Fall 2020

Finite time suboptimal control design of nonlinear systems with θ-D technique and implementation to aerospace applications

Jie Yao

FINITE TIME SUBOPTIMAL CONTROL DESIGN OF NONLINEAR SYSTEMS WITH $\theta - D$ TECHNIQUE AND IMPLEMENTATION TO AEROSPACE APPLICATIONS

by

JIE YAO

A DISSERTATION

Presented to the Graduate Faculty of the

MISSOURI UNIVERSITY OF SCIENCE AND TECHNOLOGY

In Partial Fulfillment of the Requirements for the Degree

DOCTOR OF PHILOSOPHY

in

MECHANICAL ENGINEERING

2020

Approved by

Dr.S.N.Balakrishnan
Dr.Robert G. Landers
Dr.Serhat Hosder
Dr.K.Krishnamurthy
Dr.Abhijit Gosavi

ABSTRACT

A finite time suboptimal control strategy (named $\theta - D$ approximated algorithm) was proposed in this study, which can provide the control engineers with a novel effective and efficient design tool from the finite time optimal perspective. Based on the framework of this proposed method, the original nonlinear dynamics were formulated in pseudo-linear form, and the performance index was denoted by a linear quadratic regulator prototype in this research. After that, the approximated solutions to intractable Hamilton-Jacobi-Bellman (HJB) equation were acquired by putting vanishing perturbation terms into the performance index. By tuning the parameters in perturbation terms, semi-global stability and sub-optimalilty was guaranteed. By taking the advantages of the perturbation terms, the large control was not required to cope with the large deviation at the initial time, which alleviates the severe tests of the actuators. The detailed procedure to develop this technique and corresponding stability proof were provided. The effectiveness of the proposed technique was verified by solving the two-dimensional benchmark problem, and the other three aerospace applications, including Reusable Launch Vehicle (RLV) landing problem, multiple satellites docking problem, and satellite maneuvering considering J_2 perturbation problem. In this research, contrary to the finite-time state dependent Riccati equation (FS-DRE) technique , the proposed technique did not need excessive online computation, which makes the real-time implementation in various engineering scenarios possible since the computational resources are always limited for any specific engineering application; thus, leading to the major contribution of this research for avoiding the online computation of nonlinear Riccati equation and matrix inverse operation at each sample time.

ACKNOWLEDGMENTS

First, I would like to express my sincere appreciation to my dissertation research committee, which includes Dr. Robert G. Landers, Dr. Serhat Hosder, Dr. K. Krishnamurthy, and Dr. Abhijit Gosavi. Their valuable comments and support were essential to my success.

Second, my deepest gratitude goes to my advisor, Dr. S.N.Balakrishnan, who is the Curators' Professor and world-class scientist in the Guidance, Navigation and Control (GNC) community. Reminiscing on my time with my advisor researching and learning during the past six years, the warm and appreciative current is strong. My advisor witnessed my growing up from an ordinary graduate student to a qualified PhD. My advisor has always treated me as his own child with patience, energy, and financial support. His personality, spirit of hard-working, and insight to doing research influenced me enormously in past six years, and he will impact my future career. Additionally, I would like to express my thanks to the wife of my advisor. She always prepared wonderful food for research team parties, which gave me a special feeling of home and let me enjoy the happy reunion moment.

Third, I would like to give my thanks to my colleagues. Thank you for sharing your ideas in the team meetings and your company the past six years. Additionally, I want to thanks to all professors and staff on the campus who helped me in the past six years. Wish you all the best in the future !

Finally, I want to give my special thanks to my mother, and especially, to my wife Ms.Meng Xia, for your moral support and encouragement during my PhD journey. Thank you for always be there for me and for everything you have done for me. My life became wonderful because of you. Thank you for your company and never-ending support in the past six years, love you forever! To my Dad, may your soul in heaven rest in peace !

TABLE OF CONTENTS

Page

LIST OF ILLUSTRATIONS

Figure Page

LIST OF TABLES

Table Page

NOMENCLATURE

Symbol	Description
C_D	Drag Coefficient
C_L	Lift Coefficient
C_{D_0}	Zero-lift Drag Coefficient
C_{L_0}	Zero-angle-of Attack Lift Coefficient
D	Drag Force, lb
H	Scale Height, $8.5KM$
J_2	Perturbation Coefficient, $1.08262668 \times 10^{-3}$
K_I	Lift-induced Drag Coefficient Parameter
L	Lift Force, lb
LEO	Low Earth Orbit
$LVLH$	Local Vertical Local Horizontal
S_a	Aerodynamic Reference Area, ft^2
T	Period of the Chief Satellite
V	Velocity Magnitude, ft/s
X	Downrange, ft
X_f	Fixed Final Downrange, ft
$[\omega\times]$	Skew-symmetric Matrix

$\bar{q}$	Dynamic Pressure, lb/ft^2
$\mathbf{\Omega}$	Right Ascension of the Ascending Node
α	Angle of Attack, deg
γ	Flight Path Angle, deg
$\mathbf{R}$	Reference Length
ω	Angular Velocity of the LVLH Frame
$\rho = [x, y, z]^T$	the Radial, Along-track, and Cross-track Distance of the Deputy Satellite Relative to the Chief Satellite
$\mathbf{d}$	Disturbance
$\mathbf{x_d}$	Reference State
$\mathcal{F}$	Vector of the Force
$\mathcal{T}$	Reference Time
μ	Gravitational Coefficient, $3.986 \times 10^5 km^3/sec^2$
$\overline{\mathbf{F}}$	Normalized Control Force in the Inertial Frame
$\overline{\mathbf{r}}$	Position Vector within the Inertial Frame
ρ	Air Density, $slugs/ft^3$
ρ_0	Sea-level Air Density, 0.0027 $slugs/ft^3$
$\mathbf{r}$	Position Vector of Satellite from the Gravitational Center
a	Orbital Semi-major Axis

$c_{(*)}$	Cosine Operation
e	Eccentricity
h	Altitude, ft
i	Inclination
m	Reusable Launch Vehicle Mass, $slugs$
r_0	Position Vector of the Chief Satellite
$s_{(*)}$	Sine Operation

1. INTRODUCTION

1.1. NONLINEAR CONTROL BACKGROUND

The development of the control design techniques were based on the increasingly complicated control objects, which originated from the requirement for the industrialization and scientific developments. In 1788, James Watts's invention of the governor was designed to regulate the speed of the rotary steam engine. It was the first time that humankind touched the concept of control. Up to this day, control engineers can design more complex algorithms to multiply satellites formation flying Liu *et al.* (2020b); Mashtakov *et al.* (2020), hundreds of drones' flying Bertizzolo *et al.* (2020), space vehicles Yedavalli (2020), and precision landing of SpaceX rockets Blackmore (2016), just to name a few. The past two centuries witnessed the enormous progress of control techniques and related theories. In broad terms, the field of control theory can be divided into two branches: linear control theory and nonlinear control theory. Due to the relatively simple characteristics, the control techniques for linear systems are comparatively perfect and mature Chen (1996). Unfortunately, those linear control techniques cannot satisfy the requirement for growing complexity control objects, which are evolving with nonlinear dynamic property. As a result, the development of the nonlinear control synthesis theories and techniques are of practical significance, which attract a large number of scientists and engineers getting involved in this field. Because of scholars' effort in the past half century, there are numerous papers about the synthesis of nonlinear control methods, which fall into the following categories: feedback linearization Chiasson (1998), sliding mode control (SMC) Edwards and Spurgeon (1998), backstepping Liu *et al.* (2020a), control Lyapunove functions (CLF) Garg *et al.* (2020), etc. There is no universal method to satisfy all of application scenarios. Then, each nonlinear control synthesis strategy has its advantages, but it also hold its own innate limitations which stem

from the theoretical background and restrictive applicability scope. If one is interested in those detailed derivation and analysis, one can refer to the comprehensive nonlinear control textbooks for the further reading, such as Slotine *et al.* (1991), Isidori (2013), and Khalil and Grizzle (2002).

Feedback Linearization technique is a well-studied and widely-used approach in controlling nonlinear systems. Researchers can intends to come up with a proper coordinate transformation to the given nonlinear system through a change of state variables and control inputs, such that the final closed-loop system renders linear dynamics. After that, plenty of linear control design methods were applied to transformed systems to meet the pre-designed performance requirements. However, there was a prerequisite: this coordinate transformation does exist for a given nonlinear system. Unfortunately, not all nonlinear system has this valid transformation. Theoretically, since this method originated from the differential geometry, the word "diffeomorphism" is taken from that. The prerequisite is that the transformation must be a "diffeomorphism" to ensure that the transformed system is an exactly equivalent representation of the original nonlinear system. Put simply, the transformation has to satisfy two conditions: 1. It is inevitable; 2. Both the transformation and its inverse are smooth so that the property of differentiability of original coordinate system can be held in the new one. The second limitation was zero dynamics, which implies some states can not be observed from the output measurement. Feedback linearization can still be designed with the nonlinear systems, which have a relative degree that is less than the dimension of state vector(one can get the relative degree though the Lie derivative). Then, the transformed system must include zero dynamics, which could be unstable and have fatal effects to the whole system since some internal states could blow up in finite time. The third drawback was that feedback linearizaiton cannot utilize some beneficial nonlinearities since all of them can be completely removed by the linerization process. The operation could result in the actuator generating strong large control signal which is not energy efficient. Actually, feedback linearization has been implemented in many

areas, such as Zhang *et al.* (2020), Autonomous landing of UAVs Tripathi *et al.* (2020), diesel engines Xu *et al.* (2020), etc. Feedback linearization is still an active research field. Some researchers and engineers team with other concepts or techniques and extend to other applications in the engineering community. A few typical examples are: Ammar *et al.* (2020) incorporated a sliding mode observer into the feedback linerizaiton and took this technique into induction motor drive control. Feedback linearization was also introduced into the reinforcement learning framework to solve the double pendulum, quadrotor, and 7-DOF manipulator arm problems Westenbroek *et al.* (2020). Cooperative game theory and feedback linerization were employed to addressed the fault-tolerant control for four-wheel independent actuated electric vehicle Zhang and Lu (2020).

Sliding mode control (SMC) is another power tool for the control engineers to use for designing the control for nonlinear systems, which sometimes could be coupled with some bounded disturbances or uncertainties. The most marked feature of SMC is that the control action is a discontinuous function of time, and can switch between continuous structures, which need to be designed such that the trajectories of nonlinear systems can move forward around the adjacent areas with different structures. This new type of motion of system, as it slides along those boundaries, is named a sliding mode. The geometrical locus, including those boundaries, is called sliding hypersuface (or manifold). Since SMC practically employs high gain to force the trajectories of nonlinear dynamics to slide along the restricted sliding mode surface, SMC is robust and it is insensitive to parameter variations and can actively reject the disturbances or uncertainties. This robustness property is of practical importance when doing control synthesis work for some nonlinear systems with uncertainties. However, engineers have to implement SMC with more care since the actuators have delays or other imperfections, which can result in large chatter, excitation of unmodified dynamics, energy loss, and plant damage. More detailed information and progress of SMC can be found in the survey papers Qureshi and Salim (2020); Zambelli and Ferrara (2020). Current research is extending the application scope of the SMC, and also

attempting to eliminate the chattering phenomenon Gao and Weng (2020); Hosseinabadi *et al.* (2020); Wan *et al.* (2020).

Originating from the application of the direct Lyapunov method, control Lyapunov function (CLF) was employed to obtain a Lyapunov function for the close loop system, and a control can be derived to force the trajectories of the system to the equilibrium states (stability is guaranteed). However, the limitation of this method is finding a proper control Lyapunov function for a nonlinear dynamics since there does not exist a systematic way to find a proper CLF. After the development of the backstepping technique by Peta V. Kokotovic around 1990, this technique gained more attention and progressed, which actually is an applicable extension of control Lyapunov function. Technically, backstepping control design technique is a recursive procedure to choose CLF, which allows design adaptive controllers for a class of nonlinear dynamics. Nonlinear dynamics is regraded as the consists of different subsystems. By iteratively selecting some proper function of state variables as a pseudo-control for each subsystem, the true feedback control can be obtained by virtue of the final Lyapunov function. The advantage of this technique is that it can solve adaptive control of nonlinear dynamics with high dimension. One can refer to the book Krstic *et al.* (1995) for the details. Although this control design strategy has favourable property, it can only apply to a certain type of nonlinear systems, which implies the nonlinear systems must satisfy the strict-feedback form. In addition, the selection of the pseudo-control for each subsystem and CLF is dependent on the designers' knowledge and experience. So, it is designer-originated method, the final performance of the system should be varied. In recent years, both methods have been extending to address new significant problems. The control of a hybrid dynamical system is designed by the CLF Sanfelice (2020). The CLF is considered in the sliding mode control framework Sachan *et al.* (2020). The control for the robotic systems involves the nonlinear model predictive control and CLF Grandia *et al.* (2020). Some new backstepping applications can be found in recent papers, such as, perturbed PVTOL aircraft Zheng and Yang (2020), air-breathing hypersonic

vehicle Yu *et al.* (2020), and leader-follower AUV formation control Wang *et al.* (2020) . Those aforementioned studies indicated that the research on backstepping technique is still an active research field currently.

It is obvious that the review so far only emphasised on the existing major control techniques to nonlinear systems. Actually, there exists another control synthesis method branch for nonlinear dynamics based on the optimal perspective. The $\theta - D$ technique of this dissertation is contributing to this branch. The next section will briefly review the relative works of other researchers in this field.

1.2. RELEVANT WORKS OF OPTIMAL CONTROL DESIGN FOR NONLINEAR DYNAMICS

Derived from the calculus of variationsGelfand *et al.* (2000) and got a control to optimize a cost function with a given dynamic system, the well-established optimal control strategy Lewis *et al.* (2012), which is based on the dynamic programming theory Bellman (1966) and the minimum principle theory Athans (1967), is undoubtedly an effective technique to design control for nonlinear systems. See Bryson (1996); Sussmann and Willems (1997) for further reading about the history of optimal control. It is apparent that solving the Hamilton-Jacobi-Bellman (HJB) is the critical and inevitable for optimal control design. Optimal control design for linear quadratic problems is easy to be solved since the HJB equation degenerate to the analytically solvable Riccati equation. However, tremendous applications involving nonlinear systems lead to extreme difficulty to get analytical solutions of the HJB equation, which restricts optimal control strategy of limited implementation for nonlinear systems. Consequently, numerous researches have investigated different methods to find approximated or numerical solutions to the HJB equation of nonlinear control problems, and they are systematically formed the *sub-optimal* control or *near-optimal* control for nonlinear systems, extending the optimal control strategy to more fields such as robotics, aerospace, process control, bio-engineering, economics, and finance.

Generally speaking, from time dependence perspective, nonlinear optimal control can be categorized into two groups: infinite horizon nonlinear optimal control and finite horizon nonlinear optimal control (some articles refer to infinite time and finite time, as well). Compared with the infinite horizon nonlinear optimal control case, which has been extensively investigated within the control community, research on the finite horizon nonlinear optimal control case is still under-developed, although it enjoys great engineering practical values because of the internal challenge caused by the time-dependent characteristic of the solutions to the HJB equation for the nonlinear system.

For infinite time or infinite horizon category, the time-invariant nature provides favorable condition to attract researchers, hence the numerous academic papers. Al-Tamimi and Lewis Wang *et al.* (2009) proposed a standard scheme to solve some classes of nonlinear systems using value-iteration-based heuristic dynamic programming (HDP). There are two standard neural networks (NN): a critic NN is taken to approximate the value function, and an action network is employed to approach the optimal control policy. The author emphasized that this approach allowed the implementation of HDP without knowing the internal dynamics of the system. A discrete time policy iteration adaptive dynamic programming(ADP) technique was developed by Liu Liu and Wei (2014) to solve the infinite horizon optimal control problem for nonlinear system. This research indicated that the iterative cost function was non-increasingly convergent to the optimal solution of the HJB equation. Additionally, NNs were also employed to approximate the performance index function and compute the optimal control law. Jagannathan Dierks and Jagannathan (2012) also presented an ADP to solve the infinite horizon optimal regulation control of affine nonlinear discrete-time systems in the presence of unknown internal dynamics and a known control coefficient matrix. In Liu and Wei (2013); Wei *et al.* (2014), Liu et al. developed a new iterative ADP algorithm to solve optimal control problems for infinite horizon discrete time nonlinear systems with finite approximation errors. Balakrishnan et al. proposed two improved schemes of ADP, Padhi *et al.* (2006), Ding and Balakrishnan (2011), named

Single Network Adaptive Critic (SNAC) and JSNAC, for a wide class of infinite time optimal control design of nonlinear systems. Compared with the regular schemes of ADP, the two schemes can reduce computations and storage requirements. Beard et al. Beard *et al.* (1998) proposed a numerical method, called successive Galerkin approximations, to solve HJB equations to achieve near-optimal control. Chen et al. Chen *et al.* (2004) presented an approximation solution method to infinite time nonlinear quadratic optimal control problem by solving a Riccati equations and a series of algebraic equations. The method from Fakharian et al.Fakharian *et al.* (2010) relied on the Adomian Decomposition method to solve the HJB arising in nonlinear optimal control problem. An iterative method was presented by Xuesong et al. Chen and Chen (2017) to solved the generalized HJB (GHJB) equation. This method converted the GHJB equation to a set of algebraic equations. Then, the proposed algorithm solved equations numerically for value points around the origin by the linearization of the non-linear equations under a ideal initial control guess. EG Al'brekht (1961) and DL Lukes (1969) developed a recursive process to obtain sub-optimal control as a power series in states.Garrard et,al. Garrard *et al.* (1967) expanded the optimal performance index as a power series based on an auxiliary variable ε and obtained a recursive solution to the HJB equation. Wernli and Cook Wernli and Cook (1975) proposed a technique by which the original nonlinear systems are taken into apparent lineraization form. The suboptimal control led to the Taylor series expansion of the solution to a State Dependent Riccati Equation (SDRE). Actually, the SDRE strategy Çimen (2008, 2010); Cloutier (1997); Cloutier *et al.* (1996); Shamma and Cloutier (2003); Stansbery and Cloutier (2000) is also a powerful tool to design optimal control for nonlinear system. By representing a nonlinear dynamics to resemble linear-form structure, the strategy allowed the designers to adopt linear quadratic regulator (LQR) methodology or H_∞ design technique for the synthesis of nonlinear control systems. The foregoing methods and papers are few of the primary studies on infinite time/horizon suboptimal/nearoptimal control design for nonlinear systems (refer to Lewis and Liu (2013); Liu *et al.* (2017); Zhang *et al.* (2019) for more reading).

Regarding the finite time/horizon category, there exists a striking contrasting phenomenon. On the one hand, the property of time dependence poses a critical challenge to design sub-optimal control for nonlinear system within engineering community. However, on the other hand, it has great practical merits. For example, it is applicable in path-planning problem for the approach and landing phase of a reusable launch vehicle (RLV) Harl and Balakrishnan (2010), UAV rendezvous within certain time Yamasaki and Balakrishnan (2010), and missile hitting targets problem Harl *et al.* (2010), etc. With the effort of Wang *et al.* (2012, 2010), Liu et al. provided insight into solving the finite-horizon nonlinear optimal control problem using the ADP strategy. Together with the regular ADP scheme, Zhao et al. Zhao *et al.* (2014) presented a novel way to solve finite horizon optimal control design problem with unknow the system dynamics, which further expanded the application scopes. In the same year, Xu and Jagannathan Xu and Jagannathan (2014) proposed a finite horizon optimal control design method to the stochastic nonlinear network system with a similar logic in Zhao *et al.* (2014). Employing the same scheme of ADP, Kim et al. Kim *et al.* (2020) adopted the Deep Neural Network (DNN), to replace the regular NN (shallow NN), to approximately solve the HJB of finite-horizon optimal control in a nonlinear control-affine system. The investigation showed that with appropriate training, the use of DNN can be applied to high-dimensional problems and improve the performance of a learned policy in the presence of uncertainty. Duan et al. Duan *et al.* (2020) posed an optimal control problem for finite-time missile-target interception systems. In the study, an event-based periodic adaptive dynamic programming (ADP) algorithm was employed to find the Nash equilibrium solution for the designed Hamilton-Jacobi-Issac (HJI) equation. A single critic neural network was employed to implement the proposed event-based optimal control algorithm, which not only alleviated some approximating errors but also simplified regular structures of the ADP. In the past few years, Balakrishnan and his team has published some works in the finite time category Heydari and Balakrishnan (2011a, 2013a, 2015, 2012, 2013b, 2014). The finite-time optimal control of nonlinear discrete

system with input constraint was considered by taking an offline training strategy Heydari and Balakrishnan (2011a, 2012). The time-varying property of finite horizon was tackled by a single NN, which incorporated constant weights and time-variant active functions. Actually, the philosophy of Heydari and Balakrishnan (2011a, 2012) is a regular direct heuristic dynamic programming (DHDP)-based scheme which employed policy/value iterations. The terminal constraint was satisfied by using an augmented vector incorporating the terminal value of the co-state. The strategy of Heydari and Balakrishnan (2011a, 2012) was used to solve a tracking problem in Heydari and Balakrishnan (2014). Later on, a closed-form solution Heydari and Balakrishnan (2015) was creatively proposed to establish finite horizon sub-optimal control of nonlinear systems based on the SDRE technique. In the research, a detailed proof was provided to guarantee the validation of this method. In Heydari and Balakrishnan (2013a), which is an application of Heydari and Balakrishnan (2015), the path-planning problem of the reentry phase of a reusable launch vehicle(RLV) was considered. Regardless of the ADP schemes employed, the online or offline proper training of neural networks is inevitably required. This requirements increases the complicity of implementation and restricts the applications of the schemes to some extent. The ADP strategy is a time-consuming process and requires great computational efforts due to its iterative property and the required training process, needless to say finite time sub-optimal control design for the high-dimensional nonlinear system. To summarize the main idea of the ADP and its variants were trying to approximate either the cost function or the optimal control expressions with different types of neural networks architectures. However, the synergistic relationship between the co-state and the resulting solutions is not exploited in those studies. Another limitation is the online or offline training of the neural network. If the dimension of the states of system is high, the difficulty in training a reliable neural network increases, and it is a time-consuming work. For numerical methods, the computational cost is very expensive if we would like to get resulting solutions with good accuracy. Although Heydari and Balakrishnan (2015) offered a closed-form solution

which provides a convenient and effective way to handle the finite time problem, the major limitation of this method is the tedious requirement of the online computation the algebraic Riccati equation at each sample time. As the system order increases, this computation load would make real-time implementation difficult.

Recently, Xin and Balakrishnan proposed a novel $\theta - D$ methodology and a series of applications Balakrishnan *et al.* (2007); Drake *et al.* (2004); Ming *et al.* (2006); Xin and Balakrishnan (2002, 2003, 2004, 2005); Xin *et al.* (2004a, 2005, 2007, 2008, 2004b, 2003, 2004c,d); Xin and Pan (2011). This method was first proposed in Xin and Balakrishnan (2002) and applied to the missile guidance law design problem. Later on, a more comprehensive research Xin and Balakrishnan (2005) on this method was presented to control community. The rest of papers were a series of applications, including missile autopilot design Ming *et al.* (2006); Xin and Balakrishnan (2003); Xin *et al.* (2003, 2004c), spacecraft position and attitude control Xin *et al.* (2004b); Xin and Pan (2011), ascent phase of reusable launch vehicles Drake *et al.* (2004), wing rock motion control Xin and Balakrishnan (2004), station-keeping problem of satelliteXin *et al.* (2008, 2004d), and spacecraft formation Balakrishnan *et al.* (2007); Xin *et al.* (2004a, 2005, 2007). However, the expertise in Xin and Balakrishnan (2002, 2005) and the rest of the aforementioned applications only considered the infinite time/horizon case. So,since many important mechanical and aerospace appreciations fall under finite horizon/ time control, for example, trajectory design for space vehicle and missile guidance, it is necessary to develop a finite time/horizon $\theta - D$ technique which can inherit the effective and efficient advantages of the infinite time/horizon version.

One of important nonlinear control design areas is aerospace field, which attracts lots of scientists and engineers to develop new effective and efficient control algorithms. In this research, a novel finite time optimal control strategy is developed to some aerospace applications, including Reusable Launch Vehicle (RLV) landing problem, multiple satellites docking problem and satellite maneuvering with considering J2 perturbation problem. The brief description of the background is given in the next section.

1.3. AEROSPACE APPLICATION BACKGROUND

Reusable Launch Vehicles returning from outer space is the final stage of the whole space exploration mission. Return or reentry from space is similar to skipping rocks on the surface of a lake. In order to make the stone skip several times over the water before finally plunging into the lake, one must make the stone strike the water's surface at a precise angle and proper velocity. Otherwise, there is no skipping, only a noisy splash. With the same logic, the RLV must be controlled to ensure the atmospheric layer is at an accurate angle and speed for a safe landing. Otherwise, the RLV will either skip off the atmospheric layer and return back to icy outer space, or it will experience a fiery journey due to the friction with the air. The challenges of ice and fire promotes the development of the RLV reentry technology. In this research, the focus was on the approaching and landing (A&L) phase, the final step of the whole reentry process, which includes the reentry step, the terminal area energy management(TAEM) step and, the A&L step.

At the end of TAEM phase when sufficient energy has already been dissipated, the A&L phase will be initialized, which begins at 10,000 feet altitude and ends with landing on the runway. The autoland guidance control of this A&L phase are required to guide the RLV to follow a predefined landing trajectory, and finally to land on a proper runway with less than 9 feet/second of vertical velocity and near-zero flight path angle James (1988). Although engineers have considered a wide range of possible scenarios to make this autoland guidance controller more robust, all RLV-faced circumstances can not be predicted in advance since there are too many uncertainties in the two previous stages. Also, the RLV might have some structural, or unpredictable damage and perturbations. In order to guide the RLV to land safely within the finite horizon, it is necessary to design a feasible trajectory online based on the currently-available flight data of RLV, instead of the pre-designed trajectory.

Actually, there exists some but not many, previous works about finite horizon (called *finite time* in some academic papers) guidance control design of the A&L phase. The three-

dimensional A&L case was considered in Xiangdong *et al.* (2017). By exploiting the higher-order sliding mode control technique, a multiple sliding surface guidance technique (MSSG) was developed. Due to the inherent property of reaching sliding surface within finite time, MSSG was regarded as finite time guidance control. Combining integral sliding control concepts with polynomial feedback control methods, a new finite time sliding mode control law was created in Liao and Chen (2016). This study claims that the robustness was ensured along the motion, the convergence time can be selected in advance and guaranteed, and system states can be formed in an analytical way. Another finite-time approach and landing guidance law was discussed in Li and Hu (2018). Based on all-coefficient adaptive control theories, a predictor-corrector guidance control law was proposed. The author indicated that the law can generate the new trajectories online according to the current states and final state conditions. Finally, the stability and finite time convergence of this guidance law were studied. Based on the techniques of extended-state observer and non-singular fast terminal sliding mode control, a finite-time controller was designed in presence of the disturbance in Zhang *et al.* (2018). The stability analysis and numerical simulation were given to verity the validation of this method. Harl and Balakrishnan (2010) developed a finite-time guidance law based on the second-order sliding mode concept, which allowed for the design of the trajectories offline. They were then generated online by a closed-loop law. This method employs the finite-time-reaching phase of the sliding mode control to ensure that any desired state constraints can be fulfilled in a finite time. The techniques mentioned above are involved with the concepts of adaptive control or sliding mode control to fulfil the guidance control law with the finite horizon.

Another typical problem of formation control design for multiple satellites was adopted and numerically simulated to demonstrate the performance of the proposed method. Satellite formation flying is a challenging task, but a real cutting edge, which implies that several satellites forming a group and working together will accomplish space exploration missions. Most missions were taken by a single larger, more complicated, and more expen-

sive satellite decades ago. Normally, more complicated systems are vulnerable to failure because of small part malfunctions. Fortunately, formation flying groups of satellites can avoid this situation, and it can also provide for limited degradation of performance during the period of the satellite malfunction. This means that the overall space mission will be at risk if a single larger satellite has a system fault. However, if only a single satellite in a group fails, the rest of the satellites in this formation may continue to accomplish the mission with the sacrifice of some performances. Another advantage of the formation flying is that it can offer flexibility to space exploration mission designers in that each satellite of a formation can be re-positioned to satisfy different tasks' requirement. For example, a ground-observing space-based sensor should be designed as formation flying, which can increase the aperture size as compared to constructing of a larger satellite. This formation flying system can provide the sensor more flexibility since the aperture size and orientation are adjustable in orbit. Actually, docking operation is one kind of formation flying that ensures satellites can find each other and keep station in the same orbit.

Over the past fifty years, with the development of the space exploration, many researchers have been devoted to developing effective control algorithms for the formation flying due to the aforementioned beneficial properties. Zhou *et al.* (2013) developed a quaternion-based finite time nonlinear control law to force the the attitude of the rigid spacecraft (follower) to synchronize the attitude of the leader. Meanwhile, the angular velocity will converge to zero in finite time. Additionally, employing the a finite time sliding-mode estimator, a modified control law was invented to reduce the heavy communication burden. Jin (2016) created a interesting fault tolerant finite time leader-follower control strategy, which aimed at multiple under-actuated autonomous surface vessels involved with the partially known control gain functions. Also, there exists two constrained conditions: line-of-sight and angle tracking errors. Recently, A paper by Hao *et al.* (2020) addressed the problem of attitude synchronization and tracking control of formation flying with external disturbance. By adopting the neural network to estimate the upper bound

of the disturbance, a hyperbolic tangent function-based sliding mode control method is designed to fulfil the consensus purpose. The output feedback finite time attitude containment control problem of formation flying was considered by Chen and Zhao (2020) with a novel finite time command filtered backstepping containment control strategy. From finite time/horizon optimal perspective, there also exists some researches about the formation flying. Heydari and Balakrishnan (2011a) proposed a single network adaptive critics strategy to solve the finite time optimal control problem involving input constraint. Two years later, a model-based reinforcement learning algorithm was developed by Heydari and Balakrishnan (2013b) for fixed-final-time optimal control of nonlinear systems with soft and hard terminal constraints. A state dependent Riccati equation(SDRE) based dynamic programming method was proposed in Geng *et al.* (2020) to address the fixed time optimal re-pointing maneuvers problem with the terminal constraints. Actually, the researches about the finite time optimal control for formation flying are not many. However, this research direction is of practical significance to control satellite or spacecraft formation flying in the space. Additionally, when there is one design control algorithm for satellite flying, the J_2 perturbation is unavoidable concern due to the fact that the Earth is an oblate spheroid. It is an obvious physical property that the centrifugal force will definitely bulge the equator of the earth when it rotates along the axis. The word "J_2" is based on the infinite series equation which represents the the perturbational effects of oblation on the gravity of a planet. The coefficients of each item in this series, which are J_2, J_3, J_4, $\cdots$, are named zonal coefficients. The fact is that J_2 is the dominating term since J_2 is over 1000 times larger than the others and exerts the strongest perturbing influence on orbits. Some papers were presented as follows about the control design from optimal perspective with the J_2 influence. Vadali *et al.* (1999) developed a fuel-optimal, low-thrust, variable Isp propulsion control scheme to the satellite formation flying involving the J_2 perturbation. Two techniques, Mixed-integer Linear Programming and the Particle Swarm Optimization, were used to solve the fuel minimum in-plane satellite reconfiguration maneuver in J_2 perturbed

near-circular orbits. Franco and dos Santos (2020)'s paper, the linear model in Cartesian coordinates, called Clohessy-Wiltshire Equations was considered. Then, the optimal control approach, described by the Linear Quadratic Regulator (LQR), were taken to carry out the ITASAT-2 mission, which launched three satellites in formation flying while considering the J_2 perturbation. Bilal *et al.* (2019) provided the State-Dependent Riccati Equation (SDRE) control approach to tackle a formation flying of low Earth orbit (LEO) satellites. At the meantime, an exact nonlinear differential J_2 perturbation model was considered in the relative orbital dynamics. However, the control strategy for the satellite formation flying coupling with the J_2 perturbation from the finite time optimal perspective can not be found. However, it is useful because it can provide the designers or engineers with a freedom to control the operation times.

1.4. RESEARCH OBJECTIVES AND CONTRIBUTIONS

Based on the aforementioned discussions, researchers and engineers have made enormous progress in nonlinear control synthesis in the past half century, who generated lots of techniques and extended those techniques to different application scopes. Although each of them has its own advantages and limitations, those methods can obtain a relative good performance results from theoretical perspectives. In this research, the goal is to create an algorithm which can take "finite time","optimal" and "saving computational resources" simultaneously into consideration. If those requirements can be satisfied, this algorithm can be effectively and efficiently implemented in real time, which can provide the engineer with a promising tool in the real application practice in aerospace or other fields. Based on this guiding ideology and previous research work completed by the team, a novel finite time suboptimal nonlinear control synthesis ($\theta - D$ approximation) design strategy is proposed, which aim to find an approximately analytical solution to partial Hamilton-Jacob-Bellman (HJB) equation. The optimal cost or costate can be approximated by the summation of power series of θ, which is regarded as the auxiliary parameter. The partial HJB equation

can be replaced by a set of recursive algebraic Lyapunov equations. The perturbation terms (D terms) is added into the framework to avoid generation of the large control by the actuator to offset the possible large initial state. Note that no actuator can produce unlimited signals. Though appropriately manipulating the parameters in D terms, the semi-globally asymptotic stability can be guaranteed based on the Lyapunov stability theory.

The contributions of this research are listed as follows:

1. To develop a new optimal control technique for a class of nonlinear dynamics from the finite time optimal perspective.

2. To provide an effective and efficient tool for engineers when they design a finite time optimal controller.

3. To obtain a closed form solution and avoid the intensive computation load compared with the finite time SDRE technique, which needed to computer nonlinear Ricatti equation and twice matrix inverse operation at each sample state.

4. To avoid the large control to large initial state problem due to the existing D terms, which can effectively protect the actuators and save money.

5. To make the real-time implementation possible of the proposed algorithm with different engineering application scenarios.

6. To implement successfully the finite time $\theta - D$ method into aerospace applications, which verify the proposed finite time $\theta - D$ method is promising.

7. To offer a new tool for solving multiagent cooperation control design problem.

8. With proper transformation, non-affine control nonlinear systems can also be tackled with this proposed method, which implies both affine-control and non-affine control nonlinear dynamics can be handled with the proposed method.

9. Other project-oriented independent variables (altitude,down-ranges,etc) could be formulated "time" in the finite time $\theta - D$ framework, which can extend the application scope.

10. The modeled disturbances or uncertainties can be rejected with this proposed method.

1.5. ORGANIZATION OF THIS DISSERTATION

The overall development of finite the time $\theta - D$ algorithm is presented in Section 2. In this section, the theoretical part of this technique will be discussed, including the goal, the algorithm, and the related necessary proof. After that, a two dimensional benchmark nonlinear problem are studied by the proposed method to show the related advantage properties. At the same time, the comparison work is carried out with finite-time SDRE technique Heydari and Balakrishnan (2015) from performance, cost, and overall run time to verify the effective and efficient characteristics of the proposed method.

Section 2 and Section 3 are about the applications of the proposed finite time $\theta - D$ method. The optimal path planning of RLV landing problem is investigated in this section. Actually, this dynamics of the RLV landing is a non-affine control system. The method is employed to convert this non-affine control into finite time $\theta - D$ framework. Besides, the independent variable "downrange" is considered as "time" in the proposed method. Additionally, a certain robustness property of this finite time $\theta - D$ technique is demonstrated. In Section 3, two applications can be found: multiple satellite consensus problem and satellite orbit maneuvering problem with J_2 perturbation. This part can show that the proposed method can be extended to multi-agent cooperative control and disturbance rejection work. The final Section 5 gives the final conclusion and the list of future research direction.

2. FINITE TIME SUBOPTIMAL CONTROL OF A CLASS OF NONLINEAR SYSTEMS

2.1. PROBLEM STATEMENT

In this part, the objective is to develop closed-from suboptimal controllers for nonlinear dynamic systems. Focus will be on time-invariant nonlinear system of the form

$$\dot{x} = f(x) + B(x)u \tag{2.1}$$

where $x \in \Omega \subset \Re^n$, $f(x) : x \in \Omega \rightarrow \Re^n$,$B(x) : x \in \Omega \rightarrow \Re^{n\times m}$, and $u \in U \subset \Re^m$

The goal is to seek a controller which can minimize the quadratic cost function $J(x,u)$, which is defined by

$$J(x,u) = \frac{1}{2}x(t_f)^T S_f x(t_f) + \frac{1}{2}\int_0^{t_f} (x^T Q x + u^T R u)dt \tag{2.2}$$

where $Q \in \Re^{n\times n}$, $R \in \Re^{m\times m}$, and $S_f \in \Re^{n\times n}$. The matrices Q and S_f are semi-positive definite, and R is a positive definite. The known final time is denoted by t_f.

The following assumptions are specified to guarantee that the above optimal control design problem is a well-posed one:

(A1) Ω is a compact set which includes origin as an interior point; U is an admissible control set which is also a compact set.

(A2) $f(x)$ is continuously differentiable on Ω, and $f(0) = 0$.

(A3) the dynamic system (2.1) is controllable over the compact set Ω.

(A4) the dynamic system (2.1) is zero-state observable Byrnes *et al.* (1991) over Ω. With the dynamic system given by (2.1) and the above assumptions $(A1) - (A4)$, the minimization of the cost function, given by (2.2) leads to the following partial differential equation for

the optimal cost:

$$V_x^T f(x) - \frac{1}{2} V_x^T B(x) R^{-1} B^T(x) V_x + \frac{1}{2} x^T Q x = -V_t \tag{2.3}$$

where $V_x = \frac{\partial V(x,t)}{\partial x}$ and $V_t = \frac{\partial V(x,t)}{\partial t}$. $V(x,t)$ is the optimal cost, i.e.

$$V(x,t) = \min_u \left(\frac{1}{2} x(t_f)^T S_f x(t_f) + \frac{1}{2} \int_0^{t_f} (x^T Q x + u^T R u) dt \right) \tag{2.4}$$

with $V(x,t) > 0$ and $V(0) = 0$. The necessary condition to get optimality results in

$$u = -R^{-1} B(x)^T V_x \tag{2.5}$$

Remark 1. From 2.5, we know that V_x is required to compute the optimal controller. Unfortunately, the HJB equation is extremely hard to solve in general, hence the limited use of optimal control techniques for nonlinear systems. There exists some research in intelligent control or neural network literature that approximated the cost function or the optimal expression using various kinds of neural network schemes. The adaptive dynamic programming (ADP) or related variants were employed to approximate the co-state or the Lagrange's multiplier within those literature. However, those studies did not exploit the synergistic relations between the costate and the resulting solution because the those papers hardly addressed the fundamental problem with HJB equation, which is that it leads to a two point boundary value problem.

Remark 2. The crux of the whole optimal control problem is that the boundary conditions for the costate are specified at the final time. Once the costate is known at each point in time, optiaml control can be obtained easily. The method proposed in this dissertation is to approximate the costate. A critical problem exists in the fact that it represents the partial derivative of the cost with respect to the state, and the optimal cost is a function of state and

time in a finite time problem. That is, how can we retrieve $V(x,t)$ from $\partial V(x)/\partial x$? In the next part, an approach is outlined with a series expansion that approximates the costates. Then, we further show recurrence relations.

2.2. FINITE TIME $\theta - D$ SUBOPTIMAL CONTROL DEVELOPMENT

An infinite power series is added into the cost function for operating the approximation procedure and assuming a power series solution to be the gradient of the optimal cost V.

Now, let us consider a perturbation term $\sum_{i=1}^{\infty} D_i\theta^i$ to be added to the cost function

$$J(x,u) = \frac{1}{2}x(t_f)^T S_f x(t_f) + \frac{1}{2}\int_0^{t_f} \left[x^T\left(Q + \sum_{i=1}^{\infty} D_i\theta^i\right)x + u^T Ru\right]dt \tag{2.6}$$

where θ is a scalar and D_i is a matrix. θ and D_i are chosen such that $\left(Q + \sum_{i=1}^{\infty} D_i\theta^i\right)$ is semi-positive definite.

The original dynamic equation (2.1) can be re-arranged as

$$\dot{x} = f(x) + B(x)u = \left[A_0 + \theta\left(\frac{A(x)}{\theta}\right)\right]x + \left[g_0 + \theta\left(\frac{g(x)}{\theta}\right)\right]u \tag{2.7}$$

where A_0 and g_0 are constant matrices such that (A_0, g_0) is a stablizable pair and $\left[\left(A_0 + A(x)\right), \left(g_0 + g(x)\right)\right]$ is pointwise controllable.

Define the costate as

$$\lambda = V_x \tag{2.8}$$

Assume a power series expansion of λ based on θ

$$\lambda = \left(T_0 + \sum_{i=1}^{\infty} T_i(x)\theta^i\right)x \tag{2.9}$$

where matrices T_0, $T_i(1 \leq i < \infty)$ are to be determined, and they are assumed to be symmetric. In order to motivate the solution of the HJB equation, first, consider only two terms of the expression on the RHS of (2.9).

With the assumed expression of λ in (2.9), the next step is to get an expression for the optimal cost function, called V_x. We now motivate this part by taking only the first two terms of the θ-based series expansion for V_x as

$$\frac{\partial V(x)}{\partial x} = \Big[T_0 + T_1(x)\theta\Big]x \tag{2.10}$$

Then, the optimal cost function can be written as

$$\begin{aligned} V(x,t) &= \int \left(\frac{\partial V(x)}{\partial x}\right)^T dx + c(t) \\ &= \int x^T \Big(T_0 + T_1(x)\theta\Big)^T dx + c(t) \\ &= \frac{1}{2}x^T T_0 x + \theta w(x) + c(t) \end{aligned} \tag{2.11}$$

where $c(t)$ is a function of time satisfying the boundary condition and $w(x)$ is a function of x only

$$w(x) = \int x^T T_1^T(x)dx \tag{2.12}$$

Note that, in (2.10), only two items are considered. Actually, if we take all the items of (2.9) into account, $w(x) = \int x^T \big(\sum_{i=1}^{\infty} \theta^{i-1} T_i(x)\big)^T dx$. We can easily identify that $w(x)$ is still a function of x.

At $t = t_f$ and with (2.11), $V(x(t_f), t_f)$ is given by

$$V(x(t_f), t_f) = \frac{1}{2}x(t_f)^T T_0(t_f)x(t_f) + \theta w(x_{t_f}) + c(t_f) \tag{2.13}$$

From the cost function definition in (2.2)

$$V(x(t_f), t_f) = \frac{1}{2}x(t_f)^T S_f x(t_f) \tag{2.14}$$

By equating (2.13) and (2.14) and assuming that $w(x_{t_f}) = 0$ and $\{c(t) = 0 | t \in [0, t_f]\}$, we get for all x

$$\frac{1}{2}x(t_f)^T T_0(t_f)x(t_f) = \frac{1}{2}x(t_f)^T S_f x(t_f) \tag{2.15}$$

Consequently:

$$T_0(t_f) = S_f \tag{2.16}$$

With the previous assumption of $\{c(t) = 0 | t \in [0, t_f]\}$

$$\begin{aligned} \frac{\partial V(x,t)}{\partial t} &= \frac{\partial}{\partial t}\left[\frac{1}{2}x^T T_0 x + \theta w(x) + c(t)\right] \\ &= \frac{\partial}{\partial t}\left[\frac{1}{2}x^T T_0 x\right] \\ &= \frac{1}{2}x^T \dot{T}_0 x \end{aligned} \tag{2.17}$$

since $w(x)$ is a function of x only.

Generalizing this argument for all the terms in the series expression for λ in (2.9), the HJB equation (2.3) can be rewritten as

$$\begin{aligned} & V_t + V_x^T f(x) - \frac{1}{2}V_x^T B(x)R^{-1}B^T(x)V_x + \frac{1}{2}x^T\big(Q + \sum_{i=1}^{\infty} D_i\theta^i\big)x = 0 \\ \implies & \frac{1}{2}x^T\dot{T}_0 x + x^T\left(T_0 + \sum_{i=1}^{\infty} T_i(x)\theta^i\right)^T\Big(A_0 + A(x)\Big)x \\ & - \frac{1}{2}x^T\left(T_0 + \sum_{i=1}^{\infty} T_i(x)\theta^i\right)^T\Big(g_0 + g(x)\Big)R^{-1}\Big(g_0 + g(x)\Big)^T \\ & \times\left(T_0 + \sum_{i=1}^{\infty} T_i(x)\theta^i\right)x + \frac{1}{2}x^T\big(Q + \sum_{i=1}^{\infty} D_i\theta^i\big)x = 0 \end{aligned} \tag{2.18}$$

Note that each item in the HJB equation is premultiplied by x^T and postmultiplied by x. Equating the coefficients of powers of θ to zero in (2.18) leads to the following series of equation:

$$T_0 A_0 + A_0^T T_0 - T_0 g_0 R^{-1} g_0^T T_0 + Q = -\dot{T}_0 \tag{2.19}$$

$$\begin{aligned} &T_1(A_0 - g_0 R^{-1} g_0^T T_0) + (A_0^T - T_0 g_0 R^{-1} g_0^T) T_1 \\ &= -\frac{T_0 A(x)}{\theta} - \frac{A^T(x) T_0}{\theta} + T_0 g_0 R^{-1} \frac{g^T(x)}{\theta} T_0 + T_0 \frac{g(x)}{\theta} R^{-1} g_0^T T_0 - D_1 \end{aligned} \tag{2.20}$$

$$\begin{aligned} &T_2(A_0 - g_0 R^{-1} g_0^T T_0) + (A_0^T - T_0 g_0 R^{-1} g_0^T) T_2 \\ &= -\frac{T_1 A(x)}{\theta} - \frac{A^T(x) T_1}{\theta} + T_0 g_0 R^{-1} \frac{g^T(x)}{\theta} T_1 + T_0 \frac{g(x)}{\theta} R^{-1} g_0^T T_1 \\ &+ T_0 \frac{g(x)}{\theta} R^{-1} \frac{g^T(x)}{\theta} T_0 + T_1 g_0 R^{-1} g_0^T T_1 + T_1 g_0 R^{-1} \frac{g^T(x)}{\theta} T_0 \\ &+ T_1 \frac{g(x)}{\theta} R^{-1} g_0^T T_0 - D_2 \end{aligned} \tag{2.21}$$

$$\begin{aligned} &T_n(A_0 - g_0 R^{-1} g_0^T T_0) + (A_0^T - T_0 g_0 R^{-1} g_0^T) T_n \\ &= -\frac{T_{n-1} A(x)}{\theta} - \frac{A^T(x) T_{n-1}}{\theta} + \sum_{j=0}^{n-2} T_j \frac{g(x)}{\theta} R^{-1} \frac{g^T(x)}{\theta} T_{n-2-j} \\ &+ \sum_{j=0}^{n-1} T_j \left[g_0 R^{-1} \frac{g^T(x)}{\theta} + \frac{g(x)}{\theta} R^{-1} g_0^T \right] T_{n-1-j} + \sum_{j=1}^{n-1} T_j g_0 R^{-1} g_0^T T_{n-j} - D_n \end{aligned} \tag{2.22}$$

Note that there exists only one nonlinear differential equation(2.19) with the final condition (2.14) which has the same form in a linear quadratic problem, that is for T_0, and can be solved *offline* to provide a closed-form solution. The rest of the $T_i(x)$ equations are all *linear* Lyapunov equation, and a closed-form solution can be solved for each one of them since each $T_i(x)$ equation is the function of the current state x, which is known, and of the

coefficient $T_{i-1}(x)$. Hence, with (2.9), a closed-form solution for optimal control can be expressed as the follows:

$$u = -R^{-1}B^T(x)\sum_{i=0}^{\infty} T_i(x)\theta^i x \tag{2.23}$$

Remark 3. Since (2.19) can be solved offline and we can get all T_0 value at each sample time in advance, we can rewrite (2.9) as a compact form $\sum_{i=0}^{\infty} T_i(x)\theta^i x$ for a concise reason.

Remark 4. In the rest of the dissertation, (2.19) − (2.23) will be named as finite-time $\theta - D$ technique. If the D term does not exist, this technique will be called finite-time θ approximation.The limitation of θ approximation is that when the nonlinear systems face a large initial value (the most serious challenge for controllers of nonlinear systems), the controllers have to generate a large initial control signal to nonlinear system, which is a tough trial for any actuators in real engineering applications. Sometimes, the large initial control signal will result in an intensively varied transient process, even leading to instability of the nonlinear system.

Now, we design D_i term as follows: $i = 1, \cdots, n$

$$D_1 = k_1 \exp^{-l_1 t}\left[-\frac{T_0 A(x)}{\theta} - \frac{A^T(x)T_0}{\theta} + T_0 g_0 R^{-1}\frac{g^T(x)}{\theta}T_0 + T_0\frac{g(x)}{\theta}R^{-1}g_0^T T_0\right] \tag{2.24}$$

$$\begin{aligned} D_2 = k_2 \exp^{-l_2 t}\Bigg[&-\frac{T_1 A(x)}{\theta} - \frac{A^T(x)T_1}{\theta} + T_0 g_0 R^{-1}\frac{g^T(x)}{\theta}T_1 + T_0\frac{g(x)}{\theta}R^{-1}g_0^T T_1 \\ &+ T_0\frac{g(x)}{\theta}R^{-1}\frac{g^T(x)}{\theta}T_0 + T_1 g_0 R^{-1}g_0^T T_1 + T_1 g_0 R^{-1}\frac{g^T(x)}{\theta}T_0 + T_1\frac{g(x)}{\theta}R^{-1}g_0^T T_0\Bigg] \end{aligned} \tag{2.25}$$

$$\begin{aligned} D_n = k_n \exp^{-l_n t}\Bigg[&-\frac{T_{n-1}A(x)}{\theta} - \frac{A^T(x)T_{n-1}}{\theta} + \sum_{j=0}^{n-2} T_j\frac{g(x)}{\theta}R{-}1\frac{g^T(x)}{\theta}T_{n-2-j} \\ &+ \sum_{j=0}^{n-1} T_j\left[g_0 R^{-1}\frac{g^T(x)}{\theta} + \frac{g(x)}{\theta}R^{-1}g_0^T\right]T_{n-1-j} + \sum_{j=1}^{n-1} T_j g_0 R^{-1}g_0^T T_{n-j}\Bigg] \end{aligned} \tag{2.26}$$

where $k_i > 0$ and $l_i > 0$; $i = 1, \cdots, n$ are freedom and problem-originated variables which should be tuned properly .

Remark 5. The effect of the large initial value has been stated in remark 4. The philosophy that we design (2.24),(2.25) and (2.26) to mitigate this effect will be stated as follows:Let us observe the (2.20). Without considering the term D_1, one can find that at each sample time, A_0, g_0, T_0, θ are known and $A(x)$ is a state-dependent variable and the only term which can directly affect the magnitude of T_1. This T_1 will further affect the following $T_2, T_3, \cdots, T_n$ and finally determinate the magnitude of control. This observation leads to find ways to alleviate this effect. We realize that the vanishing perturbation terms in the cost function provide the D_i terms on the RHS of (2.20),(2.21) and (2.22). With the D_i terms in the RHS, our goal is to design a proper D_i which could decrease the impact of RHS terms in (2.20),(2.21) and (2.22) to the T_i and could further offset the large control problem without compromising the performance of the original nonlinear system. This could happen if those extra terms (2.24),(2.25) and (2.26) are small enough and decrease quickly with time.

With the D_i terms of (2.24),(2.25) and (2.26), the (2.20),(2.21) and (2.22) will change to

$$
\begin{aligned}
&T_1(A_0 - g_0R^{-1}g_0^TT_0) + (A_0^T - T_0g_0R^{-1}g_0^T)T_1 \\
&= \varepsilon_1(t)\bigg[- \frac{T_0A(x)}{\theta} - \frac{A^T(x)T_0}{\theta} + T_0g_0R^{-1}\frac{g^T(x)}{\theta}T_0 + T_0\frac{g(x)}{\theta}R^{-1}g_0^TT_0\bigg]
\end{aligned} \tag{2.27}
$$

$$
\begin{aligned}
&T_2(A_0 - g_0R^{-1}g_0^TT_0) + (A_0^T - T_0g_0R^{-1}g_0^T)T_2 \\
&= \varepsilon_2(t)\bigg[- \frac{T_1A(x)}{\theta} - \frac{A^T(x)T_1}{\theta} + T_0g_0R^{-1}\frac{g^T(x)}{\theta}T_1 + T_0\frac{g(x)}{\theta}R^{-1}g_0^TT_1 \\
&+ T_0\frac{g(x)}{\theta}R^{-1}\frac{g^T(x)}{\theta}T_0 + T_1g_0R^{-1}g_0^TT_1 + T_1g_0R^{-1}\frac{g^T(x)}{\theta}T_0 \\
&+ T_1\frac{g(x)}{\theta}R^{-1}g_0^TT_0\bigg]
\end{aligned} \tag{2.28}
$$

$$
\begin{aligned}
&T_n(A_0 - g_0R^{-1}g_0^TT_0) + (A_0^T - T_0g_0R^{-1}g_0^T)T_n \\
&= \varepsilon_n(t)\Bigg[- \frac{T_{n-1}A(x)}{\theta} - \frac{A^T(x)T_{n-1}}{\theta} + \sum_{j=0}^{n-2} T_j \frac{g(x)}{\theta} R^{-1} \frac{g^T(x)}{\theta} T_{n-2-j} \\
&+ \sum_{j=0}^{n-1} T_j \left[g_0R^{-1}\frac{g^T(x)}{\theta} + \frac{g(x)}{\theta}R^{-1}g_0^T \right] T_{n-1-j} + \sum_{j=1}^{n-1} T_j g_0 R^{-1} g_0^T T_{n-j} \Bigg]
\end{aligned} \tag{2.29}
$$

where $\varepsilon_i(t) = 1 - k_i e^{-l_i t}$, $(i = 1, \cdots, n)$ is a small enough number that should be within the interval $[0, 1)$.

Remark 6. $\varepsilon_i(t)$ is to employed to avoid the large magnitude value of T_i in (2.20), (2.21) and (2.22). The choice of $\varepsilon_i(t)$ should satisfy the convergence and stability requirement which will be stated in the next section. The term $e^{-l_i t}$ $(l_i > 0)$ guarantees the perturbation terms in the cost function and HJB equation to diminish as time passes, which restrict the perturbation term just could affect the sample times at beginning.

Remark 7. From (2.19) to (2.29) provide sufficient, rather than necessary, condition of $V_x = \sum_{i=0}^{\infty} T_i(x)\theta^i x$ to be the solution of the corresponding HJB equation. The reason is that at the very beginning, we assume that the gradient of an *optimal cost function* is of the form $\sum_{i=0}^{\infty} T_i(x)\theta^i x$. To get an optimal control, another condition is made: this solution is also the gradient of a positive definite function with $V(0) = 0$. There is a proposition in the Remark 2.2 of Xin and Balakrishnan (2005) which guarantees such an optimal cost function exists. Now, we summarize all the step of the finite-time $\theta - D$ method as follows:

Note that:

(1). Once A_0, g_0, Q, and R are determined, the differential Riccati matrix equation (2.19) can be solved backward to get T_0 since the final time state $T_0(t_f)$ is given with (2.16). This step can be done *offline*. Note that T_0 is a non-negative definite matrix;

(2). Let us observe the (2.27). This is a general form of linear Lyapunov equation. At each sample time, $(A_0 - g_0R^{-1}g_0^TT_0)$ and $(A_0^T - T_0g_0R^{-1}g_0^T)$ are constant matrices. They can be computed *offline*. Based on matrices theory, and denoting all of items of the RHS of (2.27) as Q_1, the close-formed solution of (2.27) can be expressed as $Vec(T_1) =$

Algorithm 1 : Finite-time $\theta - D$ Sub-optimal Control Design Algorithm

Input:
S_f: terminal state weight matrix; Q: state weight matrix;
R: control weight matrix; $x_{initial}$: initial value of state;
θ, k_i, l_i : adjustable parameters;
A_0, g_0: factorize $A(x)$ from $f(x)$, $g(x)$ from $B(x)$ with $x = x_{initial}$
t_f: the final time; dt: sample time;
Output: x: state under the suboptimal control

1: **for** each $i \in [1, t_f/dt]$ **do**
2: solve the differential Riccati equation (2.19) with S_f to get solutions of T_0;
3: **end for**
4: **for** each $j \in [1, t_f/dt]$ **do**
5: calculate $A(x)$,$g(x)$;
6: compute T_1 with the equation (2.27);
7: compute T_2 with the equation (2.28);
8: $\cdots$
9: compute $u = -R^{-1}B^T(x)(T_0 + \theta T_1 + \theta^2 T_2 + \cdots)x$;
10: with the dynamic equation (2.1), one can compute the state with the above control;
11: store the state for the next iteration;
12: **end for**

$\left(I \otimes (A_0^T - T_0 g_0 R^{-1} g_0^T) + (A_0^T - T_0 g_0 R^{-1} g_0^T) \otimes I\right)^{-1} Vec(Q_1)$Brewer (1978). We can realize that the inverse operation of $\left(I \otimes (A_0^T - T_0 g_0 R^{-1} g_0^T) + (A_0^T - T_0 g_0 R^{-1} g_0^T) \otimes I\right)$ can also be calculated offline and in advance. What we need to compute online are some simple matrix multiplication and additions, leading to an effectively and efficiently solved finite time nonlinear optimal control problem online with high reliability. The rest of the equations could be solved with the same logic.

(3). How many T_is are needed for computing the control u should depend on the specific problems. Normally, three items T_0, T_1, T_2 are enough.

(4). There does not exist a criteria to factorize $A(x)$ from $f(x)$. Fortunately, based on SDRE, Cloutier Cloutier (1997); Cloutier *et al.* (1996) and Cimen Çimen (2008, 2010) have investigated how to factorize $A(x)$ with theoretical analysis and some real applications. With the finite time scenario, Heydari and Balakrishnan (2011a) demonstrated a theoretical proof about the stability property involving the different $A(x)$.

2.3. THE CONVERGENCE AND STABILITY ANALYSIS

Before starting the analysis, we make some assumptions to ensure that the control design problem we investigate in this dissertation is a well posed one.

(C1) $x \in \Omega$, where Ω is a compact set within n-dimensional Euclidean space.

(C2) With properly factorized from $f(x), B(x), A(x)$ and $g(x)$ are continuous over compact set Ω, which implies that all entries of $A(x)$ and $g(x)$ should be continuous. Besides, $\|A(x)\|_2 \neq 0$, $\|g(x)\|_2 \neq 0$, $\forall x \in \Omega$.

(C3) (A_0, g_0) is a stabilized pair.

(C4) $\lambda_{max}\left[(A_0 - g_0 R^{-1} g_0^T T_0) + (A_0^T - T_0 g_0 R^{-1} g_0^T)\right] < 0$, where λ_{max} denotes the largest eigenvalue

Note that:

(N1) To simplify the notation, the argument x in $A(x), g(x), T_i(x)$ and t in $\varepsilon_i(t)$ will be omitted. However, in some places, the argument will be added to avoid confusion.

(N2) We introduce a set of new variables: $\widehat{T}_0 = \theta^0 T_0; \widehat{T}_1 = \theta^1 T_1; \widehat{T}_2 = \theta^2 T_2; \cdots; \widehat{T}_n = \theta^n T_n$. Then (2.19), (2.27), (2.28), (2.29) will lead to

$$\widehat{T}_0 A_0 + A_0^T \widehat{T}_0 - \widehat{T}_0 g_0 R^{-1} g_0^T \widehat{T}_0 + Q = -\dot{\widehat{T}}_0 \tag{2.30}$$

$$\begin{aligned}&\widehat{T}_1 (A_0 - g_0 R^{-1} g_0^T \widehat{T}_0) + (A_0^T - \widehat{T}_0 g_0 R^{-1} g_0^T)\widehat{T}_1 \\ &= -\varepsilon_1 \left[\widehat{T}_0 A + A^T \widehat{T}_0 - \widehat{T}_0 g_0 R^{-1} g^T \widehat{T}_0 - \widehat{T}_0 g R^{-1} g_0^T \widehat{T}_0\right]\end{aligned} \tag{2.31}$$

$$\begin{aligned}&\widehat{T}_2 (A_0 - g_0 R^{-1} g_0^T \widehat{T}_0) + (A_0^T - \widehat{T}_0 g_0 R^{-1} g_0^T)\widehat{T}_2 \\ &= -\varepsilon_2 \Bigg[\widehat{T}_1 A + A^T \widehat{T}_1 - \widehat{T}_0 g_0 R^{-1} g^T \widehat{T}_1 - \widehat{T}_0 g R^{-1} g_0^T \widehat{T}_1 - \widehat{T}_0 g R^{-1} g^T \widehat{T}_0 \\ &- \widehat{T}_1 g_0 R^{-1} g_0^T \widehat{T}_1 - \widehat{T}_1 g_0 R^{-1} g^T \widehat{T}_0 - \widehat{T}_1 g R^{-1} g_0^T \widehat{T}_0\Bigg]\end{aligned} \tag{2.32}$$

$$\widehat{T}_n(A_0 - g_0R^{-1}g_0^T\widehat{T}_0) + (A_0^T - \widehat{T}_0g_0R^{-1}g_0^T)\widehat{T}_n$$
$$= -\varepsilon_n\Bigg[\widehat{T}_{n-1}A + A^T\widehat{T}_{n-1} - \sum_{j=0}^{n-2}\widehat{T}_jgR^{-1}g^T\widehat{T}_{n-2-j}$$
$$- \sum_{j=0}^{n-1}\widehat{T}_j\Bigg[g_0R^{-1}g^T + gR^{-1}g_0^T\Bigg]\widehat{T}_{n-1-j} - \sum_{j=1}^{n-1}\widehat{T}_jg_0R^{-1}g_0^T\widehat{T}_{n-j}\Bigg] \tag{2.33}$$

2.3.1. Mathematical Preparation. Lemma 1. Jacobson (1970); Kučera (1973) With $S \geq 0, Q \geq 0, R > 0$, the solutions of differential Riccati equation $-\dot{P} = PA + A^TP - PBR^{-1}B^TP + Q$, $P(t_f) = S$, are bounded on the time interval $[t_0, t_f]$, regardless of S and t_f.

Lemma 2. Rudin *et al.* (1964) Let f and g be continuous functions on a metric space X. Then $f + g, fg, f/g$ are continuous on X.

Lemma 3. Rudin *et al.* (1964) If f is a continuous mapping of a compact metric space X into $\Re^k$, then $f(X)$n is closed and bounded. Thus, f is bounded.

Lemma 4. Rudin *et al.* (1964) Suppose f is a continuous real function on a compact metric space X and $M = sup_{p\in X}f(p)$, $m = inf_{p\in X}f(p)$. Then there exist points $p, q \in X$ such that $f(p) = M$ and $f(q) = m$.

Lemma 5. Zedek (1965) If the coefficient of a polynomial, some of whose leading coefficients are zeros, are varied continuously, the existing roots of the polynomial vary continuously.

Lemma 6. If $x \in \mathcal{D} \subset \Re^n$, where $\mathcal{D}$ is a compact set within Euclidean space, and there is a continuous function $\Pi(x)$, where $\Pi(x) : \mathcal{D} \to \Re^{m\times n}$), then the matrix function $\Pi(x)$ is bounded.

Proof. With lemma 3, the image of a compact space under a continuous mapping is compact. So, one can conclude that the continuous function $\Pi(x) : \mathcal{D} \to \Re^{m\times n}$ is a compact set within $\Re^{m\times n}$. Thus, $\Pi(x)$ is closed and bounded. In particular, each coordinate lives within a compact subset $\Re$.

Lemma 7. If $x \in \mathcal{D} \subset \Re^n$, where $\mathcal{D}$ is a compact set within Euclidean space, and there is a continuous function $\Pi(x)$, where $\Pi(x) : \mathcal{D} \rightarrow \Re^{m \times m}$, which implies each entry is continuous, then the eigenvalue function $\lambda_i(x), 0 \leq i \leq m$ are continuous function of x. Further, the bound of $\lambda_i(x)$ exist.

Proof. Let us consider the characteristic polynomial

$$p(\lambda, x) = det(\lambda I - \Pi(x)) \tag{2.34}$$

we can see that the coefficient $p_i(x)$ of $p(\lambda, x) = \sum_{i=0}^{m} p_i(x)\lambda^i$ depends continuously on $\pi_{ij}(x)$, which is the i^{th} row and j^{th} column entry of matrix $\Pi(x)$. With lemma 2, we can state that the coefficient $p_i(x)$ is also a continuous function of x. Thus, with lemma 5, we can conclude root $\lambda_i(x)$ of the $p(\lambda, x) = \sum_{i=0}^{m} p_i(x)\lambda^i$ or the eigenvalue function of $\Pi(x)$ is a continuous function of x. Further, the bound of each $\lambda_i(x)$ exists within the compact set $\mathcal{D}$, based on lemma 4.

Lemma 8. Mori and Deresei (1984) Given a continuous Lyapuvnov equation

$$A^T P + PA = -Q \tag{2.35}$$

where $A, P, Q \in \Re^{n \times n}$, if A is a stable matrix, we have the norm bound for P

$$\|P\|_\bullet = \frac{\|Q\|_\bullet}{-\mu_\bullet(A^T) - \mu_\bullet(A)} \tag{2.36}$$

where $\mu_\bullet(A)$ is a matrix measure of A induced form $\|\|_\bullet$. In this study, 2-norm is employed

$$\mu_2(A) = \frac{1}{2}\lambda_{max}(A + A^T) \tag{2.37}$$

2.3.2. Convergence Analysis. The goal is to prove that $\sum_{i=0}^{\infty} T_i\theta^i$ is a point-wise convergent series under the conditions C(1), C(2), C(3) and C(4). With (N2), we otherwise prove that $\sum_{i=0}^{\infty} \widehat{T_i}$ is a point-wise convergent series.

Proof:

Step One: Let us consider equation (2.31) first.

With the optimal control theory, if (C3) and $\widehat{T_0}$ from differential Riccati equation (2.30) are satisfied, $(A_0 - g_0R^{-1}g_0^T\widehat{T_0})$ is a stable matrix. Based on (36) and (37), we can get:

$$\|\widehat{T_1}\| \leq -\varepsilon_1 \frac{\|\widehat{T_0}A + A^T\widehat{T_0} - \widehat{T_0}g_0R^{-1}g^T\widehat{T_0} - \widehat{T_0}gR^{-1}g_0^T\widehat{T_0}\|}{\lambda_{max}\left[(A_0 - g_0R^{-1}g_0^T\widehat{T_0}) + (A_0^T - \widehat{T_0}g_0R^{-1}g_0^T)\right]} \tag{2.38}$$

Define

$$C = -\frac{1}{\lambda_{max}\left[(A_0 - g_0R^{-1}g_0^T\widehat{T_0}) + (A_0^T - \widehat{T_0}g_0R^{-1}g_0^T)\right]} \tag{2.39}$$

Due to $\widehat{T_0} = \theta^0 T_0$ defined by (N2), (C4) can be rewritten as $\lambda_{max}\left[(A_0 - g_0R^{-1}g_0^T\widehat{T_0}) + (A_0^T - \widehat{T_0}g_0R^{-1}g_0^T)\right] < 0$

(2.38) will lead to

$$\begin{aligned} \|\widehat{T_1}\| &\leq \varepsilon_1 C\|\widehat{T_0}A + A^T\widehat{T_0} - \widehat{T_0}g_0R^{-1}g^T\widehat{T_0} - \widehat{T_0}gR^{-1}g_0^T\widehat{T_0}\| \\ &\leq \varepsilon_1 C\left(\|A\| + \|A^T\| + 2\|\widehat{T_0}\|\|R^{-1}\|\|g_0\|\|g\|\right)\|\widehat{T_0}\| \end{aligned} \tag{2.40}$$

With lemma 6, we know that $A(x)$ and $g(x)$ are bounded within the compact set Ω. With lemma 1, we also can also conclude that $\|\widehat{T_0}\|$ is bounded within a time interval $[0, t_f]$. Now, we suppose the item $(\|\widehat{T_0}\|\|R^{-1}\|\|g_0\|\|g\|)$ can pick the largest value when $\|\widehat{T_0}\|$ and $\|g\|$ can get the maximum value over the compact set.

Define

$$C_A = Sup_{x\in\Omega}\left[\|A\| + \|A^T\|\right] \tag{2.41}$$

$$C_{g1} = Sup_{x\in\Omega}\left[\|R^{-1}\|\|g_0\|\|g\|\right] \tag{2.42}$$

$$C_{t0} = \max_{t\in[0,t_f]}(\|\widehat{T}_0\|) \tag{2.43}$$

Thus, (2.40) becomes:

$$\|\widehat{T}_1\| \leq \varepsilon_1 C\big(C_A + 2C_{t0}C_{g1}\big)\|\widehat{T}_0\| \tag{2.44}$$

Therefore, by choosing enough small ε_1, we can make

$$\varepsilon_1 C\big(C_A + 2C_{t0}C_{g1}\big) \leq q < 1 \tag{2.45}$$

where q is a constant scalar number within interval $(0, 1)$.

Then,

$$\|\widehat{T}_1\| \leq q\|\widehat{T}_0\| \tag{2.46}$$

Step Two: let us consider (2.32).

Following the logic of the previous step, we can get

$$\begin{aligned}\|\widehat{T}_2\| \leq \varepsilon_2 C\|&\widehat{T}_1 A + A^T\widehat{T}_1 - \widehat{T}_0 g_0 R^{-1} g^T\widehat{T}_1 - \widehat{T}_0 g R^{-1} g_0^T\widehat{T}_1 - \widehat{T}_0 g R^{-1} g^T\widehat{T}_0 \\ &- \widehat{T}_1 g_0 R^{-1} g_0^T\widehat{T}_1 - \widehat{T}_1 g_0 R^{-1} g^T\widehat{T}_0 - \widehat{T}_1 g R^{-1} g_0^T\widehat{T}_0\|\end{aligned} \tag{2.47}$$

Define

$$C_{g2} = Sup_{x\in\Omega}\left[\|R^{-1}\|\|g\|\|g\|\right] \tag{2.48}$$

$$C_{g_0} = \|R^{-1}\|\|g_0\|\|g_0\| \tag{2.49}$$

Thus, (2.47) becomes

$$\begin{aligned}\|\widehat{T}_2\| &\leq \varepsilon_2 C\left[\big(C_A + 4C_{t0}C_{g1} + qC_{g0}\big)\|\widehat{T}_1\| + C_{g2}C_{t0}\|\widehat{T}_0\|\right] \\ &\leq \varepsilon_2 C\left[\big(C_A + 4C_{t0}C_{g1} + qC_{g0}\big)q + C_{g2}C_{t0}\right]\|\widehat{T}_0\|\end{aligned} \tag{2.50}$$

We can choose a sufficiently small ε_2 to make

$$\varepsilon_2 C\left[\left(C_A + 4C_{t0}C_{g1} + qC_{g0}\right)q + C_{g2}C_{t0}\right] \leq q^2 < 1 \tag{2.51}$$

Thus, we can get

$$\|\widehat{T}_2\| \leq q^2\|\widehat{T}_0\| \tag{2.52}$$

Step Three: Suppose we can select the parameters $\varepsilon_3, \cdots, \varepsilon_{n-1}$ to make $\|\widehat{T}_3\| \leq q^3\|\widehat{T}_0\|$, $\cdots$, $\|\widehat{T}_{n-1}\| \leq q^{n-1}\|\widehat{T}_0\|$ valid. Let us consider (2.33)

$$\begin{aligned}
\|\widehat{T}_n\| \leq{}& \varepsilon_n C\Bigg(\left\|\widehat{T}_{n-1}A + A^T\widehat{T}_{n-1}\right\| + \left\|\sum_{j=0}^{n-2}\widehat{T}_j g R^{-1} g^T \widehat{T}_{n-2-j}\right\| \\
&\left\|\sum_{j=0}^{n-1}\widehat{T}_j\left(g_0 R^{-1} g^T + g R^{-1} g_0^T\right)\widehat{T}_{n-1-j}\right\| + \left\|\sum_{j=1}^{n-1}\widehat{T}_j g_0 R^{-1} g_0^T \widehat{T}_{n-j}\right\|\Bigg) \\
&\leq \varepsilon_n C\Bigg(C_A\|\widehat{T}_{n-1}\| + C_{g2}\sum_{j=0}^{n-2}\|\widehat{T}_j\|\|\widehat{T}_{n-2-j}\| + 2C_{g1}\sum_{j=1}^{n-1}\|\widehat{T}_j\|\|\widehat{T}_{n-1-j}\| \\
&+ C_{g0}\sum_{j=1}^{n-1}\|\widehat{T}_j\|\|\widehat{T}_{n-j}\|\Bigg) \\
&\leq \varepsilon_n C\Bigg(C_A q^{n-1} + (1/2)n(n-1)q^{n-2}C_{g2}C_{t0} + n(n-1)C_{g1}C_{t0}q^{n-1} \\
&+ (1/2)n(n-1)C_{g0}C_{t0}q^n\Bigg)\|\widehat{T}_0\| \\
&\leq \varepsilon_n C\Bigg(C_A q^{-1} + (1/2)n(n-1)C_{g2}C_{t0}q^{-2} + n(n-1)C_{g1}C_{t0}q^{-1} \\
&+ (1/2)n(n-1)C_{g0}C_{t0}\Bigg)q^n\|\widehat{T}_0\|
\end{aligned} \tag{2.53}$$

From (2.53), we can find that it is reasonable to manipulate ε_n to make

$$\varepsilon_n C\left(C_A q^{-1} + (1/2)n(n-1)C_{g2}C_{t0}q^{-2} + n(n-1)C_{g1}C_{t0}q^{-1} + (1/2)n(n-1)C_{g0}C_{t0}\right) < 1$$

Thus, we can get

$$\|\widehat{T}_n\| \leq q^n \|\widehat{T}_0\| \tag{2.54}$$

Thus, from the above analysis, we can realize that

$$\sum_{i=0}^{n} \|\widehat{T}_i\| \leq (1 + q + q^2 + \cdots + q^n)\|\widehat{T}_0\| \tag{2.55}$$

We can see that when n approaches to infinity, the RHS of (2.55) is a convergent geometric series, since $0 < q < 1$.

Thus, we can conclude that $\sum_{i=0}^{\infty} \widehat{T}_i$ is a convergent series, which implies that $\sum_{i=0}^{\infty} T_i\theta^i$ is convergent.

2.3.3. Positive Definite Analysis. Now, we have already proven that $\sum_{i=0}^{\infty} T_i\theta^i$ is convergent. Since our goal is stability analysis, we have to show that $\sum_{i=0}^{\infty} T_i\theta^i$ is positive definite. With (N2), we just need to show that $T_s = \sum_{i=0}^{\infty} \widehat{T}_i$ is positive definite.

Proof:

The first step is to rewrite equation (2.30) as the form of equation (2.31). The idea is to add $-\widehat{T}_0 g_0 R^{-1} g_0^T \widehat{T}_0$ to the both sides of the equation (2.30).

After that operation, the equation (2.33) can be changed to (2.56). Since $(A_0 - g_0 R^{-1} g_0^T \widehat{T}_0)$ is stable, and $\widehat{T}_0$ is semi-positive definite, then the RHS of (2.56) is equally semi-negative definite.

$$\begin{aligned}
&\widehat{T}_0 A_0 + A_0^T \widehat{T}_0 - \widehat{T}_0 g_0 R^{-1} g_0^T \widehat{T}_0 + Q = -\dot{\widehat{T}}_0 \\
\Longrightarrow\ &\widehat{T}_0 A_0 + A_0^T \widehat{T}_0 - \widehat{T}_0 g_0 R^{-1} g_0^T \widehat{T}_0 - \widehat{T}_0 g_0 R^{-1} g_0^T \widehat{T}_0 \\
&= -Q - \dot{\widehat{T}}_0 - \widehat{T}_0 g_0 R^{-1} g_0^T \widehat{T}_0 \\
\Longrightarrow\ &\widehat{T}_0 (A_0 - g_0 R^{-1} g_0^T \widehat{T}_0) + (A_0^T - \widehat{T}_0 g_0 R^{-1} g_0^T)\widehat{T}_0 \\
&= -Q - \dot{\widehat{T}}_0 - \widehat{T}_0 g_0 R^{-1} g_0^T \widehat{T}_0
\end{aligned} \tag{2.56}$$

Now, we can add (2.56), (2.31), (2.32), (2.33) together when $n \to \infty$; then, one can obtain

$$
\begin{aligned}
&T_s(A_0 - g_0R^{-1}g_0^T\widehat{T}_0) + (A_0^T - \widehat{T}_0g_0R^{-1}g_0^T)T_s \\
&= [-Q - \dot{\widehat{T}}_0 - \widehat{T}_0g_0R^{-1}g_0^T\widehat{T}_0] - \sum_{k=1}^{\infty}\varepsilon_k[\widehat{T}_{k-1}A + A^T\widehat{T}_{k-1}] \\
&+ \sum_{k=2}^{\infty}\varepsilon_k(\sum_{j=0}^{k-2}\widehat{T}_jgR^{-1}g^T\widehat{T}_{k-2-j}) + \sum_{k=1}^{\infty}\varepsilon_k(\sum_{j=0}^{k-1}\widehat{T}_j\big(g_0R^{-1}g^T + gR^{-1}g_0^T\big)\widehat{T}_{k-1-j}) \\
&+ \sum_{k=2}^{\infty}\varepsilon_k(\sum_{j=1}^{k-1}\widehat{T}_jg_0R^{-1}g_0^T\widehat{T}_{k-j})
\end{aligned} \tag{2.57}
$$

In order to justify that $\sum_{i=0}^{\infty}\widehat{T}_i$ is positive-definite, we just need to show that the RHS of (2.57) is negative definite since $(A_0 - g_0R^{-1}g_0^T\widehat{T}_0)$ is stable.

Equivalently, with (2.56), one can show that the following expression is positive definite:

$$
\begin{aligned}
&x^T\Bigg[-\Big(\widehat{T}_0(A_0 - g_0R^{-1}g_0^T\widehat{T}_0) + (A_0^T - \widehat{T}_0g_0R^{-1}g_0^T)\widehat{T}_0\Big) + \sum_{k=1}^{\infty}\varepsilon_k[\widehat{T}_{k-1}A + A^T\widehat{T}_{k-1}] \\
&- \sum_{k=2}^{\infty}\varepsilon_k(\sum_{j=0}^{k-2}\widehat{T}_jgR^{-1}g^T\widehat{T}_{k-2-j}) - \sum_{k=1}^{\infty}\varepsilon_k(\sum_{j=0}^{k-1}\widehat{T}_j\big(g_0R^{-1}g^T + gR^{-1}g_0^T\big)\widehat{T}_{k-1-j}) \\
&- \sum_{k=2}^{\infty}\varepsilon_k(\sum_{j=1}^{k-1}\widehat{T}_jg_0R^{-1}g_0^T\widehat{T}_{k-j})\Bigg]x > 0
\end{aligned} \tag{2.58}
$$

Define several symbols to represent the items of (2.58), to simplify the deviation

$$t_1 = x^T\Big(-\widehat{T}_0(A_0 - g_0R^{-1}g_0^T\widehat{T}_0) - (A_0^T - \widehat{T}_0g_0R^{-1}g_0^T)\widehat{T}_0\Big)x \tag{2.59}$$

$$t_2 = x^T\Big(\sum_{k=1}^{\infty}\varepsilon_k[\widehat{T}_{k-1}A + A^T\widehat{T}_{k-1}]\Big)x \tag{2.60}$$

$$t_3 = x^T\Big(\sum_{k=2}^{\infty}\varepsilon_k(\sum_{j=0}^{k-2}\widehat{T}_jgR^{-1}g^T\widehat{T}_{k-2-j})\Big)x \tag{2.61}$$

$$t_4 = x^T\left(\sum_{k=1}^{\infty} \varepsilon_k (\sum_{j=0}^{k-1} \widehat{T}_j \left(g_0 R^{-1} g^T + g R^{-1} g_0^T\right) \widehat{T}_{k-1-j})\right)x \tag{2.62}$$

$$t_5 = x^T\left(\sum_{k=2}^{\infty} \varepsilon_k (\sum_{j=1}^{k-1} \widehat{T}_j g_0 R^{-1} g_0^T \widehat{T}_{k-j})\right)x \tag{2.63}$$

The first item can be expressed as

$$\begin{aligned} t_1 =& x^T\left(- \widehat{T}_0(A_0 - g_0 R^{-1} g_0^T \widehat{T}_0) - (A_0^T - \widehat{T}_0 g_0 R^{-1} g_0^T)\widehat{T}_0\right)x \\ \geq& C_{\lambda_1} \|x\|^2 \end{aligned} \tag{2.64}$$

where $C_{\lambda_1} = \lambda_{min}\left(- \widehat{T}_0(A_0 - g_0 R^{-1} g_0^T \widehat{T}_0) - (A_0^T - \widehat{T}_0 g_0 R^{-1} g_0^T)\widehat{T}_0\right) > 0$. Since $\widehat{T}_0$ is bounded within $[0, t_f]$, and other A_0, g_0, R are constant, then minimal eigenvalue exists within $[0, t_f]$. For the T_2 term,

$$t_2 = x^T\left(\sum_{k=1}^{\infty} \varepsilon_k [\widehat{T}_{k-1} A + A^T \widehat{T}_{k-1}]\right)x \geq x^T\left(\varepsilon_m \sum_{k=1}^{\infty} \widehat{T}_{k-1}[A + A^T]\right)x \tag{2.65}$$

where if $t_2 > 0$, then $\varepsilon_m = min(\varepsilon_i, i = 1, \cdots, \infty)$ within $[0, t_f]$; if $t_2 < 0$, then $\varepsilon_m = max(\varepsilon_i, i = 1, \cdots, \infty)$ within $[0, t_f]$.

Since $A(x)$ is continuous on the compact set Ω, and T_s is also a continuous function of x on Ω, then they are bounded on the compact set Ω (lemma 3, lemma 4).

$$t_2 \geq \varepsilon_m x^T\left(T_s[A + A^T]\right)x \geq \varepsilon_m C_{\lambda_2} \|x\|^2 \tag{2.66}$$

where $C_{\lambda_2} = \lambda_{min}\left(T_s[A + A^T]\right)$.

Note that lemma 7 guarantees the above minimal eigenvalue C_{λ_2} exists over the compact set Ω.

Now, let us consider the third term t_3

$$\begin{aligned} t_3 =& x^T \left(\sum_{k=2}^{\infty} \varepsilon_k \left(\sum_{j=0}^{k-2} \widehat{T}_j g R^{-1} g^T \widehat{T}_{k-2-j} \right) \right) x \\ \leq& \|x\|^2 \sum_{k=2}^{\infty} \varepsilon_k \sum_{j=0}^{\infty} \|\widehat{T}_j\| \|g R^{-1} g^T\| \sum_{j=0}^{\infty} \|\widehat{T}_{k-2-j}\| \\ \leq& \|x\|^2 \sum_{k=2}^{\infty} \varepsilon_k \sum_{j=0}^{\infty} \|\widehat{T}_j\| \|g R^{-1} g^T\| \sum_{j=0}^{\infty} \|\widehat{T}_j\| \end{aligned} \tag{2.67}$$

Since $\sum_{j=0}^{\infty} \|\widehat{T}_j\|$ is a convergent series and equation of (2.48), we assume that $C_{\lambda_3} = \sum_{j=0}^{\infty} \|\widehat{T}_j\| \|g R^{-1} g^T\| \sum_{j=0}^{\infty} \|\widehat{T}_j\|$. Then, we can get $t_3 \leq \sum_{k=2}^{\infty} \varepsilon_k C_{\lambda_3} \|x\|^2$.

Since $(0 \leq \varepsilon_k < 1, k = 1, \cdots, \infty)$ are user-defined parameters, we can always choose a small enough ε_k such that $\sum_{k=2}^{\infty} \varepsilon_k$ is a convergent series. Assume that $\varepsilon_c = \sum_{k=1}^{\infty} \varepsilon_k$, and one will get

$$t_3 \leq \sum_{k=2}^{\infty} \varepsilon_k C_{\lambda_3} \|x\|^2 \leq \varepsilon_c C_{\lambda_3} \|x\|^2 \tag{2.68}$$

With the same logic to handle term t_3, we can analyze term t_4 and t_5 by defining

$$C_{\lambda_4} = \sum_{j=0}^{\infty} \|\widehat{T}_j\| \|g_0 R^{-1} g^T + g R^{-1} g_0^T\| \sum_{j=0}^{\infty} \|\widehat{T}_j\| \tag{2.69}$$

$$C_{\lambda_5} = \sum_{j=0}^{\infty} \|\widehat{T}_j\| \|g_0 R^{-1} g_0^T\| \sum_{j=0}^{\infty} \|\widehat{T}_j\| \tag{2.70}$$

Then, one can get

$$t_4 \leq \varepsilon_c C_{\lambda_4} \|x\|^2 \tag{2.71}$$

$$t_5 \leq \varepsilon_c C_{\lambda_5} \|x\|^2 \tag{2.72}$$

Combining (2.58),(2.64),(2.66),(2.68),(2.71),(2.72), then we get

$$
\begin{aligned}
& x^T\Bigg[-\Big(\widehat{T}_0(A_0-g_0R^{-1}g_0^T\widehat{T}_0)+(A_0^T-\widehat{T}_0g_0R^{-1}g_0^T)\widehat{T}_0\Big) \\
& +\sum_{k=1}^{\infty}\varepsilon_k[\widehat{T}_{k-1}A+A^T\widehat{T}_{k-1}]-\sum_{k=2}^{\infty}\varepsilon_k(\sum_{j=0}^{k-2}\widehat{T}_jgR^{-1}g^T\widehat{T}_{k-2-j}) \\
& -\sum_{k=1}^{\infty}\varepsilon_k(\sum_{j=0}^{k-1}\widehat{T}_j\big(g_0R^{-1}g^T+gR^{-1}g_0^T\big)\widehat{T}_{k-1-j})-\sum_{k=2}^{\infty}\varepsilon_k(\sum_{j=1}^{k-1}\widehat{T}_jg_0R^{-1}g_0^T\widehat{T}_{k-j})\Bigg]x \\
& \geq \|x\|^2(C_{\lambda_1}+\varepsilon_mC_{\lambda_2}-\varepsilon_cC_{\lambda_3}-\varepsilon_cC_{\lambda_4}-\varepsilon_cC_{\lambda_5})
\end{aligned}
\tag{2.73}
$$

Thus, by choosing proper ε_m and ε_c, the right-hand side of the inequality of (2.73) can be made positive definite, and, equivalently, the right hand side of (2.57) is negative definite. Therefore, $T_s=\sum_{i=0}^{\infty}\widehat{T}_i$ or $\sum_{i=0}^{\infty}T_i\theta^i$ is positive definite.

2.3.4. Stability Analysis. Let us choose a Lyapunov candidate function

$$
L=\frac{1}{2}x^T\sum_{i=0}^{\infty}\widehat{T}_ix \tag{2.74}
$$

Taking the derivative with respect to time, both sides of (2.74) become

$$
\frac{dL}{dt}=x^T\sum_{i=0}^{\infty}\widehat{T}_i\dot{x}+\frac{1}{2}x^T\left[\frac{d\widehat{T}_0}{dt}+\sum_{i=1}^{\infty}(I_n\otimes\dot{x}^T)\frac{\partial\widehat{T}_i}{\partial x}\right]x \tag{2.75}
$$

Since $V_x=\sum_{i=0}^{\infty}\widehat{T}_ix$, and $V_t=\frac{1}{2}x^T\dot{T}_0x$ (2.17) satisfies the HJB equation

$$
V_t+V_x^T(f(x)+B(x)u)+\frac{1}{2}u^TRu+\frac{1}{2}x^T\big(Q+\sum_{i=1}^{\infty}D_i\theta^i\big)x=0 \tag{2.76}
$$

The above equation can be rearranged as

$$
\begin{aligned}
x^T\sum_{i=0}^{\infty}\widehat{T}_i(f(x)+B(x)u) &= -V_t-\frac{1}{2}u^TRu-\frac{1}{2}x^T\big(Q+\sum_{i=1}^{\infty}D_i\theta^i\big)x \\
&= -\frac{1}{2}x^T\dot{T}_0x-\frac{1}{2}u^TRu-\frac{1}{2}x^T\big(Q+\sum_{i=1}^{\infty}D_i\theta^i\big)x
\end{aligned}
\tag{2.77}
$$

Substituting (2.77) into (2.75), and with $u = -R^{-1}B^T \sum_{i=0}^{\infty} \widehat{T}_i x$

$$\begin{aligned}
\frac{dL}{dt} &= -\frac{1}{2}x^T \dot{T}_0 x - \frac{1}{2}u^T R u - \frac{1}{2}x^T \big(Q + \sum_{i=1}^{\infty} D_i \theta^i\big)x \\
&\quad + \frac{1}{2}x^T \left[\frac{d\widehat{T}_0}{dt} + \sum_{i=1}^{\infty}(I_n \otimes \dot{x}^T)\frac{\partial \widehat{T}_i}{\partial x}\right]x \\
&= -\frac{1}{2}u^T R u - \frac{1}{2}x^T \big(Q + \sum_{i=1}^{\infty} D_i \theta^i\big)x + \frac{1}{2}x^T \left(\sum_{i=1}^{\infty}(I_n \otimes \dot{x}^T)\frac{\partial \widehat{T}_i}{\partial x}\right)x \\
&= -\frac{1}{2}x^T \left(Q + \sum_{i=1}^{\infty} D_i \theta^i + \sum_{i=0}^{\infty} \widehat{T}_i B R^{-1} B^T \sum_{i=0}^{\infty} \widehat{T}_i\right)x \\
&\quad + \frac{1}{2}x^T \left(\sum_{i=1}^{\infty}(I_n \otimes \dot{x}^T)\frac{\partial \widehat{T}_i}{\partial x}\right)x
\end{aligned} \tag{2.78}$$

From (2.6), we know that $Q + \sum_{i=1}^{\infty} D_i \theta^i$ is semi-positive definite. Because the whole expression $\left(Q + \sum_{i=1}^{\infty} D_i \theta^i + \sum_{i=0}^{\infty} \widehat{T}_i B R^{-1} B^T \sum_{i=0}^{\infty} \widehat{T}_i\right)$ is simple addition and multiplication operation, then the result of it is the function of x and also continuous, based on lemma 2. With lemma 7, we can conclude that

$$-\frac{1}{2}x^T \left(Q + \sum_{i=1}^{\infty} D_i \theta^i + \sum_{i=0}^{\infty} \widehat{T}_i B R^{-1} B^T \sum_{i=0}^{\infty} \widehat{T}_i\right)x \leq -\frac{1}{2}C_\lambda \|x\|^2 \tag{2.79}$$

where $C_\lambda = \lambda_{min}\left(Q + \sum_{i=1}^{\infty} D_i \theta^i + \sum_{i=0}^{\infty} \widehat{T}_i B R^{-1} B^T \sum_{i=0}^{\infty} \widehat{T}_i\right) > 0$.

The second term

$$\begin{aligned}
\frac{1}{2}x^T \left(\sum_{i=1}^{\infty}(I_n \otimes \dot{x}^T)\frac{\partial \widehat{T}_i}{\partial x}\right)x &\leq \frac{1}{2}\|x\|^2 \left(\sum_{i=1}^{\infty}\|I_n \otimes \dot{x}^T\|\|\frac{\partial \widehat{T}_i}{\partial x}\|\right) \\
&= \frac{1}{2}\|x\|^2 \left(\sum_{i=1}^{\infty}\|I_n \otimes (f(x) + B(x)u)^T\|\|\frac{\partial \widehat{T}_i}{\partial x}\|\right)
\end{aligned} \tag{2.80}$$

Let us observe the n^{th} recursive equation of $\widehat{T}_n$ (2.33). We know that (2.33) is regular form of linear Lyapunov equation. There exist a closed-form solution.

We can define

$$Q_n(x) = \Bigg[\widehat{T}_{n-1}A + A^T\widehat{T}_{n-1} - \sum_{j=0}^{n-2}\widehat{T}_j g R^{-1} g^T \widehat{T}_{n-2-j} \\ - \sum_{j=0}^{n-1}\widehat{T}_j\Big[g_0 R^{-1} g^T + g R^{-1} g_0^T\Big]\widehat{T}_{n-1-j} - \sum_{j=1}^{n-1}\widehat{T}_j g_0 R^{-1} g_0^T \widehat{T}_{n-j}\Bigg] \tag{2.81}$$

Then, (2.33) will become

$$\widehat{T}_n(A_0 - g_0 R^{-1} g_0^T \widehat{T}_0) + (A_0^T - \widehat{T}_0 g_0 R^{-1} g_0^T)\widehat{T}_n = -\varepsilon_n Q_n(x) \tag{2.82}$$

Thus,

$$Vec(\widehat{T}_n) = \varepsilon_n\Big(I \otimes (A_0 - g_0 R^{-1} g_0^T \widehat{T}_0) + (A_0^T - \widehat{T}_0 g_0 R^{-1} g_0^T) \otimes I\Big) Vec(Q_n(x)) \tag{2.83}$$

Then, we can realize that $\|\frac{\partial \widehat{T}_i}{\partial x}\|$ includes ε_i parameters. $(f + Bu)$ is also continuous function with x of the compact set Ω, which implies that it is bounded.

$$\begin{aligned} \frac{dL}{dt} &\leq -\frac{1}{2}C_\lambda\|x\|^2 + \frac{1}{2}\|x\|^2\Bigg(\sum_{i=1}^{\infty}\|I_n \otimes (f(x) + B(x)u)^T\|\|\frac{\partial \widehat{T}_i}{\partial x}\|\Bigg) \\ &\leq -\frac{1}{2}(1-\alpha)C_\lambda\|x\|^2 - \Bigg(\frac{1}{2}\alpha C_\lambda - \sum_{i=1}^{\infty}\|I_n \otimes (f(x) + B(x)u)^T\|\|\frac{\partial \widehat{T}_i}{\partial x}\|\Bigg)\|x\|^2 \end{aligned} \tag{2.84}$$

where $0 < \alpha < 1$. One can choose a sufficiently small ε_i included by term $\|\frac{\partial \widehat{T}_i}{\partial x}\|$ to ensure $\Bigg(\frac{1}{2}\alpha C_\lambda - \sum_{i=1}^{\infty}\|I_n \otimes (f(x) + B(x)u)^T\|\|\frac{\partial \widehat{T}_i}{\partial x}\|\Bigg)$ is non-negative. Therefore, $\frac{dL}{dt} < 0$.

2.4. NUMERICAL EXPERIMENT

The goal of this section is to show some properties of the proposed finite time $\theta - D$ algorithm with a two dimensional benchmark problem. The experiment will be carried out by the personal Laptop Thinkpad R480 with the CPU Intel(R) Core(TM) i3-7130U 2.70

GHZ and 16GB RAM. The first part will show the dynamic function and relative parameter selection. The scenario of without using D terms for relatively small initial conditions will be presented in second set. The third set will cover the analysis of T_i term selection. The final set is about the D term influence to the control when encountering large initial state values..

2.4.1. Nonlinear Dynamics and Penalty Matrices Selection. Finding a control $u = [u_1, u_2]^T$ to minimize the cost function:

$$J = \frac{1}{2}x(t_f)^T S_f x(t_f) + \frac{1}{2}\int_0^{t_f} (x^T Q x + u^T R u)dt \tag{2.85}$$

where $S_f = \begin{bmatrix} 5 & 0 \\ 0 & 5 \end{bmatrix}$; $Q = \begin{bmatrix} 1 & 0 \\ 0 & 1 \end{bmatrix}$; $R = \begin{bmatrix} 2 & 0 \\ 0 & 2 \end{bmatrix}$; $t_f = 4$ time unit.

with the dynamic function described by

$$\dot{x}_1 = x_1 - x_1^3 + x_2 + u_1 \tag{2.86}$$

$$\dot{x}_2 = x_1 + x_1^2 x_2 - x_2 + u_2 \tag{2.87}$$

We can factorize the $f(x)$ as $A_0 = \begin{bmatrix} 1 & 1 \\ 1 & -1 \end{bmatrix}$; $A = \begin{bmatrix} -x_1^2 & 0 \\ 0 & x_1^2 \end{bmatrix}$.

2.4.2. Case I: Relatively Small Initial Conditions and without using D Terms. In this case, we consider an arbitrarily small initial condition $[1, -1]$. The auxiliary parameter θ is set to 1 while the D terms are not adopted in this case. The finite time SDRE (FSDRE) technique Heydari and Balakrishnan (2015) is also employed as a comparison. Also, three T_i terms are used as usual. From Figure.2.1, we can observe the state history over the four seconds. After applying the control from the proposed method, we can get the almost the similar performance by the FSDRE technique. Both techniques can force

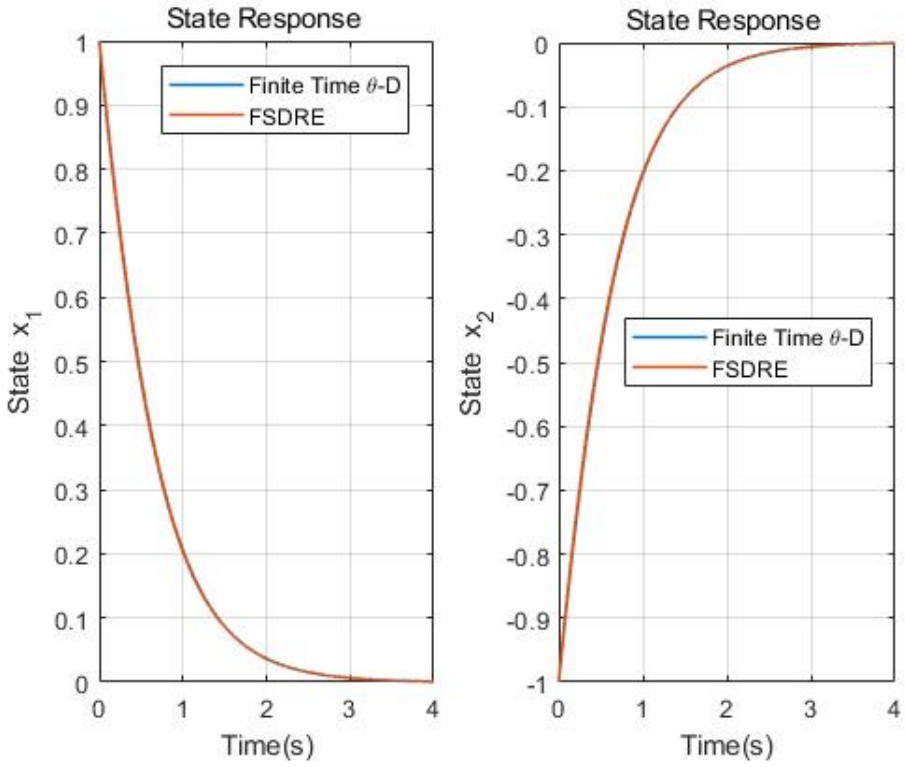

Figure 2.1. State Responses: x_0=[1,-1], without using D Term

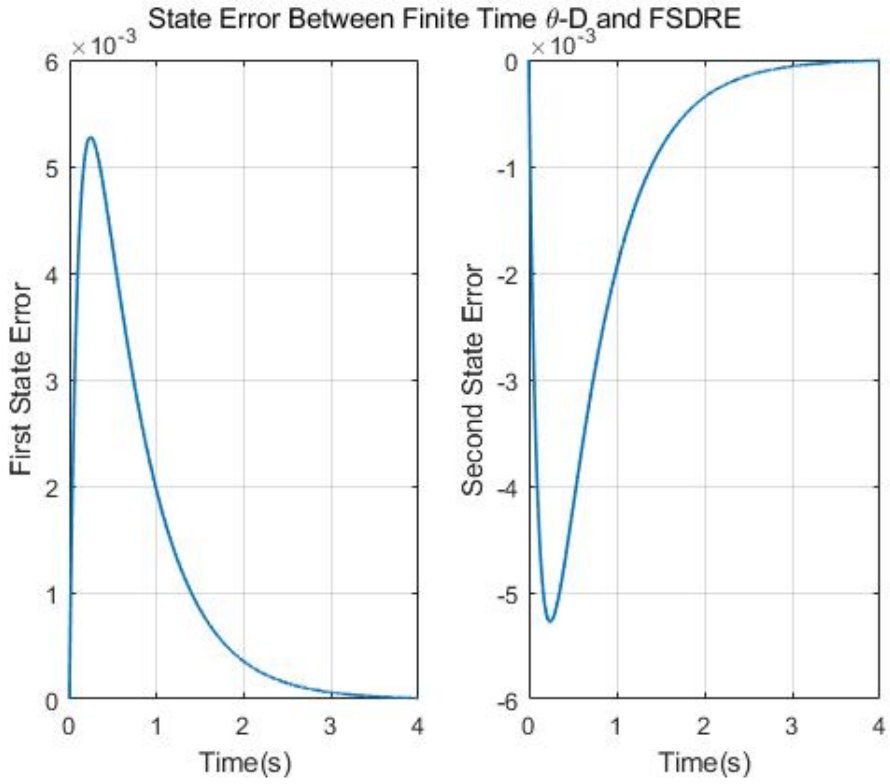

Figure 2.2. State Error Responses: x_0=[1,-1], without using D Term

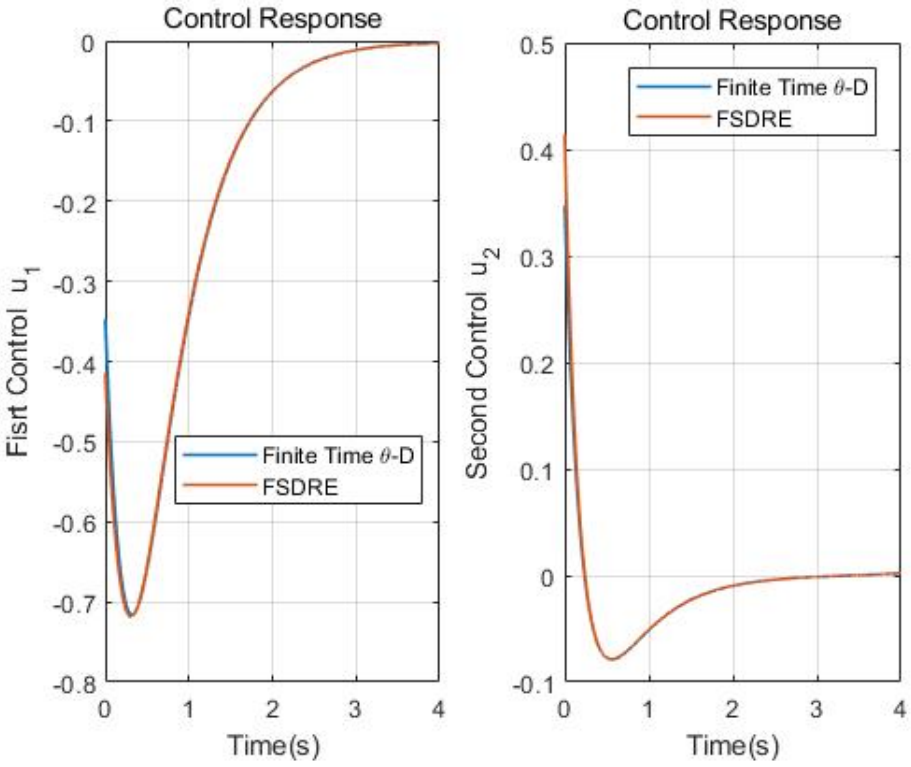

Figure 2.3. Control Responses: x_0=[1,-1], without using D Term

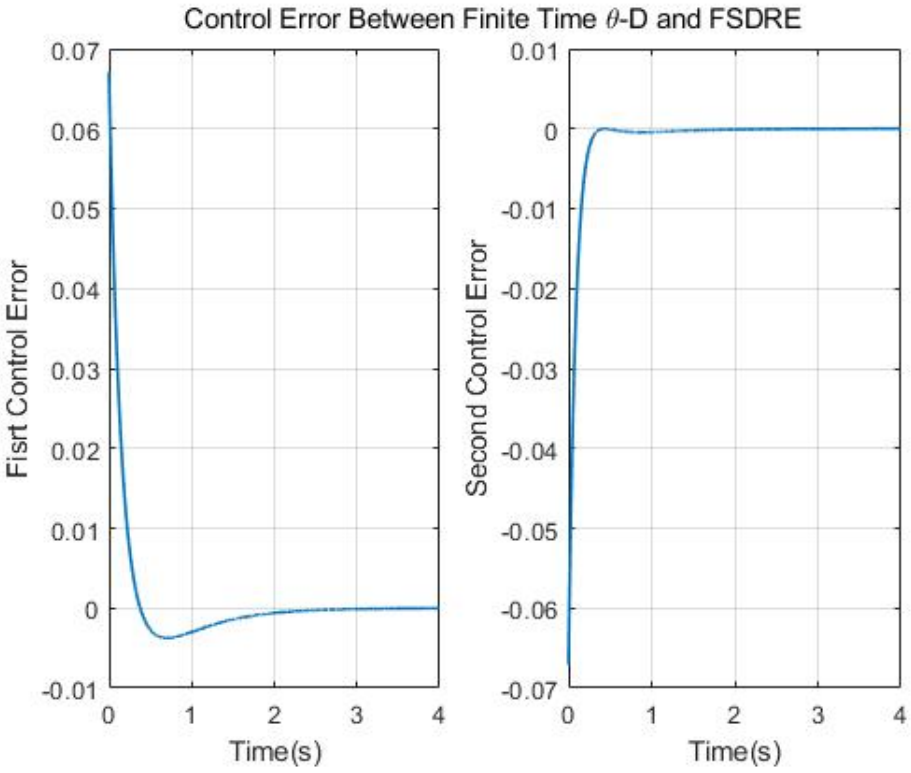

Figure 2.4. Control Error Responses: x_0=[1,-1], without using D Term

the states to arrive zero at the final time of 4 seconds. Since the state difference of those two methods can not easily identified, Figure.2.2 provides more detailed insight of the state error history. Notice that the maximum value of the difference are 5×10^{-3} of first state and -5×10^{-3} of second state, which can verify the **effectiveness** of the proposed method since it can achieve the almost same performance of FSDRE technique. For the FSDRE method, the overall run time is *8.751358 seconds* with the cost of 1.049×10^3 . However, the run time of the proposed method is only *1.638861 seconds* with the cost of 1.048×10^3. It is an attractive property that the run time of the proposed technique is one fourth of that of the FSDRE while both of them have comparable cost value, which can prove that the proposed method is **efficient** one and is ideally suitable for online implementation. In this case, three terms T_0, T_1 and T_2 are used to calculated the finite time $\theta - D$ control. The Figure.2.3 shows that the control history by three terms is good enough to approximate the control getting from the FSDRE. To get more detailed view of both controls, the history of control error is demonstrated in Figure.2.4. One can find that there exist a relatively large different at the beginning of 1 second. After that, there are almost no difference which implies that the tree terms are enough for the practical engineering problems.

2.4.3. Case II: T_i Terms Selection and without using D Terms. Practically, we take T_0, T_1 and T_1 to calculate the control in the finite time $\theta - D$ framework. This case will show how to influence the performance with more T_i terms selection. Similarly, we still consider initial condition of $[1, -1]$. The θ is set to 1 while the D terms are also not used in this case. The five T_i terms are employed in this case as a comparison with the three T_i terms. Figure.2.5 shows the state history with the FSDRE control, three T_i terms control and five T_i terms control. We can find that the overall trend is almost same with those three controls. But it is not clear to identify the details. When zoom in some part of the state history in Figure.2.6, we can observe that the states of five T_i term control will be more closer to states of FSDRE control than the states of three T_i term control. The same phenomenon can be found in the state error history of Figure.2.7. The control history in

Figure.2.8., control zoom in plot of Figure.2.9 and the control error history in Figure.2.10. also indicate that five T_i term finite time $\theta - D$ control is more closer to the control of FSDRE than three T_i term finite time $\theta - D$ control. Based on this simulation results, we can get a conclusion that more T_i terms will certainly generate better performance. But it will take more run time of *4.244108 seconds* than *1.638861 seconds* of three T_i terms calculation. So, the engineers can determinate how many T_i terms will be employed to calculate finite time $\theta - D$ control based on the the project performance requirement. The contribution of each T_i term to total finite time $\theta - D$ control are displayed in Figure.2.11 and Figure.2.12. One can observe that the fourth term and fifth term do less contribution to the final control since they are close to zero, which implies that the first term, second term and third term are denominating part for the total control. From practical perspective, we can save some computational resources with sacrificing some insignificant terms.

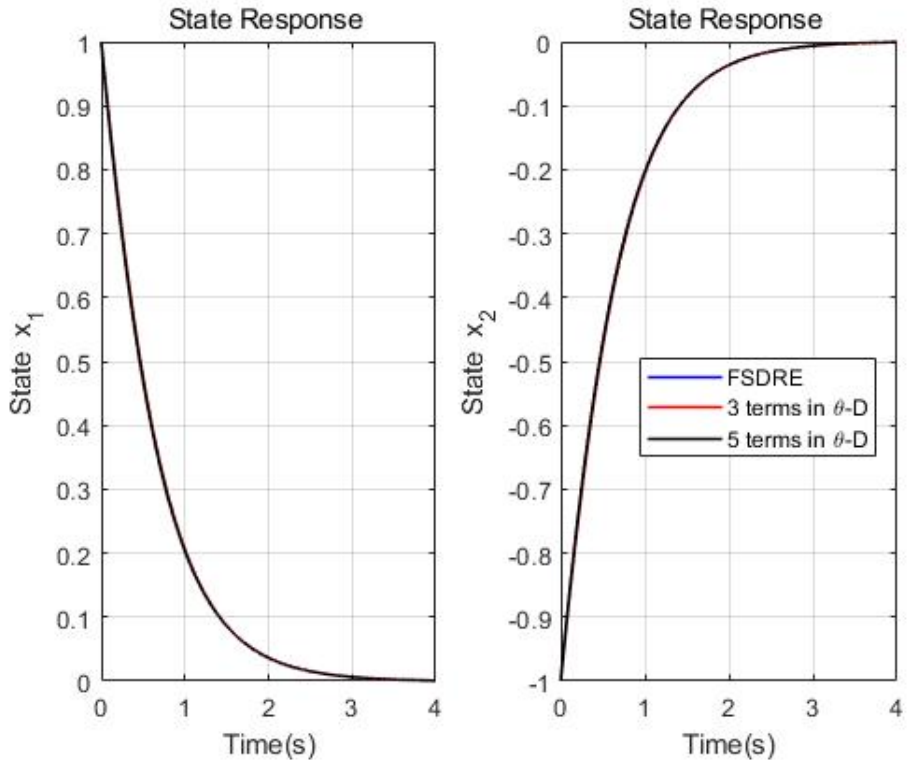

Figure 2.5. State Responses: x_0=[1,-1], without using D Term

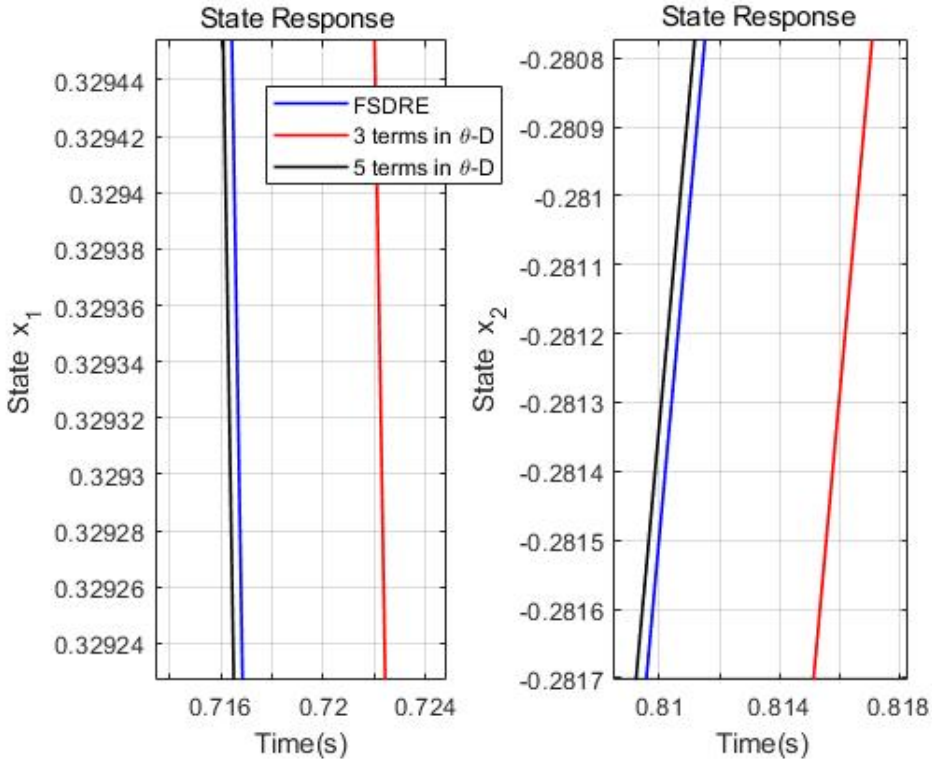

Figure 2.6. State Error Responses Zoom in: x_0=[1,-1], without using D Term

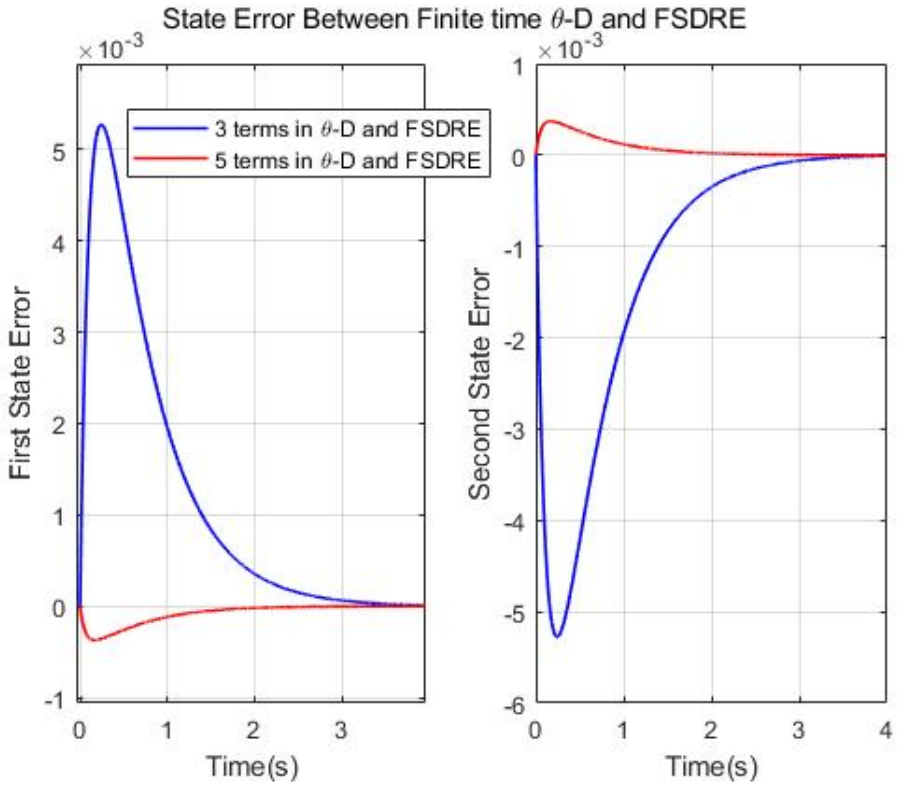

Figure 2.7. State Error Responses: x_0=[1,-1], without using D Term

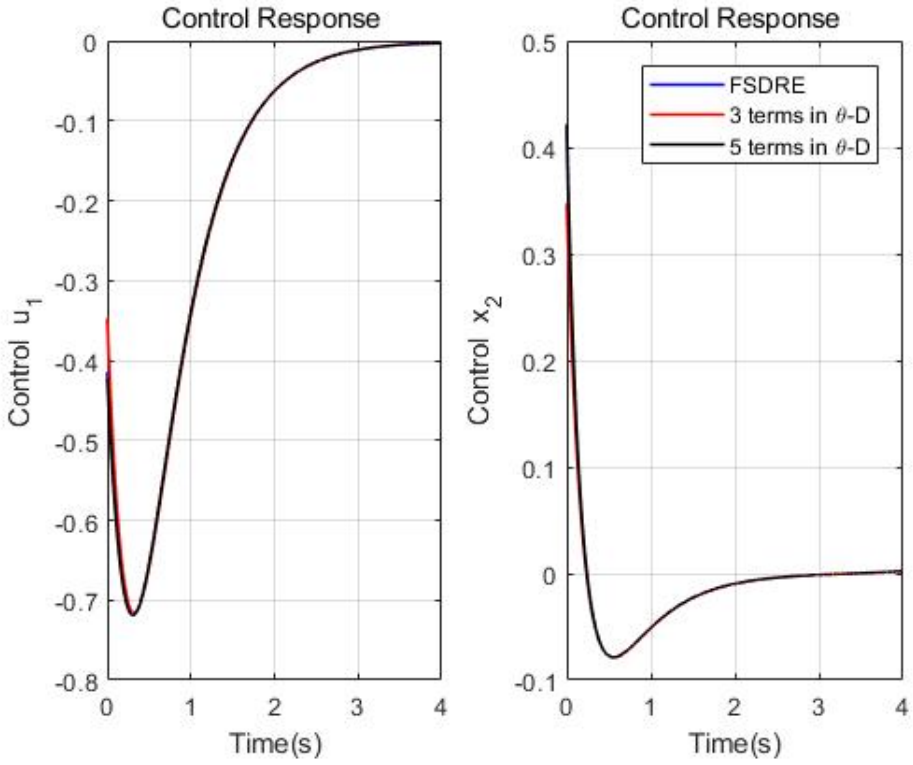

Figure 2.8. Control Responses: x_0=[1,-1], without using D Term

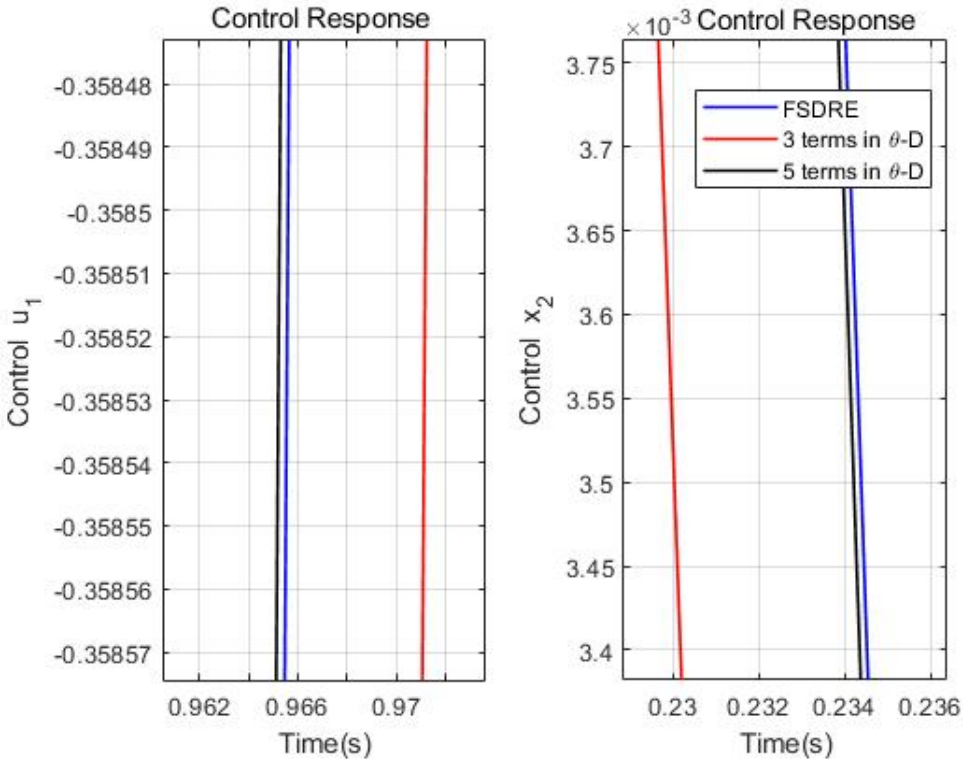

Figure 2.9. Control Responses Zoom in: x_0=[1,-1], without using D Term

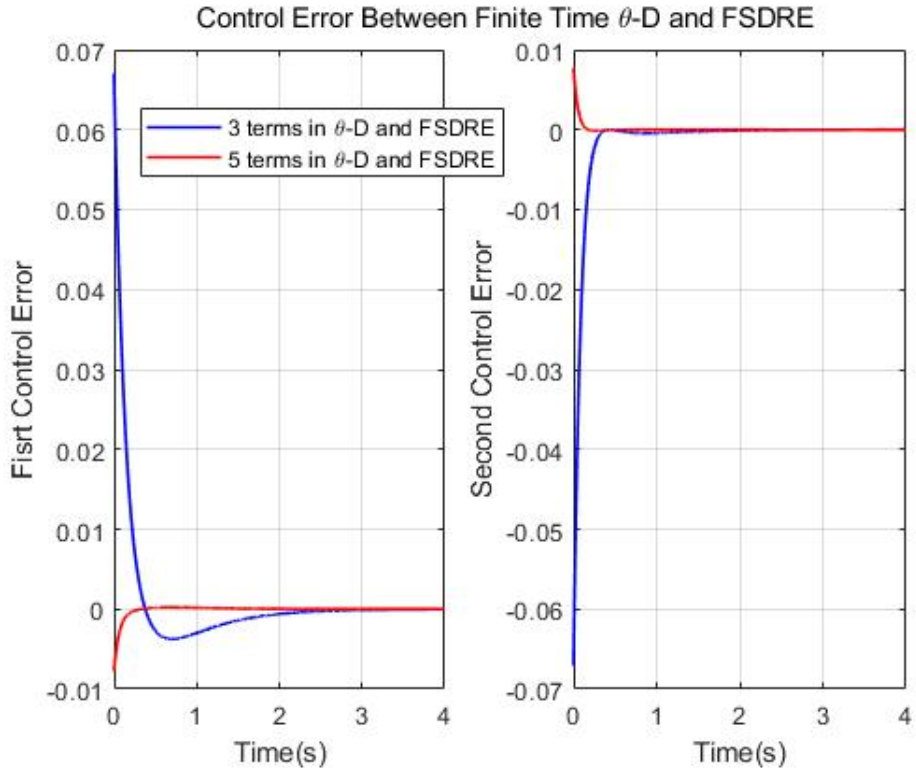

Figure 2.10. Control Error Responses : x_0=[1,-1], without using D Term

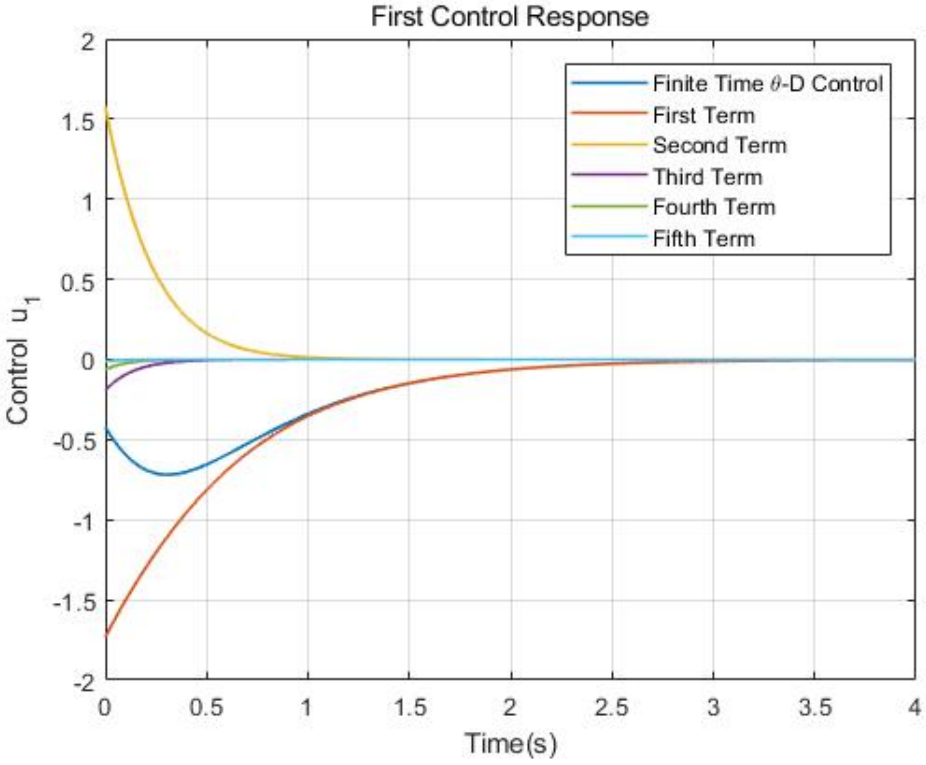

Figure 2.11. First Control Items Responses: x_0=[1,-1], without using D Term

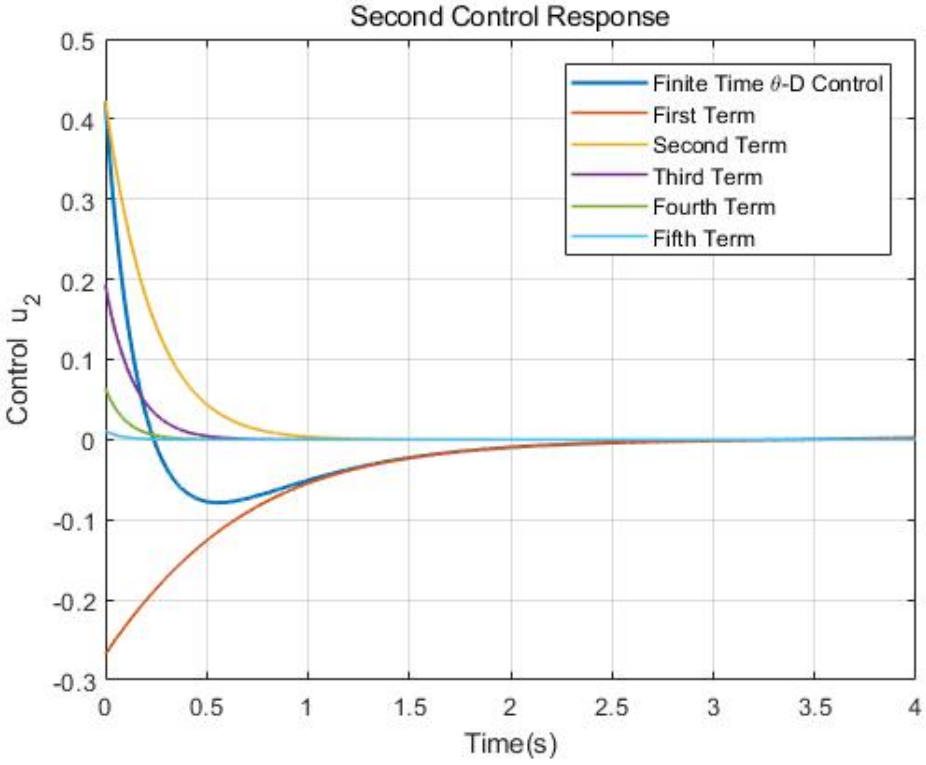

Figure 2.12. Second Control Items Responses: x_0=[1,-1], without using D Term

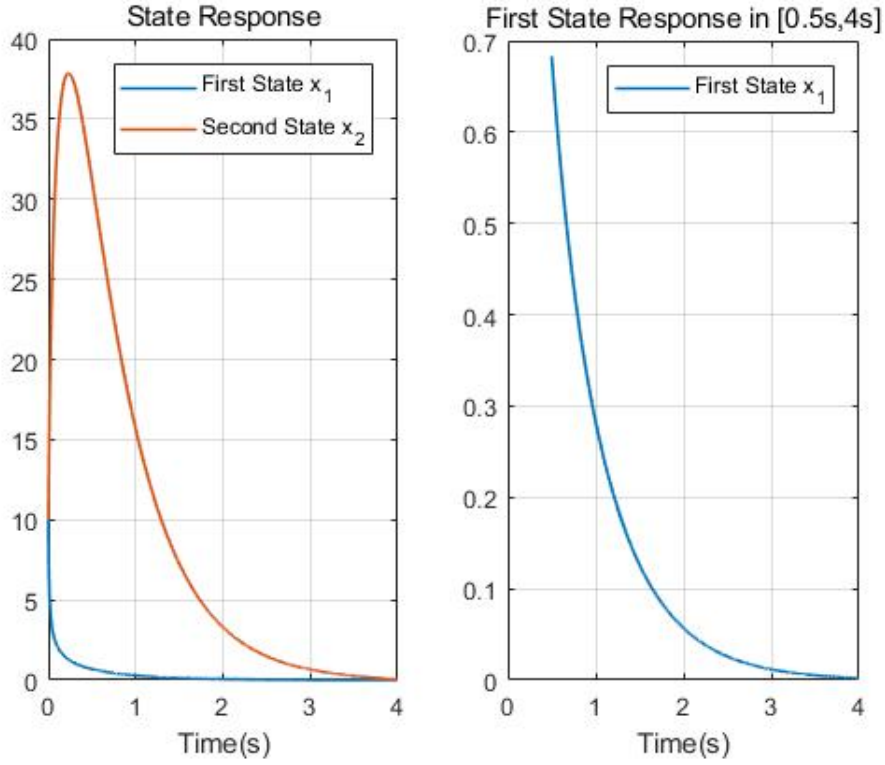

Figure 2.13. State Responses: x_0=[10,10], without using D Term

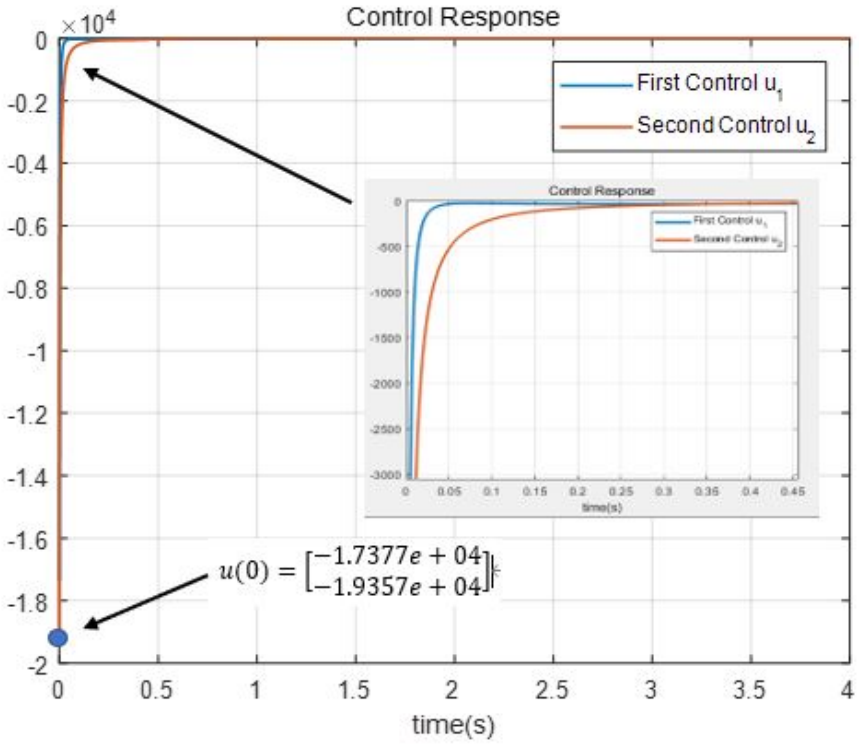

Figure 2.14. Control Responses: x_0=[10,10], without using D Term

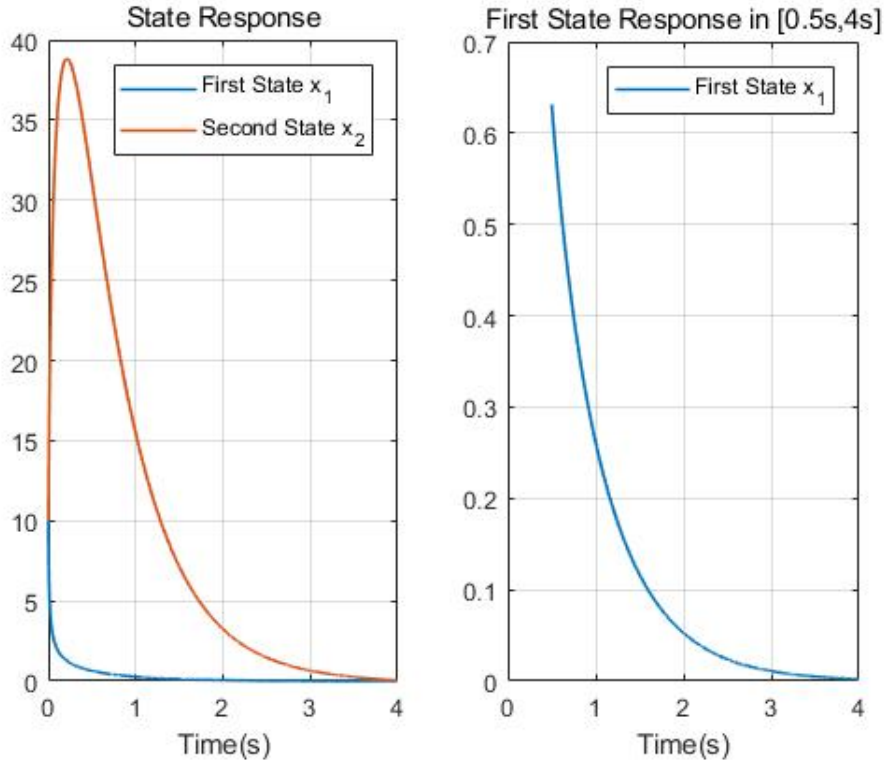

Figure 2.15. State Responses: x_0=[10,10], using D Term

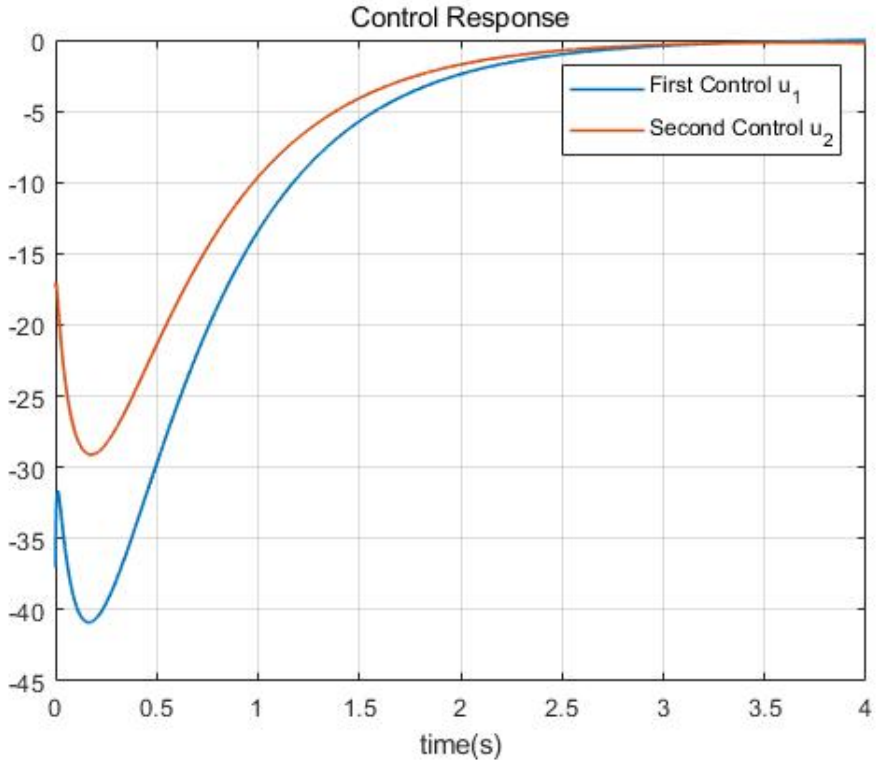

Figure 2.16. Control Responses: x_0=[10,10], using D Term

2.4.4. Case III: Adopting D Terms. The aforementioned analysis is employing the finite time $\theta - D$ algorithm without using the perturbation D term. In this case, D term will be employed to offset the large initial state challenge since actuators will generate lager control signal to large initial state. Due to this merit of D terms, the proposed method can protect the actuators in the practical applications. With the initial condition of $x_0 = [10, 10]^T$, the left plot of Figure.2.13 shows the states history without using the D terms. Certainly, three T_i terms are taken here. However, the second state history is not clear. The right plot of Figure.2.13 indicates the history of second state between $[0.5s, 4s]$.Both plots can verify that the proposed algorithm can drive the both states to zero at the final time of 4 seconds, which implies that the proposed method is working well with larger initial condition. Unfortunately, when we observe the control response, we can find that the actuator have to pay a great effort since the initial control is

$u(0) = [-1.7377e+04, -1.9357e+04]$. That is a huge control in magnitude which could jeopardize the actuators in engineering applications. It can be tackled when the D term will be involved in this algorithm. After employing the D term with, we can observe the Figure.2.15 and Figure.2.16. we can find that the state history is almost same. Attractively, from Figure.2.16, the control signal is greatly reduced as compared with Figure.2.14. Here, $k_i = 1 - \frac{1}{\|T_0 * A_0 + A_0' * T_0\|}$ and $l_i = 0.1$. Definitely, there are other selections based on the designers. The only principle to choose k_i and l_i is that the control will be insensitive to the initial states. To summarize that the D term can prevent the actuators from overloading in the real applications and can save money since control is always expensive.

3. PATH PLANNING FOR APPROACHING AND LANDING PHASE OF THE REUSABLE LAUNCH VEHICLE BY A NEW FINITE-HORIZON NEAR-OPTIMAL CONTROL DESIGN TECHNIQUE

The path planning for the approaching and landing (A&L) phase of Reusable Launch Vehicle (RLV) is re-formulated as a finite-horizon optimal control problem.The nonlinear dynamic equations are rewritten as a state-dependent pseudo-linear structure characterized with cost function of a linear quadratic regulator prototype and an intractable partial differential Hamiltonian-Jacobi-Bellman (HJB) equation. Motivated by finite time state-dependent Riccati equation (FSDRE) technique, a novel method, named finite-horizon $\theta - D$ near-optimal control design, is developed to address this challenge. Compared with the FSDRE approach, the proposed method presents a more simple closed-form solution, and it extremely reduces the online computation load, which makes the real-time implementation of this technique possible. Actually, any control algorithm working on the A&L phase of RLV must satisfy a rigid requirement such that the touchdown should occur at a fixed downrange with the sink rate (vertical velocity) near-zero and the flight path angle close to zero. Finally, the numerical simulation demonstrates that this novel control strategy offers a reliable performance, not only satisfying the strict requirement, but it also provides a certain robustness to the variant initial values.

3.1. DYNAMIC EQUATIONS OF RLV IN A&L PHASE AND PROBLEM FORMULATION

3.1.1. Mathematical Model. In this section, the dynamics of RLV in A&L phase Heydari and Balakrishnan (2011b) will be depicted (See Figure 3.1). This study is restricted the concern that the A&L phase occurs in a vertical plane and there does not exits the cross-range for the runway.

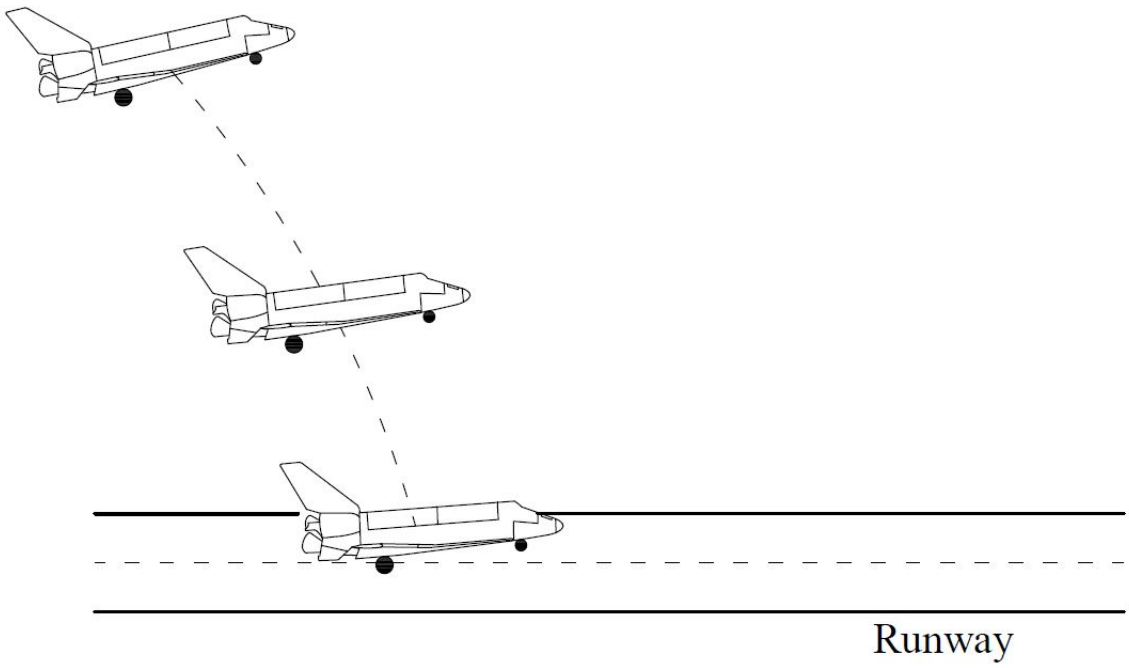

Figure 3.1. The Schematic Diagram of Landing Phase of RLV

$$\dot{v} = -\rho v^2 S_a C_D/(2 * m) - g * sin(\gamma) \tag{3.1}$$

$$\dot{\gamma} = \rho v^2 S_a C_L/(2 * m * v) - g * cos(\gamma)/v \tag{3.2}$$

$$\dot{h} = v * sin(\gamma) \tag{3.3}$$

$$\dot{X} = v * cos(\gamma) \tag{3.4}$$

where v is velocity of RLV (ft/sec), γ is flight path angle (deg), h is altitude (ft) , X is downrange (ft), ρ is air density ($slugs/ft^3$), S_a is aerodynamic reference area (ft^2). C_D is drag coefficient. C_L is lift coefficient, m is RLV mass ($slugs$), g is earth gravitational acceleration with the constant value of 32.174 ft/sec^2.

The parameters of air density ρ, lift coefficient C_L, and drag coefficient C_D can be calculated as follows Yedavalli (2020):

$$\rho = \rho_0 \exp(-h/H) \tag{3.5}$$

$$C_L = C_{L_0} * \alpha \tag{3.6}$$

$$C_D = C_{D_0} + K_I * C_L^2 \tag{3.7}$$

where ρ_0 is sea-level air density with a constant value of 0.0027 $slugs/ft^3$, H is scale height with a number of 27887.1 ft, C_{L_0} is zero angle of attack lift coefficient, α is angle of attack (deg), C_{D_0} is zero lift drag coefficient. K_I is lift-induced drag coefficient parameter. Note that (3.1)-(3.7) constitutes the dynamics of RLV in A&L phase with the state of $[v, \gamma, h, X]$ and control of α.It is important that if (3.6) is taken into (3.7), the control α will be changed to the square of α. The the dynamics of RLV in A&L phase is a control non-affine system which can not be addressed by the finite horizon $\theta - D$ technique. In order to employ the finite horizon $\theta - D$ technique, conversions must be made, that is, a new control variable u is introduced into the system as input equaling to the first derivative of α.

$$\dot{\alpha} = u \tag{3.8}$$

The state will be augmented to $[v, \gamma, h, X, \alpha]$ with new control u, which implies that the system is the control affine dynamics.

3.1.2. Finite Horizon Optimal Control Problem Formulation. The designed guidance controller can guide the RLV along a optimal trajectory with the final vertical velocity and flight path angle as small as possible with a given downrange location. Usually, the final vertical velocity is less than 9 ft/sec, and the flight path angle should be close to

zero deg when the RLV reach on the runway at the final time.Note that there is interest in the the optimal touchdown in a fixed downrange, not a fixed time in the practical engineering scenario. It is convenient for later analysis to convert the independent variable from time t to downrange X. When it is divided (3.1)-(3.3) and (3.8) by (3.4). Then the solution is

$$v' = \frac{\dot{v}}{\dot{X}} = \frac{dv}{dt} * \frac{dt}{dX} = \frac{dv}{dX} = \frac{-\rho v^2 S_a C_D/(2 * m) - g * sin(\gamma)}{v * cos(\gamma)} \tag{3.9}$$

With the same logic,

$$\gamma' = \frac{\dot{\gamma}}{\dot{X}} = \frac{d\gamma}{dX} = \frac{\rho v^2 S_a C_L/(2 * m * v) - g * cos(\gamma)/v}{v * cos(\gamma)} \tag{3.10}$$

$$h' = \frac{\dot{h}}{\dot{X}} = \frac{dh}{dX} = \tan\gamma \tag{3.11}$$

$$\alpha' = \frac{\dot{\alpha}}{\dot{X}} = \frac{d\alpha}{dX} = \frac{u}{v * cos(\gamma)} \tag{3.12}$$

The time variable will become an incidental variable, which is denoted as:

$$t' = \frac{dt}{dX} = \frac{1}{\dot{X}} = \frac{1}{v * cos(\gamma)} \tag{3.13}$$

When (3.9)-(3.13), the states is $x = [v, \gamma, h, t, \alpha]$ and control is u. New dynamics is used for the following design control.

The cost function is given as

$$J = \frac{1}{2} x^T(X_f) S_f x(X_f) + \frac{1}{2} \int_{X_0}^{X_f} \left(x^T Q x + u^T R u \right) dX \tag{3.14}$$

where $S_f \geq 0$ is final state weighted matrix, $Q \geq 0$ is state weighted matrix, $R > 0$ is control weighted matrix. X_f is denoted as a fixed downrange. The whole finite horizon optimal control problem setting is composed of (3.9)- (3.14).

3.2. NUMERICAL EXPERIMENT

3.2.1. State Dependent Coefficient $A(x)$ and $B(x)$. There is no general method to factorize $A(x)$ and $B(x)$ (refer to Çimen (2008) for more reading). In this research, the nonzero entries of matrix $A(x)$ and $B(x)$ are given as:

$$
\begin{aligned}
A(1,1) &= \frac{-\rho_0 \exp(-x_3/H) S_a (C_{D_0} + K_I C_{L_0}^2 x_5^2) - \rho S_a C_{D_0}}{4m * cos(x_2)} \\
A(1,2) &= \frac{-g * \tan(x_2)}{x_1 x_2} \\
A(1,3) &= \frac{-\rho_0 S_a C_{D_0} x_1 \exp(-x_3/H)}{4m x_3 * cos(x_2)} + \frac{\rho_0 S_a C_{D_0} x_1}{4m x_3 * cos(x_2)} \\
A(1,5) &= \frac{-\rho_0 \exp(-x_3/H) S_a K_I C_{L_0}^2 x_1 x_5}{4m * cos(x_2)} \\
A(2,1) &= -\frac{g}{x_1^3} \\
A(2,3) &= \frac{\rho_0 \exp(-x_3/H) S_a C_{L_0} x_5}{4m x_3 * cos(x_2)} - \frac{\rho_0 S_a C_{L_0} x_5}{4m x_3 * cos(x_2)} \\
A(2,5) &= \frac{\rho_0 S_a C_{L_0} (\exp(-x_3/H) + 1)}{4m * cos(x_2)} \\
A(3,2) &= \frac{\tan(x_2)}{x_2} \\
A(4,1) &= \frac{1}{x_1^2 * cos(x_2)} \\
B(5,1) &= \frac{1}{x_1 * cos(x_2)}
\end{aligned}
\tag{3.15}
$$

where $x_1 = v, x_2 = \gamma, x_3 = h, x_4 = t, x_5 = \alpha$, due to the state vector of $x = [v, \gamma, h, t, \alpha]$.

3.2.2. Selection of Related Parameters. The requisite parameters for the simulation are given, $C_{L_0} = 2.3$, $C_{D_0} = 0.0975$, $K_I = 0.1819$, $S_m/m = 0.912\ ft^2/slug$. The matrices are chosen as $R = 1$, $Q = diag([0, 0, 05, 0.01, 10^{-6}, 1])$, $S_f = diag([0, 10^6, 10^3, 0, 0])$. Note that the goal is to guide the RLV to land with a small value of vertical speed and a sharply shortened flight path angle. In the terminal penalty matrix S_f, the 2^{nd} and 3^{th} diagonal elements are endowed as a higher values since they are corresponding with the γ and h, respectively. The initial values for the simulation are 10,000 ft for altitude, 300

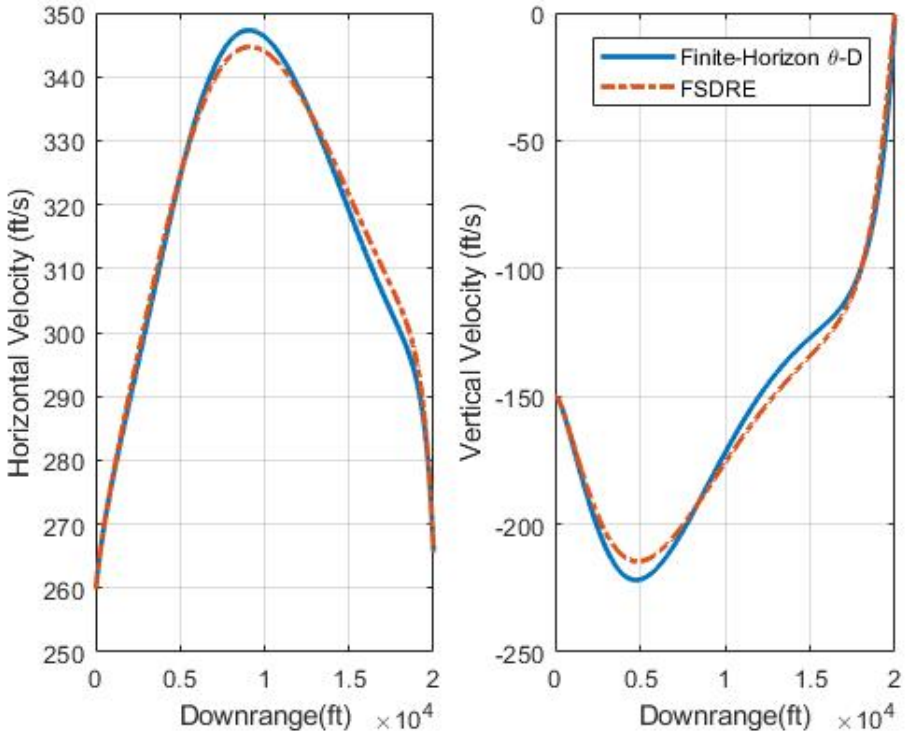

Figure 3.2. The Histories of Horizontal and Vertical Velocities by Two Techniques

ft/sec for velocity, -30 deg for the fligth path angle and 10 deg for attack angle. The fixed downrange is given as 20,000 ft. Since the independent variable is downrange X, then the sampling interval is unit of ft. In this simulation, the sampling point is every 20 ft. Additionally, The parameter of θ is set to 1. D terms are set to 0 in this case.

3.2.3. Simulation Result and Analysis. This simulation experiments are carried out in Dell OptitPlex 5070 Desktop with CPU I7-9700 and 16GB RAM. The first set of simulation are carried out with the proposed finite-horizon $\theta - D$ method as compared with the FSDRE technique in Heydari and Balakrishnan (2015). The second set leads to a robustness property of the proposed finite-horizon $\theta - D$ method to the varying initial conditions.

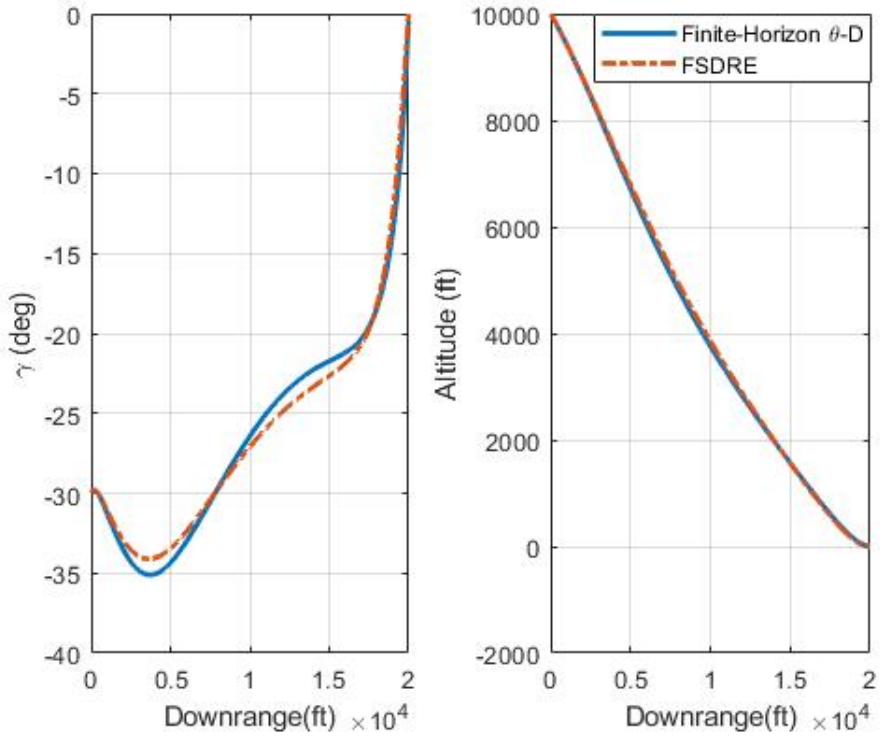

Figure 3.3. The Histories of Flight Path Angle and Altitude by Two Techniques

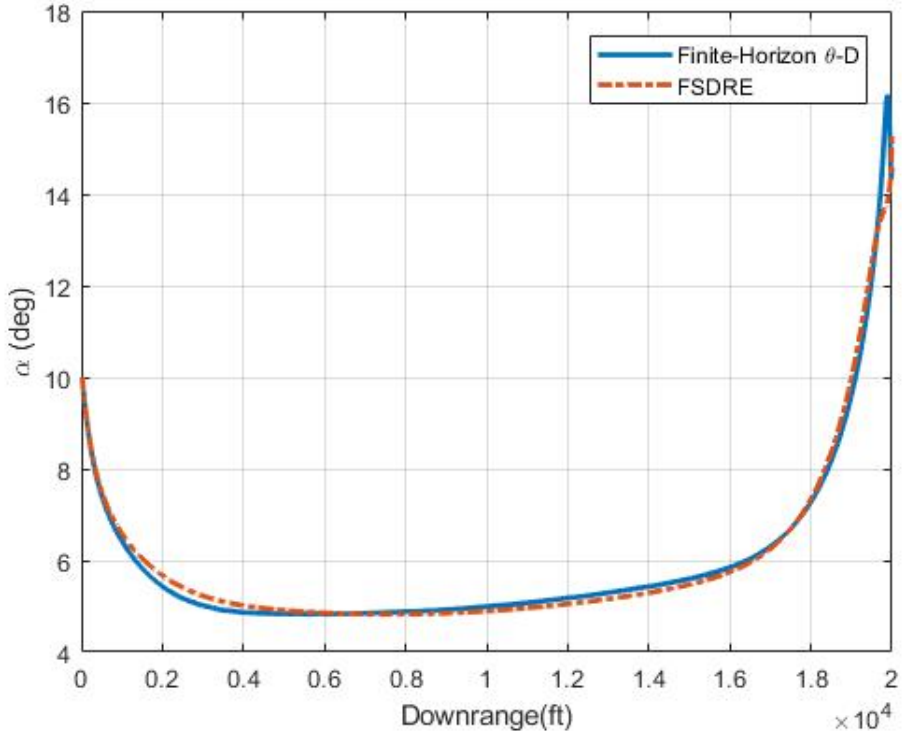

Figure 3.4. The History of Angle of Attack by Two Techniques

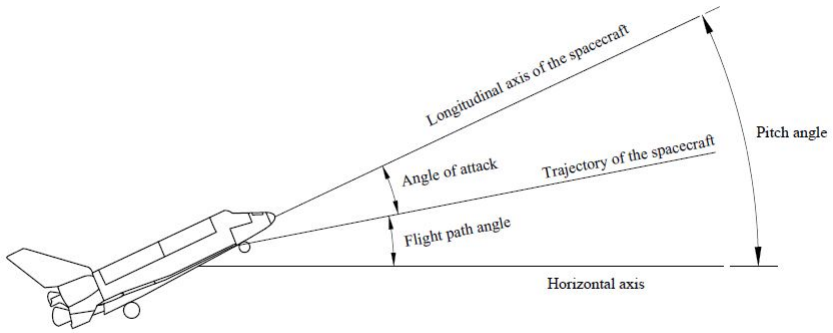

Figure 3.5. The The Schematic Diagram of Angles

3.2.3.1. Case I: finite-horizon $\theta - D$ vs FSDRE. With the same initial conditions, Figure 3.2.– Figure 3.4. show the performances by Finte-Horizon $\theta - D$ and FSDRE techniques. From Figure 3.2, the vertical velocities with two methods are close to zero. The flight path angle γ also approaches zero with two strategies based on the LHS plot of Figure 3.3. With the RHS plot of Figure 3.3, the altitudes are forced to zero. Those three figures indicate that both Finte-Horizon $\theta - D$ and FSDRE techniques are all effective to guide the A&L phase of RLV, while satisfying the designed objectives. Those figures illustrate that although the Finte-Horizon $\theta - D$ algorithm just picked three terms to calculate the control, it does not sacrifices the final performance compared with the FSDRE technique. Those three figures (Figure 3.2-Figure 3.4) can verify that our proposed finite-horizon $\theta - D$ technique is an effective tool. Besides, the total run time of FSDRE technique is 1.6517 seconds with the cost of 16.4918. At the meantime, the total run time of the proposed method is only 0.1125 seconds with the cost of 15.0135. It can be found that the run time of the proposed method is considerably less than those of FSDRE method with comparable cost of those two methods. Typically, from the run time perspective, it is clear that the proposed method in this research is a more efficient method and a better selection for practical online implementation. To summarize the proposed finite horizon $\theta - D$ technique can obtain almost same performance with the FSDRE technique with much less computation time and

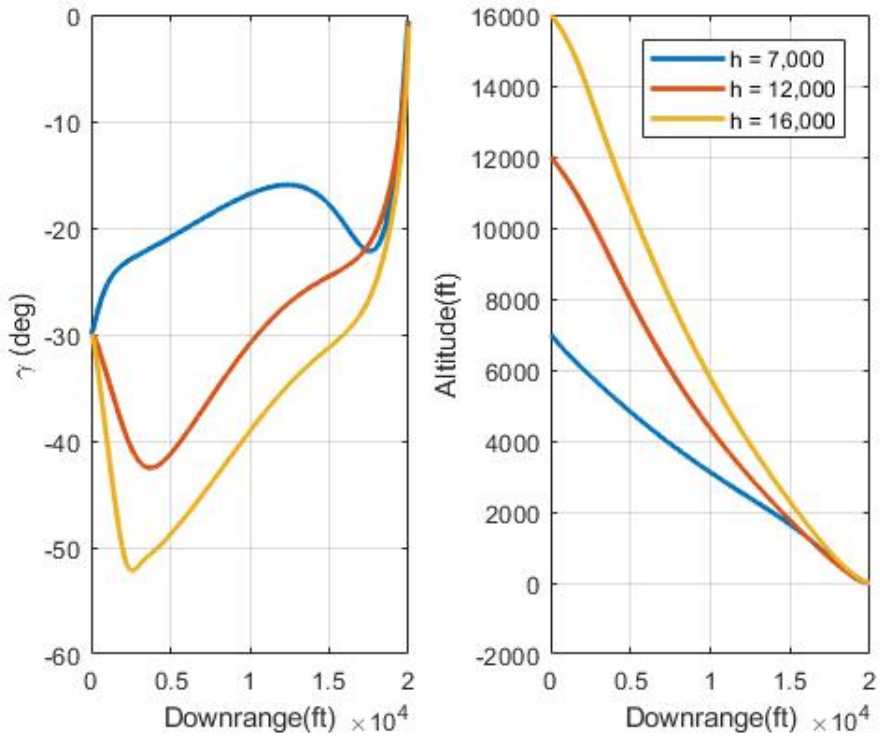

Figure 3.6. The History of γ and h with Different Initial Altitudes

cost. Additionally, for the better illustration the variables changing of the whole physical landing process, the Figure 3.5 shows a schematic diagram of the landing. When the RLV arrive the runway, it is clear that the vertical velocity will close to zero, the altitude will go to zero, and flight path angle will also be zero since the direction of trajectory of RLV should be along with the horizontal axis. However, the horizontal velocity and angle of attach will keep certain values.

3.2.3.2. Case II: robustness to the varying initial conditions. This section will displays the proposed algorithm is robust property to the some varying initial conditions, which simulates the different scenarios of RLV in A&L phases. If the RLV could start the A&L phase from different altitudes, Figure 3.6. shows that the proposed method still has a good guidance performance. Also, we choose different flight path angles, different

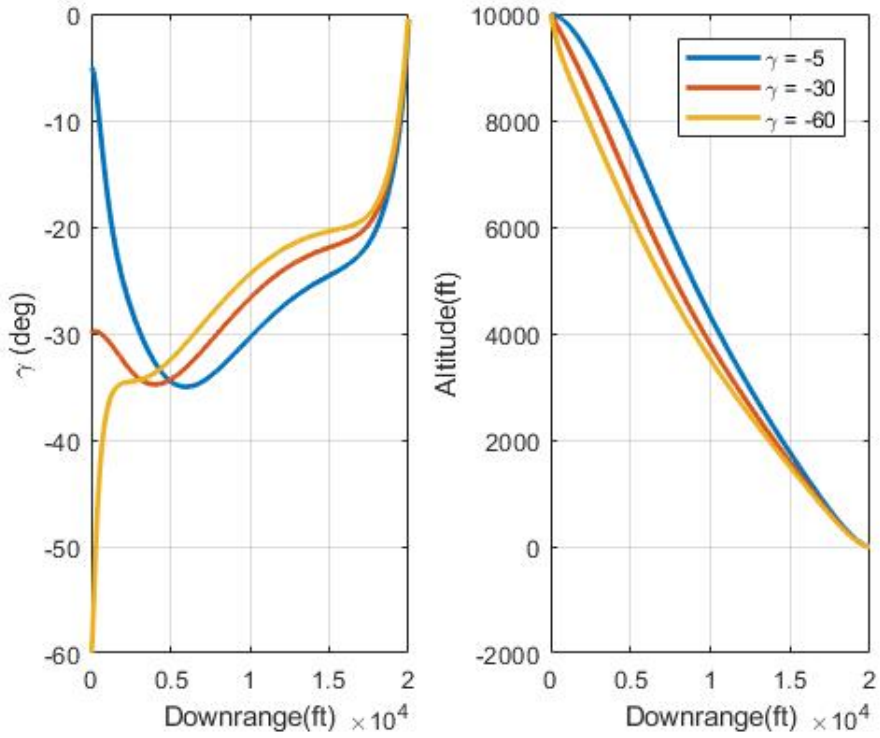

Figure 3.7. The History of γ and h with Different Initial Flight Path Angles

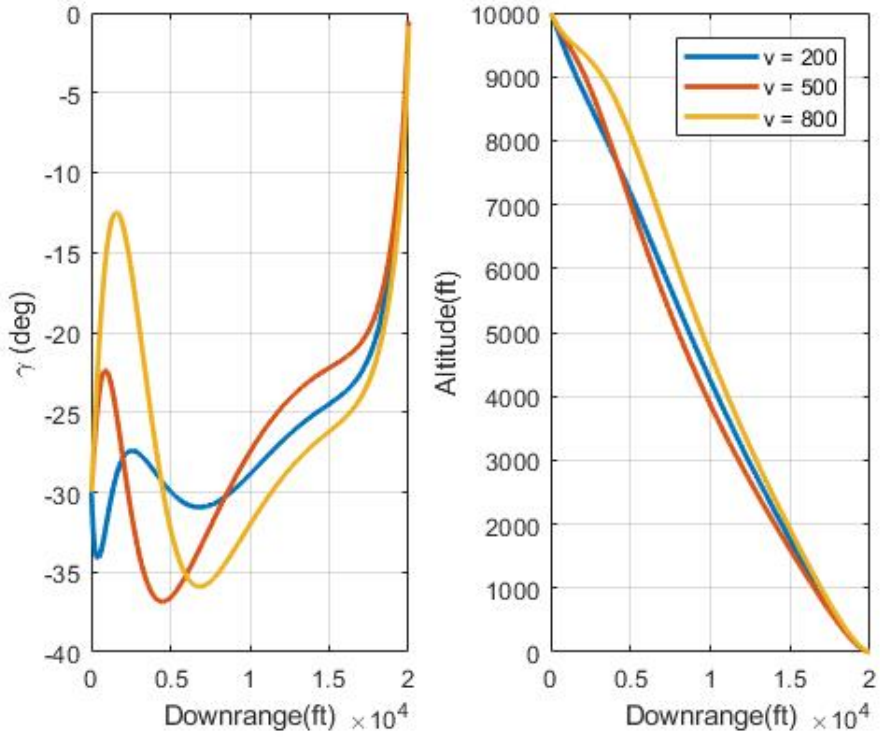

Figure 3.8. The History of γ and h with Different Initial Velocities

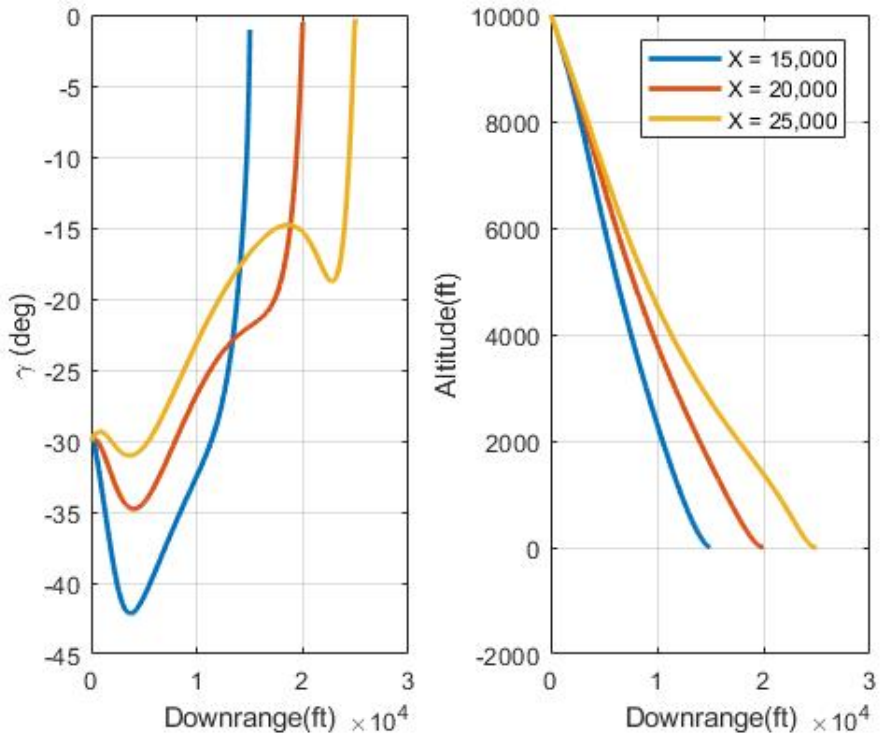

Figure 3.9. The History of γ and h with Different Initial Downranges

velocities and different downranges. It can be identified from Figures 3.7 - Figure 3.9 that the Finte-Horizon $\theta - D$ algorithm holds up well to the various situations, which can provide a reliable guidance law to help the RLV land safely.

4. FINITE TIME SUBOPTIMAL CONTROLLER DESIGN WITH $\theta - D$ TECHNIQUE FOR AEROSPACE APPLICATIONS: SATELLITE CONSENSUS PROBLEM AND SATELLITE MANEUVERING PROBLEM

In this section, two typical aerospace problems about satellites operation are investigated. Section 4.1 includes the multiply satellites consensus (or docking) operation. Nowadays, more and more space exploration missions are carried out by a group of satellites, which can avoid of totally failing of exploration missions if those missions are executed by a single larger, more complicated and more expensive satellite. Obviously, for any engineering systems, more complicated one is vulnerable to be failure due to a small malfunctional component. Put simply, the whole space exploration mission would be at risk due to an error of a single satellite. However, if the mission is carried out by a group of satellites, the rest of satellites in this group may continue to accomplish the mission with sacrificing of some limited performance if some satellites do not function properly. Meanwhile, mission with group can offer flexibility to the designers in that each satellite of the group can be re-positioned to satisfy different mission's requirement. For example, a ground-observing space-based sensor should be designed as a group of satellites' mission which can increase the aperture size as compared to the constructing a larger satellite. This group system can provide this sensor more flexibility since the aperture size and orientation are adjustable on orbit. With those aforementioned advantages, it is of practical meaning to investigate the control of a group of satellites. Inevitably, the J_2 perturbation effect to satellite movement must be considered in a successful satellite operation design, which is presented in Section 4.2. How to reject the J_2 perturbation effect deserves to do study, while the energy efficiency and successful maneuvering the satellite are considered. In this part, one can find that those two typical problems can be solved by the proposed finite time $\theta - D$ technique after a certain formulation operation.

4.1. FINITE TIME $\theta - D$ CONTROL DESIGN FOR CONSENSUS PROBLEM

In this section, four satellites (regarded as mass points) along with different orbits are taken into consideration and finite time $\theta - D$ based decentralized controller is constructed to bring them to one position for docking purpose. This problem is regarded as cooperative multi-agent tracking (leader-followers form) one characterized by nonlinear dynamics.As long as the communication topology of the four satellites satisfies a certain requirement, the states of followers can synchronize to those of leaders at finite time by adopting the proposed technique.

4.1.1. Basic Graph Topology. First, a basic introduction of graph topology is needed. A directed graph (usually called **digraph**) is represented as $\mathcal{G} = (\mathcal{V}, \mathcal{E}, \mathcal{A})$ with N nodes set $\{\mathcal{V}|v_1, v_2, \cdots, v_N\}$ and edges set $\mathcal{E} \subset \mathcal{V} \times \mathcal{V}$ with adjacency matrix $\mathcal{A} = \{w_{ij} \in \mathcal{R}^{N\times N}\}$. In this study, the time-invariant digraph is considered which implies $\mathcal{A}$ is constant real-valued matrix. An edge from node j to node i can be denoted as (v_j, v_i), which indicates the information or signal can flow from node j to node i. The value of w_{ij} represents the weight of edge (v_j, v_i) and $w_{ij} > 0$ if $\{(v_j, v_i) \in \mathcal{E}\}$, otherwise $w_{ij} = 0$. Note that this study do not involve the repeated edges and self loops, which implies $\{w_{ii} = 0, \forall i \in N\}$.

1. Defining j node is a **neighbor** of i node if $(v_j, v_i) \in \mathcal{E}$.

2. The **neighborhood set** of node i is denoted as $N_i = \{j|(v_j, v_i) \in \mathcal{E}\}$.

3. The **in-degree matrix** is $\mathcal{D} = diag\{d_i\} \in \mathcal{R}^{N\times N}$,where $d_i = \sum_{j\in N_i} w_{ij}$.

4. The **Laplacian matrix** can be define as $\mathcal{L} = \mathcal{D} - \mathcal{A}$. Apparently, $\mathcal{L}\mathbf{1}_N = 0$ where $\mathbf{1}_N \in \mathcal{R}^N$ indicates a vector with all elements to be one.

5. A **directed path** implies the existance of a sequence of successive edges $\{(v_i, v_k), (v_k, v_l), \cdots, (v_m, v_j)\}$ from i node to j node.

6. If a directed path exists from a root node to every other node in a graph, a claim can be made that there is a **spanning tree** in this graph. Actually, the consensus can be reached if

there is a spanning tree in a graph. Intuitively, this requirement condition easily understood since all of nodes(followers) can (directly or indirectly)access to the information of the root nodes(leaders).

4.1.2. Problem Formulation. The $i^{th}, i \in N$ follower satellites' dynamics can be written as:

$$\dot{x}_i = f(x_i) + Bu_i \tag{4.1}$$

where $x_i \in \mathcal{R}^n, f(x_i) \in \mathcal{R}^n, B \in \mathcal{R}^{n\times m}, u_i \in \mathcal{R}^m$.

The dynamics of the leader satellites labeled 0 is given by

$$\dot{x}_0 = f(x_0) \tag{4.2}$$

where $x_0, f(x_0)$ have the same dimensions with $x_i, f(x_i)$.

Note that: In some cases, the information of leader can be obtained by a few (or part) of the followers. If the i^{th} follower can get the information from the leader, one can say there exists a edge (v_0, v_i) with a weight $g_i > 0$. One can call the followers with $g_i > 0$ as pinned followers. Let us denote the pinning matrix as $\mathbf{G} = diag\{g_i\} \in \mathcal{R}^{N\times N}$.

Our objective of this consensus problem is to design a distributed controller u_i for all followers, which leads them to reach the leader's trajectory in finite time, which can be expressed as:

$$\lim_{t\to t_f} (x_i(t) - x_0(t)) = 0, \forall i \in N \tag{4.3}$$

4.1.3. Control Design with Finite Time $\theta - D$ Technique. In order to implement the $\theta - D$ technique, the (4.1) can be reconstructed the $\theta - D$ form as:

$$\dot{x}_i = \left[A_0 + \theta\left(\frac{A(x_i)}{\theta}\right)\right]x_i + Bu_i, i \in N \tag{4.4}$$

Definition 1. In this research, consensus error of follower i is defined as

$$e_i = \sum_{j \in N_i} w_{ij}(x_i - x_j) + g_i(x_i - x_0) \tag{4.5}$$

The cost function of the i^{th} follower is defined as:

$$J(x_i, u_i) = \frac{1}{2} x_i(t_f)^T S_f x_i(t_f) + \frac{1}{2} \int_0^{t_f} (x_i^T Q x_i + u_i^T R u_i) dt \tag{4.6}$$

The control protocol for each followers i can be designed as:

$$u_i = -c * K(x_i) * e_i \tag{4.7}$$

where $K(x_i)$ can be computed by using algorithm 1 with $K(x_i) = R^{-1}B^T(T_0 + \theta T_1(x_i) + \theta^2 T_2(x_i))$. The coupling parameter c should be picked carefully to guarantee states of followers that approach the states of leader at finite time.

Note that:

1. For any feedback tracking control, the error signal could be $(x - x_{desired})$. x is the states. $x_{desired}$ is the reference or desired states. In this problem, the error signal of i^{th} follower have to involve the leader part as $g_i(x_i - x_0)$ and also consider the other followers in its neighbourhood set as $\sum_{j \in N_i} w_{ij}(x_i - x_j)$ since the information flow might go to leader and neighbours.

2. The coupling parameter c is a positive scalar number and need to be properly selected since it determines the convergent rate.

3. $T_0, T_1(x_i)$, and $T_2(x_i)$ can be calculated by (2.19), (2.20) and (2.21).

4. Based on description of the second part about the $\theta - D$ algorithm, the control for the each follower is suboptimal. For this scenario, we can say that the local opitmality can be achieved to overall system Lewis *et al.* (2013).

4.1.4. Dynamical Mathematical Model. The dynamic equation of each satellite (point mass) in the gravitational field with an inertial frame centered at center of gravity is Curtis (2013):

$$\ddot{\mathbf{r}} = \frac{\mu}{\|\mathbf{r}\|^3}\mathbf{r} + \mathcal{F} \tag{4.8}$$

where $\mathbf{r}$ represents the position vector of the satellite from the gravitational center; the two norm form of $\|\mathbf{r}\|$ is the magnitude of the vector $\mathbf{r}$; the gravitational coefficient μ is $3.986 \times 10^5 km^3/sec^2$ and $\mathcal{F}$ denotes the vector of the force applied to the satellite per its unit of mass. Additionally, $\ddot{\mathbf{r}}$ is the second time derivative of the position vector $\mathbf{r}$ w.r.t the inertial frame.

After normalizing the parameters with some selected reference length $\mathbf{R}$ and reference time $\mathcal{T}$, one can get the normalized parameters $\bar{\mathbf{r}}$, $\dot{\bar{\mathbf{r}}}$ and $\overline{\mathcal{F}}$ as:

$$\bar{\mathbf{r}} = \frac{1}{\mathbf{R}}\mathbf{r}; \dot{\bar{\mathbf{r}}} = \frac{\mathcal{T}}{\mathbf{R}}\dot{\mathbf{r}}; \overline{\mathcal{F}} = \frac{\mathcal{T}^2}{\mathbf{R}}\mathcal{F}; \tag{4.9}$$

In this case, selecting the specific reference time as $\mathcal{T} = \sqrt{\mathbf{R}^3/\mu}$ and normalizing (32) leads to:

$$\ddot{\bar{\mathbf{r}}} = -\frac{1}{\|\bar{\mathbf{r}}\|^3}\bar{\mathbf{r}} + \overline{\mathcal{F}} \tag{4.10}$$

The position vector $\bar{\mathbf{r}}$ within the inertial frame can be denoted as $[x_1, x_2, x_3]^T$ and their rates are $[x_4, x_5, x_6]^T = [\dot{x}_1, \dot{x}_2, \dot{x}_3]^T$. Then, the overall state can be constructed as

$$x = [x_1, x_2, x_3, x_4, x_5, x_6]^T \tag{4.11}$$

The normalized control force per unit can be represented in the inertial frame as $\overline{\mathcal{F}} = [u_1, u_2, u_3]^T$. In this case,the control vector is:

$$u = [u_1, u_2, u_3]^T \tag{4.12}$$

With (4.9),(4.10) and (4.11), the mathematical dynamic equation is:

$$\begin{bmatrix} \dot{x}_1 \\ \dot{x}_2 \\ \dot{x}_3 \\ \dot{x}_4 \\ \dot{x}_5 \\ \dot{x}_6 \end{bmatrix} = \begin{bmatrix} 0 & 0 & 0 & 1 & 0 & 0 \\ 0 & 0 & 0 & 0 & 1 & 0 \\ 0 & 0 & 0 & 0 & 0 & 1 \\ -\frac{1}{(x_1^2+x_2^2+x_3^2)^{3/2}} & 0 & 0 & 0 & 0 & 0 \\ 0 & -\frac{1}{(x_1^2+x_2^2+x_3^2)^{3/2}} & 0 & 0 & 0 & 0 \\ 0 & 0 & -\frac{1}{(x_1^2+x_2^2+x_3^2)^{3/2}} & 0 & 0 & 0 \end{bmatrix} \begin{bmatrix} x_1 \\ x_2 \\ x_3 \\ x_4 \\ x_5 \\ x_6 \end{bmatrix} + \begin{bmatrix} 0 & 0 & 0 \\ 0 & 0 & 0 \\ 0 & 0 & 0 \\ 1 & 0 & 0 \\ 0 & 1 & 0 \\ 0 & 0 & 1 \end{bmatrix} \begin{bmatrix} u_1 \\ u_2 \\ u_3 \end{bmatrix} \tag{4.13}$$

Note that one can pick the state coefficient matrix as $A(x)$, the control direction matrix as B.

4.1.5. Parameter Selection. The orbital elements of four satellites are given in Table 4.1.

Table 4.1. The Orbital Elements of Four Satellites

Elements	Satellite One	Satellite Two	Satellite Three	Satellite Four
a (km)	9,000	11,000	13,000	15,000
Ω (deg)	20	0	40	50
i(deg)	20	0	40	50
e	0	0	0	0

In this table, a is orbital semi-major axis, Ω represents right ascension of the ascending node, i denotes inclination and e is eccentricity. In this case, before applying any maneuver operations for those satellites, it is considered that those four satellites are running within the equatorial plan from the Southern hemisphere to the Northern hemisphere. The objective is to maneuver the satellite two, three, four and to make them dock in the location of satellite one at finite time. This means that the satellite one keeps rotating along the orbit without any control input excreted on it and the remaining satellites are supposed to have the ability to obtain the position and speed information of satellite one and dock with it at finite time.

The communication topology among those satellites is demonstrated as follows

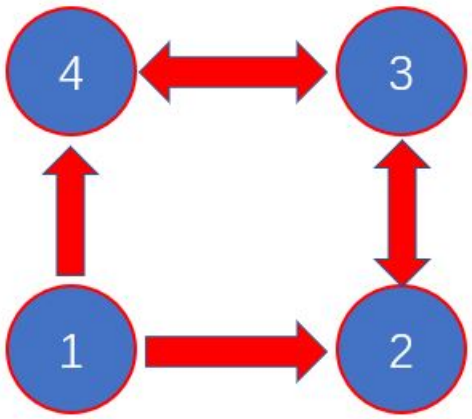

Figure 4.1. Four Satellites Communication Graphic Topology

From Figure.4.1, satellites two three, and four can directly get the information from the satellite one, while satellite three does not have direct access to satellite one. Note that in this topology exists a spanning tree with satellite one as the root.

The reference length is set as $\mathcal{R} = 9000km$, and reference time is selected as $\mathcal{T} = 1352.4s$. With this condition, each control unit is $\mathcal{R}/\mathcal{T}^2 = 4.921m/s^2$. Based on Table 4.1, the initial condition of each satellite can be computed and listed as follows:

$$\begin{aligned} x_1^0 &= [0.9397, 0.3420, 0, -0.3214, 0.8830, 0.3420]^T \\ x_2^0 &= [1.222, 0, 0, 0, 0.9405, 0]^T \\ x_3^0 &= [1.1065, 0.9285, 0, -0.4097, 0.4883, 0.5348]^T \\ x_4^0 &= [1.0713, 1.2767, 0, -0.3814, 0.3200, 0.5934]^T \end{aligned} \tag{4.14}$$

The three weight matrices of the cost function are defined as:

$$Q = diag(1200, 1100, 1600, 0, 0, 0) \tag{4.15}$$

$$S_f = diag(1000, 1000, 1000, 0, 0, 0) \tag{4.16}$$

$$R = diag(1, 1, 1) \tag{4.17}$$

In this simulation, without losing of generality, the θ is set to 1, D_i is chosen as 0 and the coupling parameter c is 0.2.

4.1.6. Simulation Result. This simulation experiment is carried out by the personal Laptop Thinkpad R480 with the CPU Intel(R) Core(TM) i3-7130U 2.70 GHZ and 16GB RAM. This first set is to show the effectiveness of finite time $\theta - D$ control to this docking problem. The second set is a comparative analysis with the FSDRE technique, which demonstrates the efficient property of the proposed method.

a. Simulation Results with Finite Time $\theta - D$ Technique

Figure.4.2 shows the history of position error between satellite two and satellite one in X, Y, and Z direction. It can be found that the error can be driven to zero at the final time of eight time unit, which implies that the proposed finite time $\theta - D$ controller is effective. The similar phenomenon also can be observed in Figure.4.3 and Figure.4.4, which represent the error histories of the satellite three to satellite one and satellite four to satellite one. Figure.4.5 shows the history of states of all satellites along the X, Y, Z direction. The red line represents the satellite one or leader, which is simulated with 30 time unit and can be found that the leader satellite is varied periodically. This plot provides an overall picture that satellite two, three, four can reach the position of satellite one at the eight time unit with the proposed finite time $\theta - D$ controller. Unfortunately, it is not clear to see what happen between the time unit interval [0, 8]. In order to get insight into this part, the state histories of those satellites within the [0, 8] are presented separately in Figure.4.6, Figure.4.7 and Figure.4.8. Figure.4.6 shows the trajectories of all of four satellites in X direction, which also verify that our proposed technique is valid. Meanwhile, Figure.4.7 and Figure.4.8 also exhibit the trajectories of all satellites in Y and Z direction. The results is quite good. Let us observe Figure.4.6, Figure.4.7 and Figure.4.8, we can find an interesting phenomena that the states in Y direction are oscillating more intensively than other two directions. The reason is arisen from the initial values. In X direction, the initial values of the four satellites are $[0.939, 1.222, 1.1065, 1.0713]$ in Z coordinate , and the initial

Table 4.2. Cost Value and Run Time with Finite Time $\theta - D$ Vs FSDRE

Techniques		Satellite Two	Satellite Three	Satellite Four
Finite Time $\theta - D$	Cost	5.1166e+03	5.0061e+03	5.1184e+03
	Run Time	7.540481 seconds		
FSDRE	Cost	5.1202e+03	5.0114e+03	5.1924e+03
	Run Time	70.116641 seconds		

values of 4 satellites is $[0, 0, 0, 0]$. But there is a large initial value difference between the satellites in Y direction $[0.3420, 0, 0.9285, 1.2767]$. Furthermore, Figure.4.9, Figure.4.10 and Figure.4.11 show the trajectories in three-dimensional coordinates, which offer a more visual perception of the movement history of the three satellites to track the leader.Note that the five-point star represents the starting point, and the circle are the reaching point. To summarize, Figure.4.2-Figure.4.11 prove that the proposed finite time $\theta - D$ technique is an effective one in this satellite docking problem.

b. Compassion Results

The aforementioned analysis reveals the proposed method is effective to control design for multi-agents problem. Furthermore, in order to show the proposed $\theta - D$ method is more efficient than the popular FSDRE technique, the simulation is operated by two methods. Table 4.2 includes the results of $FSDRE$ and finite time $\theta - D$ method. We can find the cost for the three satellites with FSDRE technique are 5.1202e+03, 5.0014e+03 and 5.1924e+03. The total run time is 70.116641 seconds. However, we also can find the cost for those satellites with the proposed method are 5.1166e+03, 5.0061e+03 and 5.1184e+03, which are comparable with the cost of FSDRE technique. Astonishingly, the run time is only 7.540481 seconds which is almost one tenth of the run time of FSDRE method. Figure.4.12 shows history of positions error between satellite two and satellite one by those two method. we can find that they are almost same. To identify what is the detailed difference between those two method, Figure.4.13 show the difference of Figure.4.12, which can be observed that the difference is very small. Figure.4.14 - Figure.4.17 also reflect the same phenomenon. So, from Figure.4.12 to Figure.4.17, those figures demonstrate that the

performance of those two techniques is quite same. To summarize, the proposed finite time $\theta - D$ can achieve the almost same performance with FSDRE technique with much less computation time can comparable cost.

4.2. FINITE TIME CONTROL DESIGN FOR SPACECRAFT FORMATION FLYING WITH J_2 PERTURBATIONS

The importance of the formation flying has been mentioned in case one. For this case, an exact nonlinear differential J_2 perturbation model is used for the relative orbital dynamics, and the $\theta - D$ finite time tracking is posed as an error regulator problem. In the aerospace engineering community, the relative movement of the deputy satellites are often depicted with a chief satellite by the relative position and velocities. For the convenient formation configuration purpose, the dynamics of relative motion are expressed within the Local Vertical Local Horizontal (LVLH) Franzini and Innocenti (2020) frame of chief satellite.

4.2.1. The Development of Dynamical Mathematical Model. If one consider a perturbed eccentric orbit for the chief satellite, the equations of relative motion for the deputy satellite are constructed as Bilal *et al.* (2019), where,

$$\frac{d^2\rho}{dt^2} = \ddot{\rho}_I - 2\omega \times \frac{d\rho}{dt} - \frac{d\omega}{dt}\rho - \omega \times (\omega \times \rho) + \mathbf{d} + \mathbf{u} \tag{4.18}$$

$$\ddot{\rho}_I = -\frac{\mu(\mathbf{r_0} + \rho)}{\|\mathbf{r_0} + \rho\|^3} + \frac{\mu}{r_0^3}\mathbf{r_0} \tag{4.19}$$

1.$\rho = [x, y, z]^T$ corresponding to the radial, along track, and cross track distance of the deputy satellite relative to the chief satellite.

2.ω indicates the angular velocity of the LVLH frame with the refenece to the inertial frame.

3.$\mathbf{u}$ and $\mathbf{d}$ are control and disturbance respectively.

4.$\mathbf{r_0}$ is the position vector of the chief satellite and denoted as $\mathbf{r_0} = [r_0, 0, 0]^T$.

5.μ is the gravitational coefficient with $3.986 \times 10^5 km^3/sec^2$.

In this case, the scenario of the formation flying of low Earth orbit(LEO) satellite is considered.There exists some perturbations for satellites, including the presence of other celestial bodies(sun and moon), the solar radiation pressure, and non-sphericity of the Earth, etc. Usually, the major disturbance for the satellite in LEO is Earth oblateness effect(or called J_2 perturbations). The modeling of the J_2 perturbations with the relative motion can be expressed as Xu and Wang (2008)

$$
\begin{aligned}
J^2 d_x &= -\eta_f^2 x - (\zeta_f - \zeta) s_i s_\theta - r(\eta_f^2 - \eta^2) \\
J^2 d_y &= -\eta_f^2 y - (\zeta_f - \zeta) s_i c_\theta \\
J^2 d_z &= -\eta_f^2 z - (\zeta_f - \zeta) c_\theta
\end{aligned} \tag{4.20}
$$

where $J^2 d_x, J^2 d_y, J^2 d_z$ are J_2 perturbation along x, y, z direction in the LVLH frame, respectively. The disturbance term in (4.18) can be specified as $\mathbf{d} = [J^2 d_x, J^2 d_y, J^2 d_z]^T$. The related parameters in (4.20) are defined as

$$\eta^2 = \frac{k_{J_2}}{r_0^5} - \frac{5 k_{J_2} s_i^2 s_\theta^2}{r_0^5} \tag{4.21}$$

$$\zeta = \frac{2 k_{J_2} s_i s_\theta}{r_0^4} \tag{4.22}$$

$$\eta_f^2 = \frac{k_{J_2}}{r^5} - \frac{5 k_{J_2} r_Z^2}{r^7} \tag{4.23}$$

$$\zeta_f = \frac{2 k_{J_2} r_Z}{r^5} \tag{4.24}$$

$$r_Z = s_i s_\theta (r_0 + x) + s_i c_\theta y + c_i z \tag{4.25}$$

$$k_{J_2} = \frac{3}{2} \mu J_2 R_e^2 \tag{4.26}$$

where, J_2 is coefficient as $1.08262668 \times 10^{-3}$. Additional, the angular velocity $\omega = [\omega_x, \omega_y, \omega_z]^T$ within the equation (4.18) is Xu and Wang (2008)

$$\omega_x = -\frac{k_{J_2} s_{2i} s_\theta}{h_0 r_0^3}; \omega_y = 0; \omega_z = \frac{h_0}{r_0^2} \tag{4.27}$$

where i is inclination, θ represents argument of latitude, r_0 indicates radial distance and h_0 stands for angular momentum of the chief satellite orbit. The radial distance of the deputy satellite is $r = \sqrt{(r_0 + x)^2 + y^2 + z^2}$. R_e represents the radius of the Earth.The $s_{(*)}$ and $c_{(*)}$ stand for the sine operation and cosine operation. Note that the chief satellite states can be represented as $[r_0, \dot{r}_0, h_0, \theta, i]$ and states propagation can be calculated by the dynamic equations of (9)-(14) in Xu and Wang (2008).

4.2.2. Tracking Problem Development. Suppose there exists a reference trajectory state is denoted as $\mathbf{x_d}(\mathbf{t})$ in LVLH frame. For brevity purpose, the notation of state as function of t will be omitted in the following statement. Also, one can define error $\mathbf{e}$ to be the difference between the satellite state vector $\mathbf{x} = [\rho, \rho]^{\mathbf{T}}$ and the the reference state $\mathbf{x_d}$.

$$\mathbf{e} = \mathbf{x} - \mathbf{x_d} = [\mathbf{e}_\rho, \mathbf{e}_\rho]^T \tag{4.28}$$

Correspondingly, the original cost function (2.2) should be reformulated as

$$J(e, u) = \frac{1}{2} e(t_f)^T S_f e(t_f) + \frac{1}{2} \int_0^{t_f} \left(e^T Q e + u^T R u \right) dt \tag{4.29}$$

In order to use $\theta - D$ technique, the equation (4.18) and (4.19) should be reformulated as error dynamics form Bilal *et al.* (2019)

$$\mathbf{e} = A(\mathbf{e})\mathbf{e} + Bu = \left[\begin{array}{c|c} \mathbf{0_{3\times3}} & \mathbf{I_{3\times3}} \\ \hline \mathbf{\Omega} + \mathbf{G(e)} & \end{array} \right] \mathbf{e} + Bu \tag{4.30}$$

where

$$\mathbf{\Omega} = -\Big[[\dot{\omega}\times] + [\omega\times][\omega\times], 2[\omega\times] \Big] \tag{4.31}$$

$$\mathbf{G(e)} = [\mathbf{\Gamma_{3\times3}}, \mathbf{0_{3\times3}}] \tag{4.32}$$

$$\mathbf{\Gamma_{3\times3}} = [\gamma, \mathbf{e}_\rho{}^T \mathbf{e}_\rho]^T \mathbf{e}_\rho{}^T \tag{4.33}$$

$$\gamma = f_g(\mathbf{e} + \mathbf{x_d}) - f_g(\mathbf{x_d}) + \mathbf{d}(\mathbf{e} + \mathbf{x_d}) - \mathbf{d}(\mathbf{x_d}) \tag{4.34}$$

$$f_g(\mathbf{x}) = \ddot{\rho}_I \tag{4.35}$$

where, $[\omega\times]$ represents the skew-symmetric matrix of ω Salkuyeh (2020) and B matrix has the same expression in (4.13). With properly choosing the weight matrices S_f, Q, R in (4.29),our goal is to design a controller by $\theta - D$ technique to make the error $\mathbf{e}$ reach zero at finite time, which implies that the deputy satellite can be driven to reach the reference trajectory at finite time.

4.2.3. Parameter Selection. In this case, the orbital elements of the chief satellite are $a = 6952km$, $e = 0.001$, $i = 97.7deg$, $\Omega = 0deg$, $\omega = 0deg$, $f = 0deg$. The deputy satellite' orbital elements are $a = 6955.10km$, $e = 0.0046$,$i = 97.3847deg$, $\Omega = 0.2406deg$, $\omega = 47.2196deg$, $f = 312.4508deg$. The reference radius(r_d) and reference phase(ϕ_d) are $r_d = 50km$ and $\phi_d = 120deg$. Additionally,the weight matrices in (4.29) are selected as

$$S_f = diag([10, 10, 10, 0, 0, 0]) \tag{4.36}$$

$$Q = diag([10^{-11}, 10^{-12}, 10^{-12}, 0, 0, 0]) \tag{4.37}$$

$$R = diag([1, 1, 1]) \tag{4.38}$$

The other parameters in $\theta - D$ algorithm are set as $\theta = 1$ and $D = 0$. The finite time is set to three different times, $0.6T$ seconds,$0.8T$ seconds and T seconds, where the T is the period of the chief satellite as $T = 2\pi\sqrt{6592^3/\mu}$ seconds.This means that the $\theta - D$ technique is employed to design a control which can drive the deputy satellite to reach the reference trajectory at the final times of $0.6T$ seconds,$0.8T$ seconds and T seconds.

4.2.4. Simulation Results. This simulation experiment is also carried out by the personal Laptop Thinkpad R480 with the CPU Intel(R) Core(TM) i3-7130U 2.70 GHZ and 16GB RAM. This first set is also to show the effectiveness of finite time $\theta - D$ control to this satellite maneuvering problem. The second set is a comparative analysis with the

Table 4.3. Cost Value and Run Time with Finite Time $\theta - D$ Vs FSDRE

Techniques		0.6T	0.8T	T
Finite Time $\theta - D$	Cost	1.7671e-05	1.7432e-05	1.7596e-05
	Run Time(seconds)	2.225677	2.955464	3.202443
FSDRE	Cost	1.777e-05	1.7503e-05	1.7679e-05
	Run Time(seconds)	10.031524	14.142157	16.962306

FSDRE technique with three time, $0.6T$ seconds, $0.8T$ seconds and T seconds, which also demonstrates the efficient property of the proposed method.

a. Simulation Results with Finite Time $\theta - D$ Technique

The Figure.4.18 is to show the position error of the deputy satellite to reference satellite. We can find that the error in X, Y and Z direction will arrive zero at the finite time $0.6T$ seconds by employing the proposed finite time $\theta - D$ control. With choosing different final times $0.8T$ seconds and T seconds, the position error will also approach the zero with the proposed method,which can be observed in Figure.4.21 and Figure.4.24. The histories of position state about deputy and reference satellite in three difference finite time are demonstrated in Figure.4.19, Figure.4.22 and Figure.4.25. Those six figures verify that the proposed method is an effective tools.Besides, it can provide the aerospace engineers a freedom to design the reaching time depended on the various task requirements. Additionally, the visualized three dimensional version of the movement of deputy satellites in three different final times can be found in Figure.4.20, Figure.4.23 and Figure.4.26.

b. Compassion Results

So far, it is easy to identify that the proposed finite time $\theta - D$ technique is quite valid to control design for the satellite orbital maneuver problem. Compared with the FSDRE control strategy, the proposed method is more efficient can be verified. The simulations are carried out with three different final times, $0.6T$ seconds, $0.8T$ seconds and T seconds. Results from the both methods are shown in Table 4.3. From the third row of this table, we can find the integrated cost function values with the FSDRE method are 1.777e-05 for $0.6T$

seconds, 1.7503e-05 for $0.8T$ seconds and 1.7679e-05 for T seconds. Correspondingly, the run time is 10.031524 seconds, 14.142157 seconds and 16.962306 seconds,respectively. From the second row of Table 4.3, note that the costs with proposed method are 1.7671e-05 for $0.6T$ seconds, 1.7432e-05 for $0.8T$ seconds and 1.7596e-05 for T seconds, which are a little bit smaller than the cost of FSDRE method. However, the run is 2.225677 seconds , 2.955464 seconds and 3.202443 seconds respectively, which is considerably less and almost one fifth of the run time of the FSDRE method. It is clear that the proposed $\theta - D$ technique is a better selection for the practical online use. From the left-hand side figures of Figure.4.27, Figure.4.28 and Figure.4.29, one can find the blue line can fit the red line very well, which indicates that those two technique can get the almost same performance in X direction. In addition, in Y and Z directions, those two methods bring some difference. One can find that the FSDRE method generate more errors. That is the reason that the cost values of FSDRE are a little bit more that the cost values of the proposed method. However, both can force the trajectories to reach zero at final time. Overall, Figure.4.27, Figure.4.28 and Figure.4.29 show that the proposed finite time $\theta - D$ can obtain similar performance with the FSDRE technique. To summarize, with the aforementioned simulation results and detailed analysis, the proposed finite time $\theta - D$ method can obtain the similar performance with FSDRE with much less computational time and comparable costs, indicating it as a the potentially powerful design tool. From the engineering practical and finite time optimal perceptive, the proposed finite time $\theta - D$ technique is a good choice when the online implementation is needed.

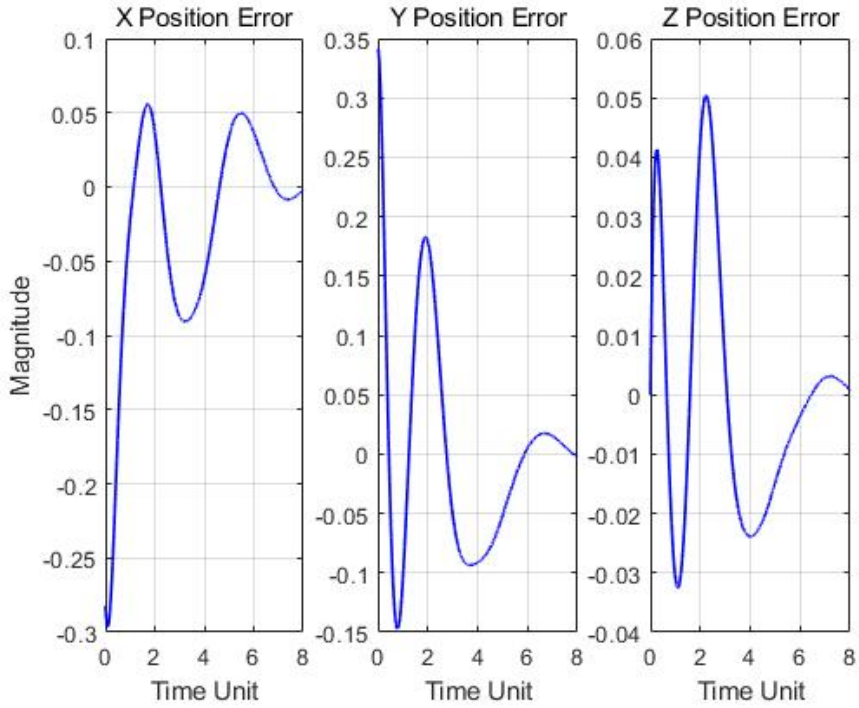

Figure 4.2. History of Position Error along X,Y,Z Direction between Satellite Two with Satellite One

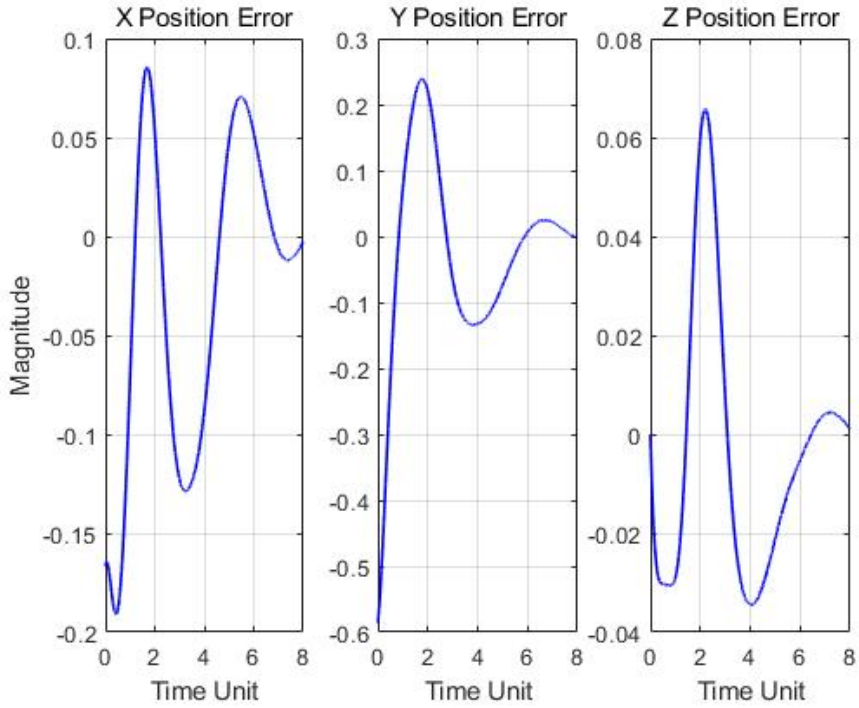

Figure 4.3. History of Position Error along X,Y,Z Direction between Satellite Three with Satellite One

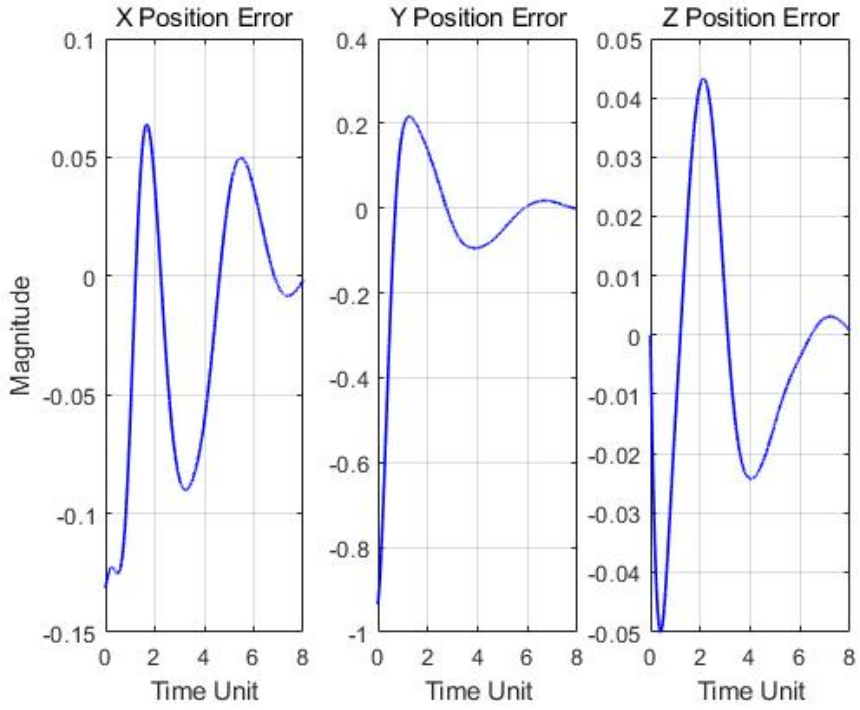

Figure 4.4. History of Position Error along X,Y,Z Direction between Satellite Four with Satellite One

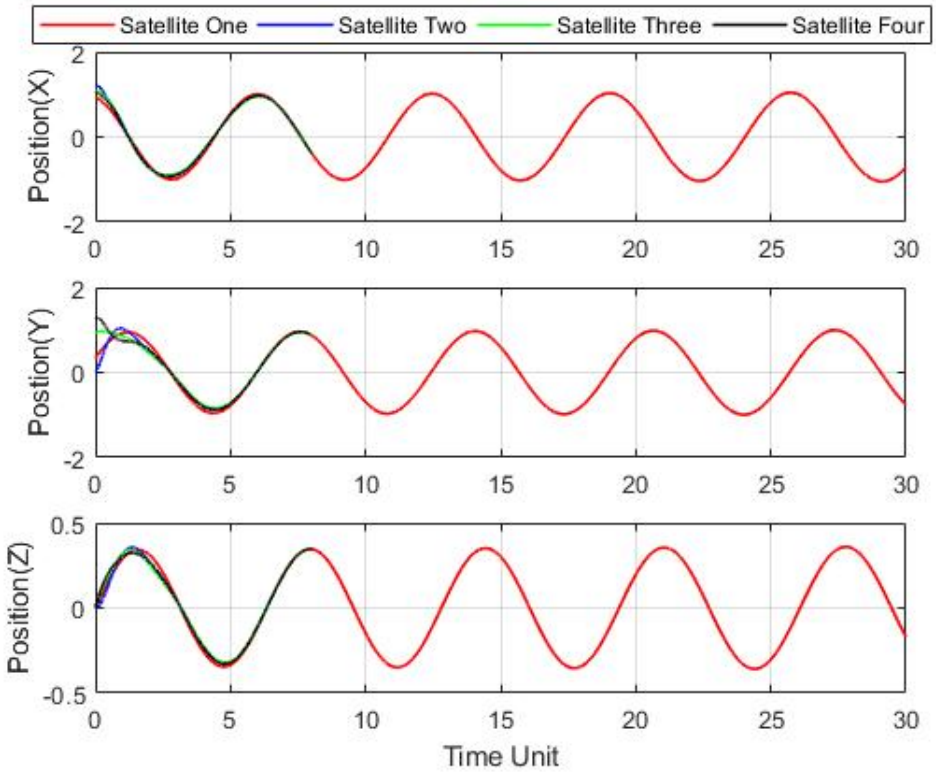

Figure 4.5. History of States of All Satellites along X,Y,Z Direction

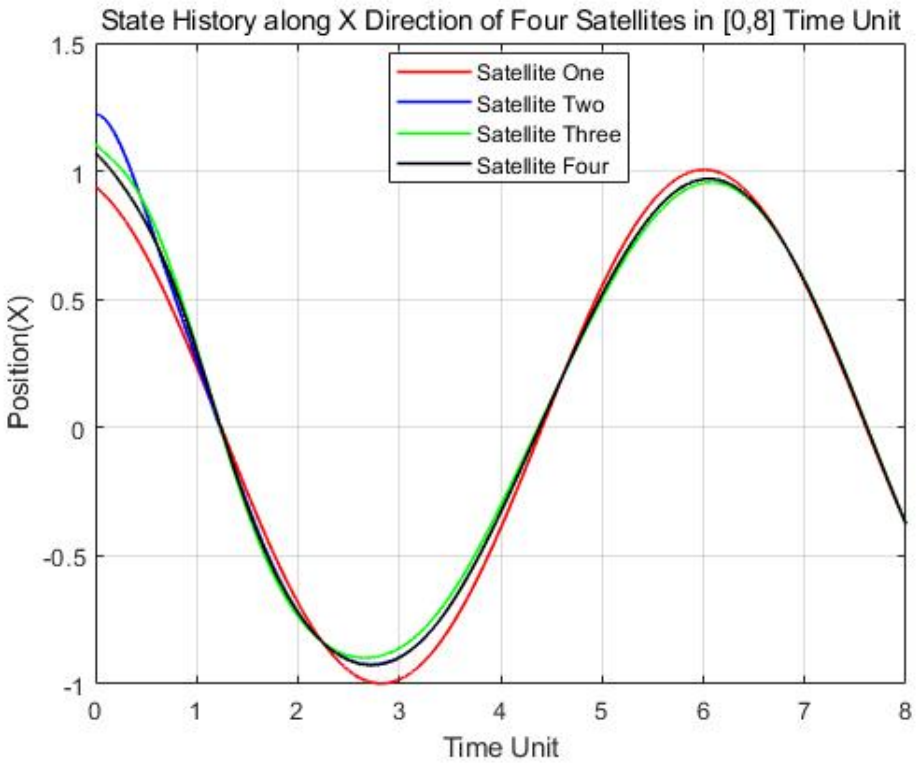

Figure 4.6. History of States of All Satellites along X Direction in [0,8] Time Unit

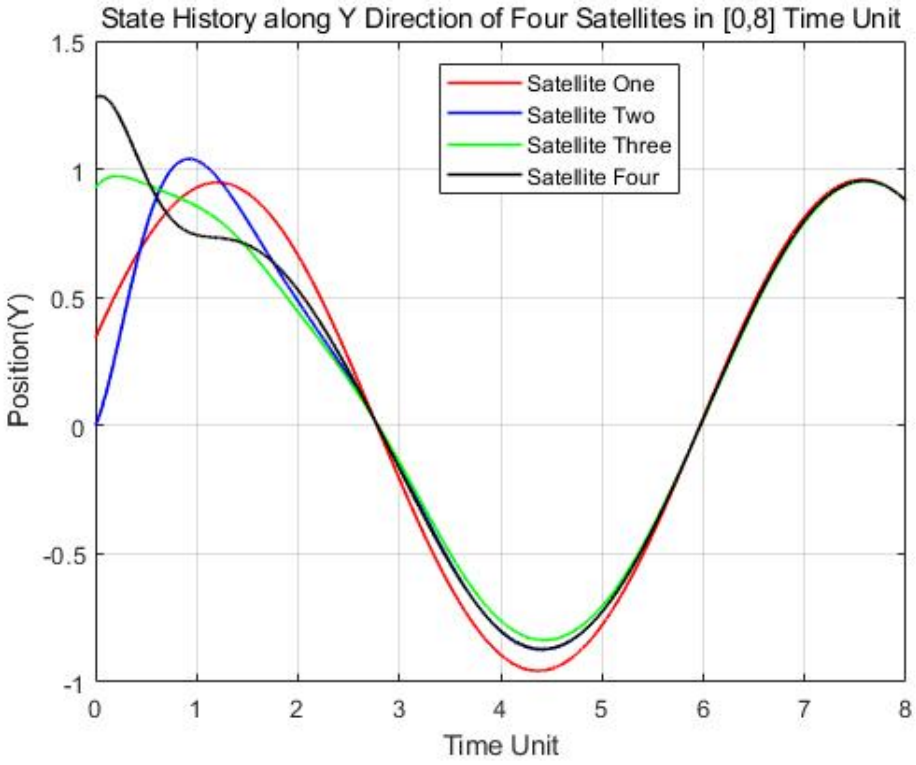

Figure 4.7. History of States of All Satellites along Y Direction in [0,8] Time Unit

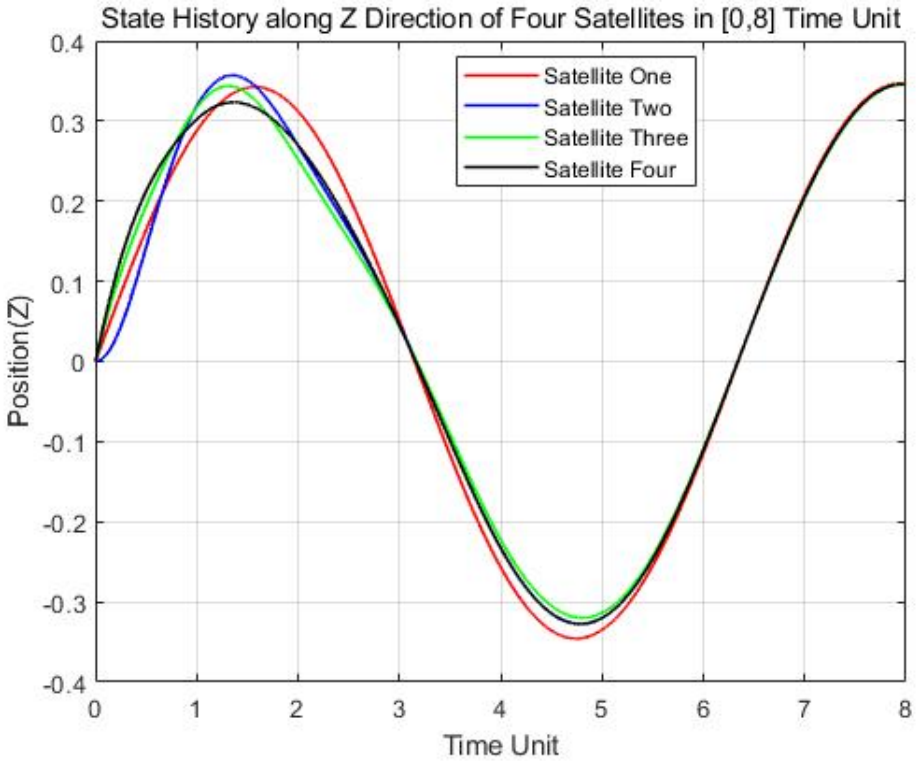

Figure 4.8. History of States of All Satellites along Z Direction in [0,8] Time Unit

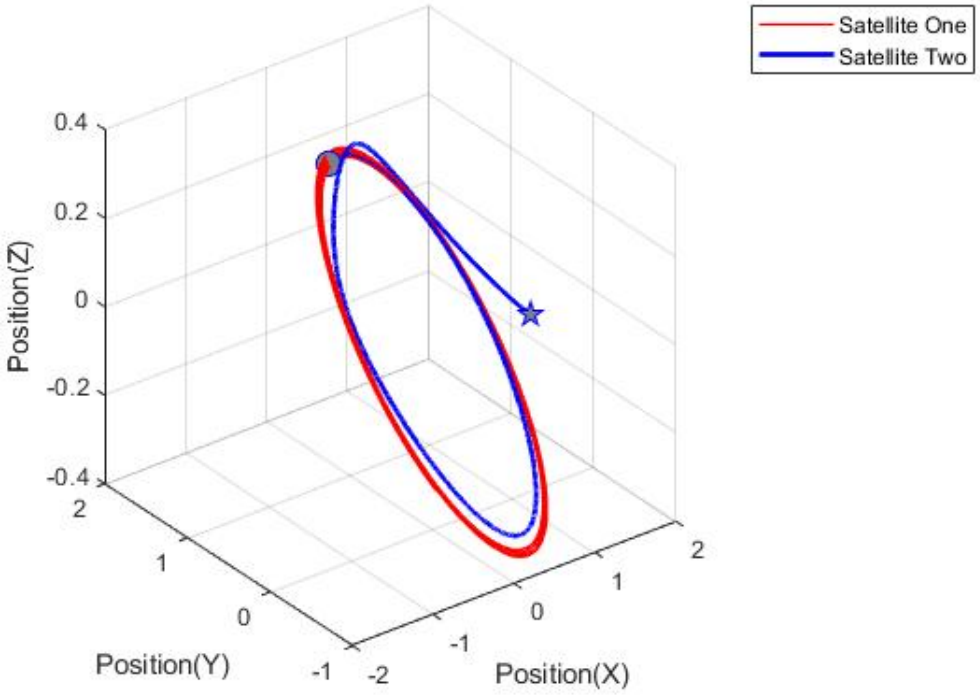

Figure 4.9. State History of Satellite Two in 3 Dimensional Frame

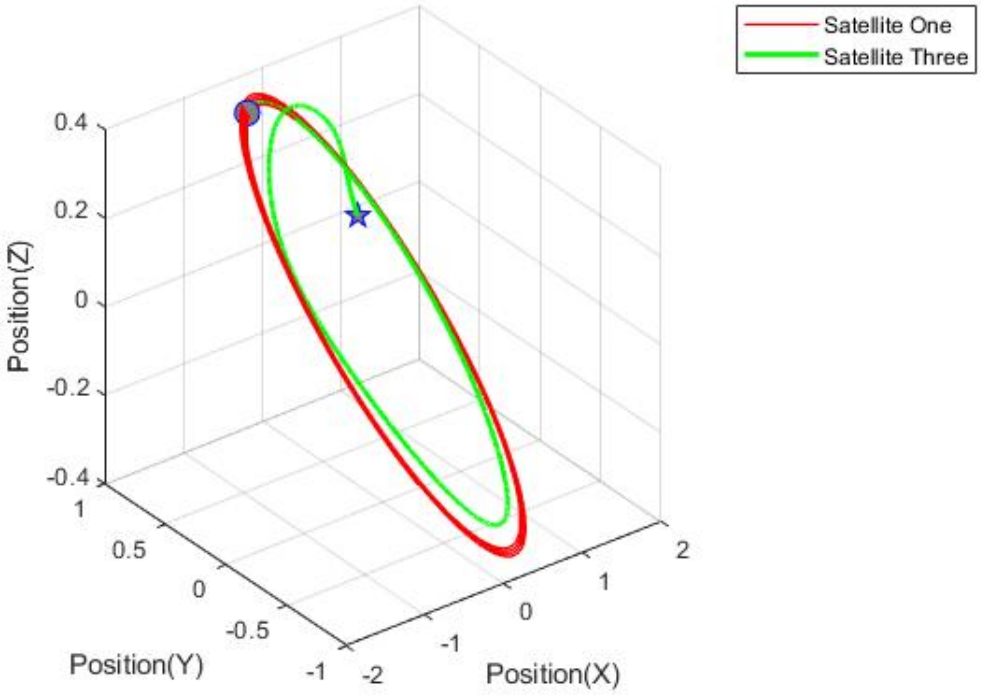

Figure 4.10. State History of Satellite Three in 3 Dimensional Frame

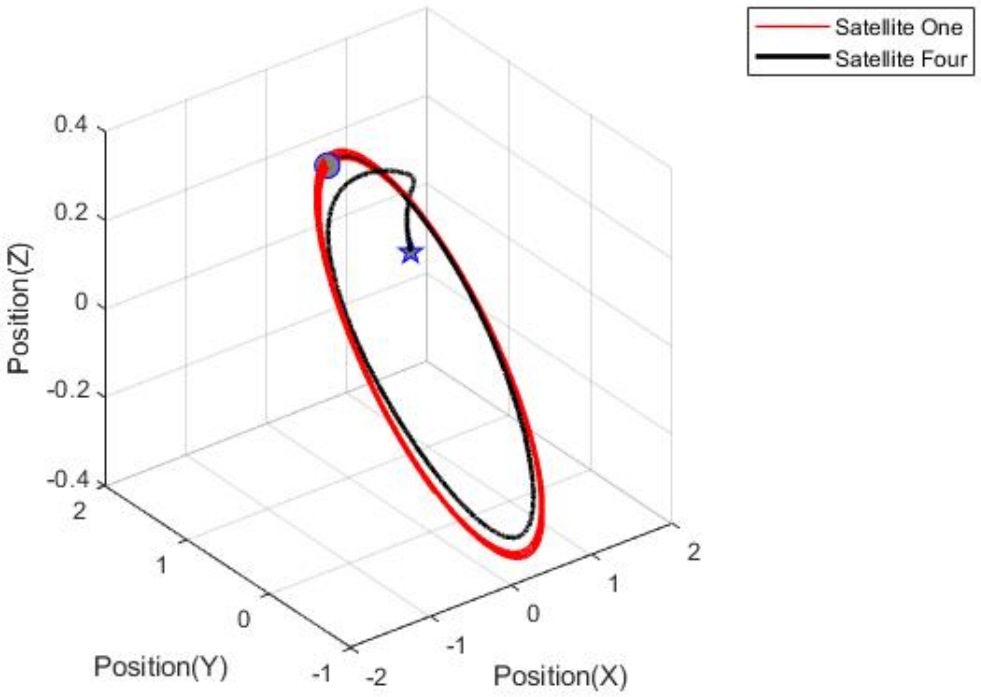

Figure 4.11. State History of Satellite Four in 3 Dimensional Frame

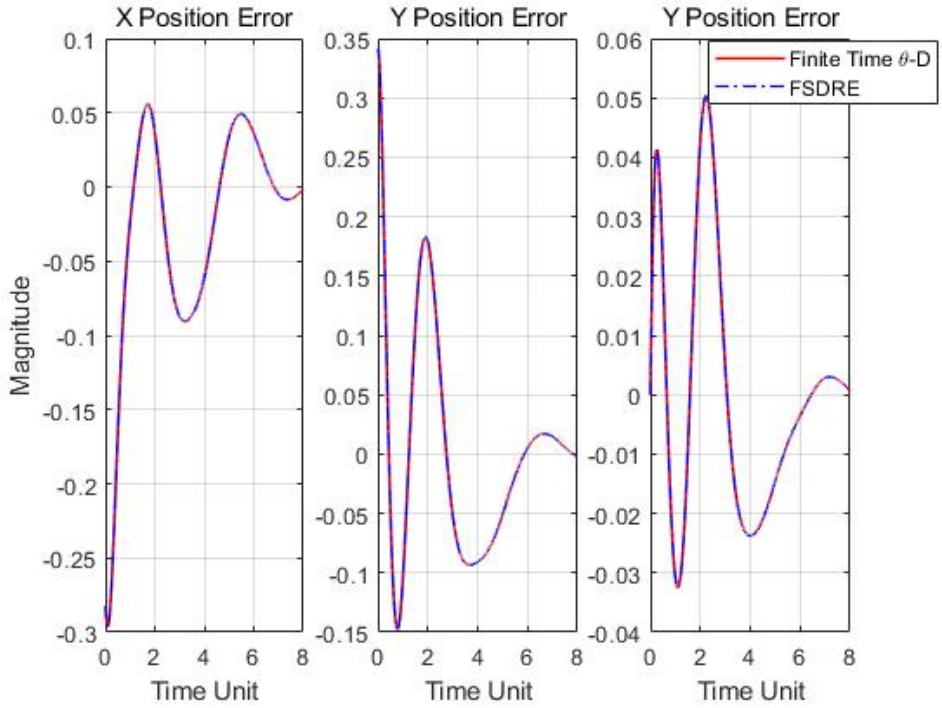

Figure 4.12. History of Position Error between Satellites Two with Satellites One by Finite Time $\theta - D$ Vs FSDRE

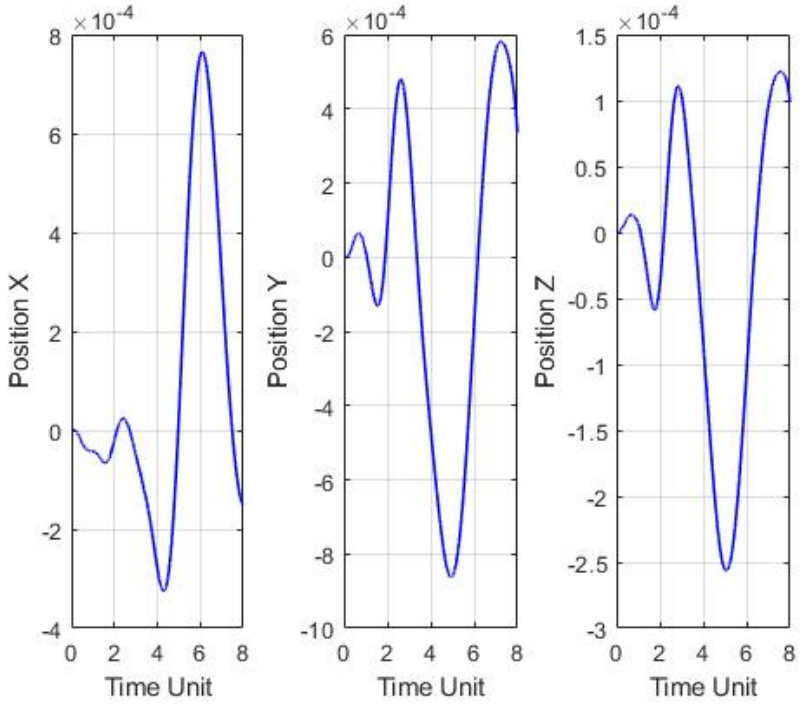

Figure 4.13. Detailed Difference by Finite Time $\theta - D$ Vs FSDRE between Satellites Two with Satellites One

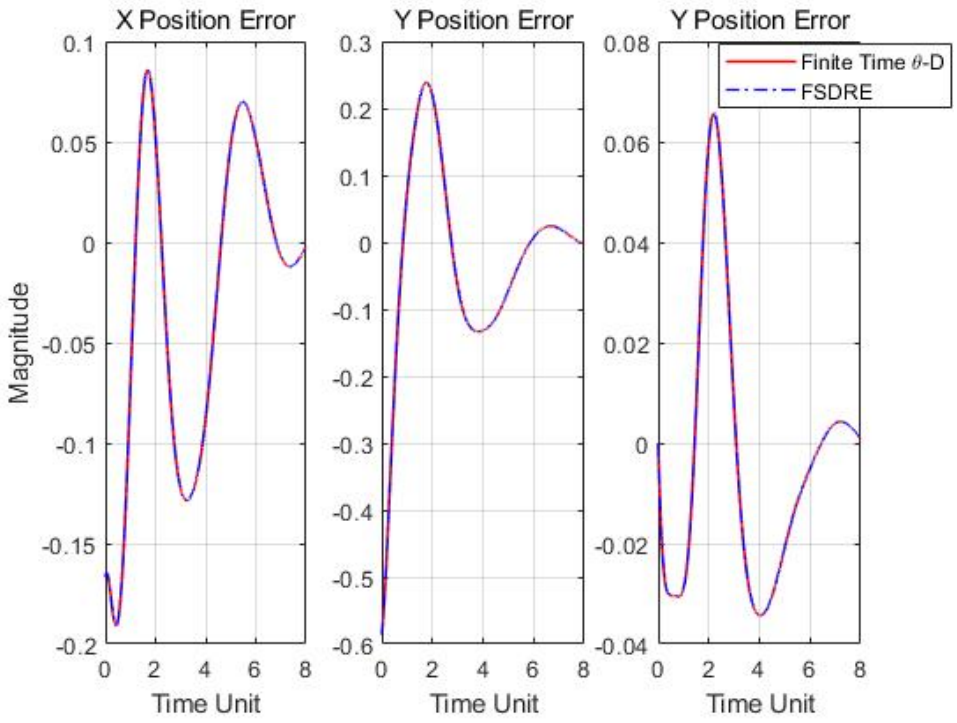

Figure 4.14. History of Position Error between Satellites Three with Satellites One by Finite Time $\theta - D$ Vs FSDRE

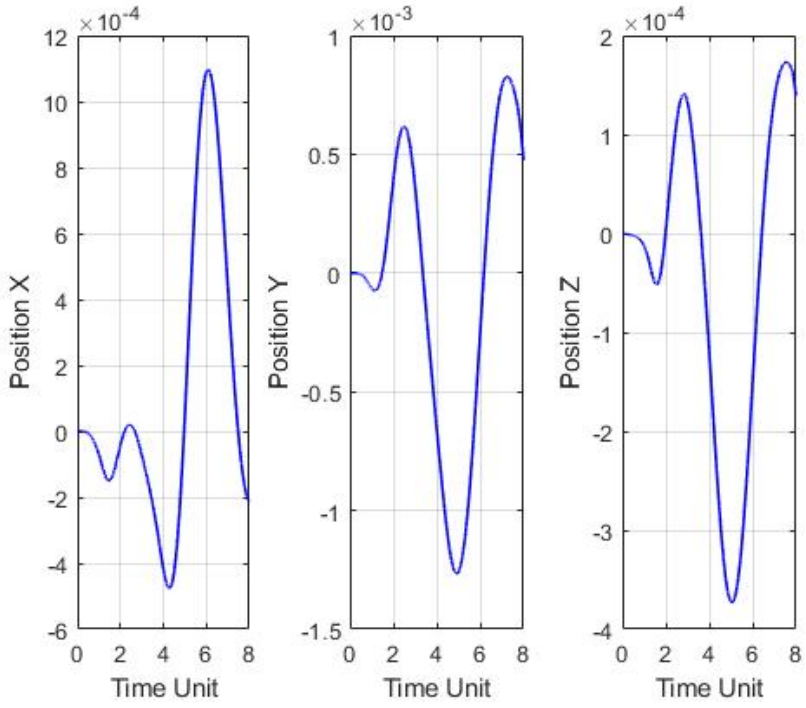

Figure 4.15. Detailed Difference by Finite Time $\theta - D$ Vs FSDRE between Satellites Three with Satellites One

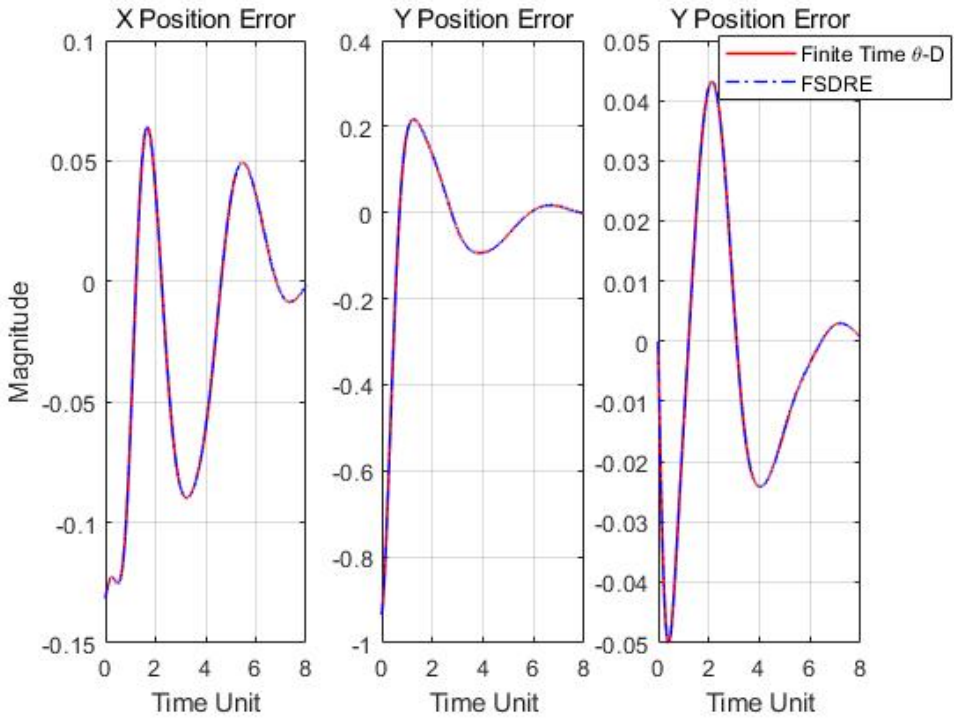

Figure 4.16. History of Position Error between Satellites Four with Satellites One by Finite Time $\theta - D$ Vs FSDRE

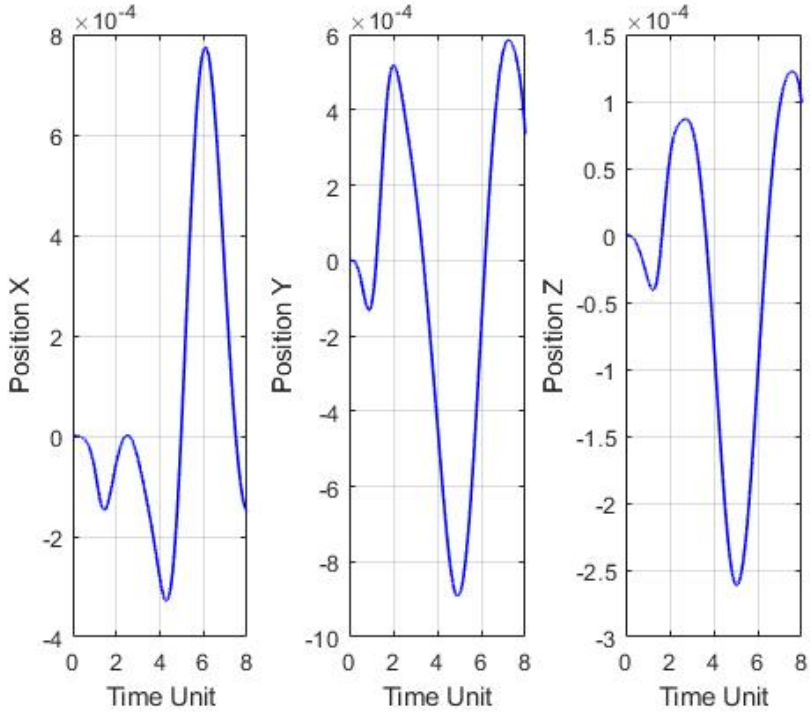

Figure 4.17. Detailed Difference by Finite Time $\theta - D$ Vs FSDRE between Satellites Four with Satellites One

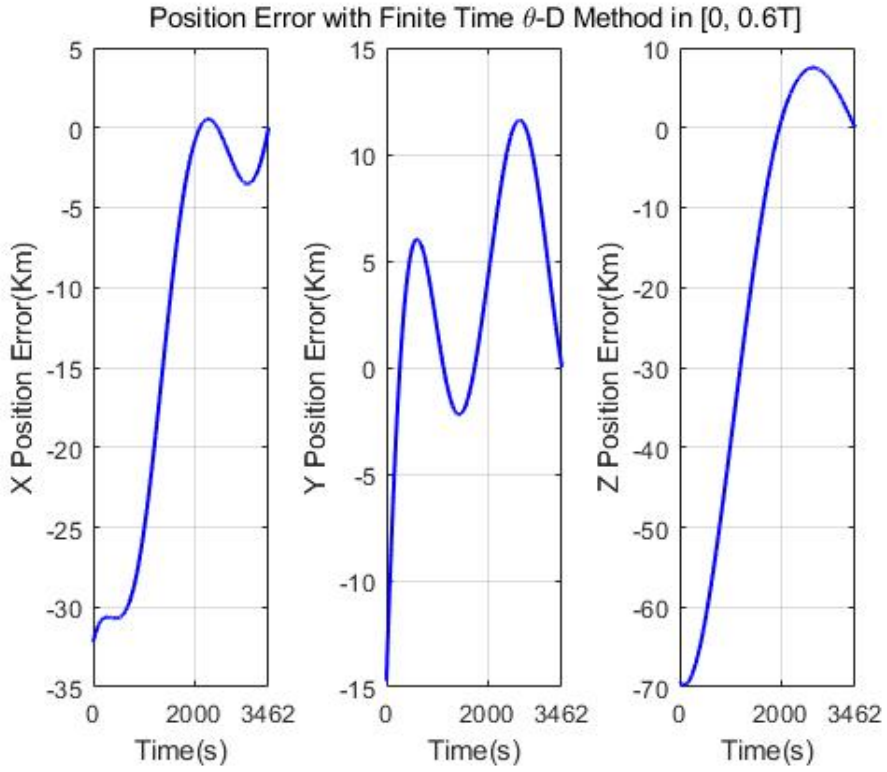

Figure 4.18. History of Position Error in [0,0.6T]

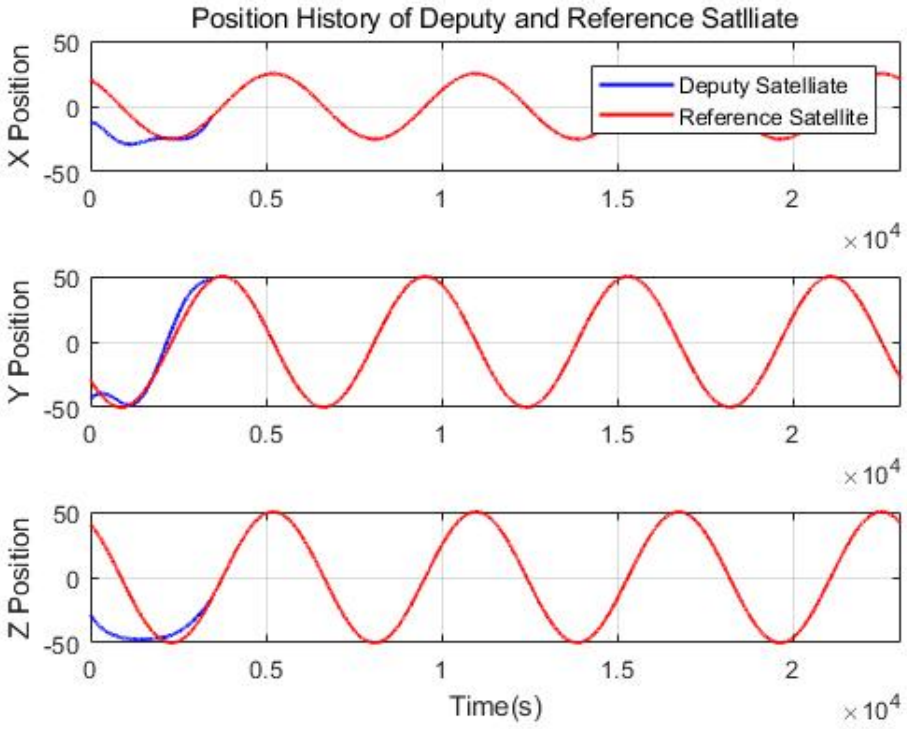

Figure 4.19. State History of Deputy and Reference Satellite

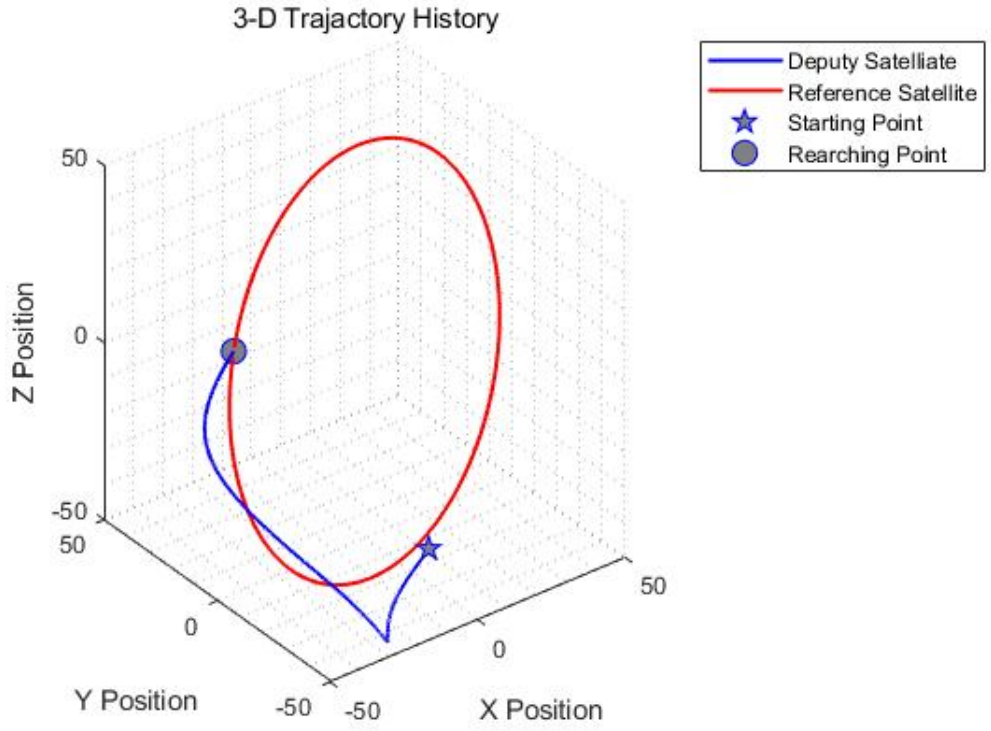

Figure 4.20. State History in 3 Dimensional Frame

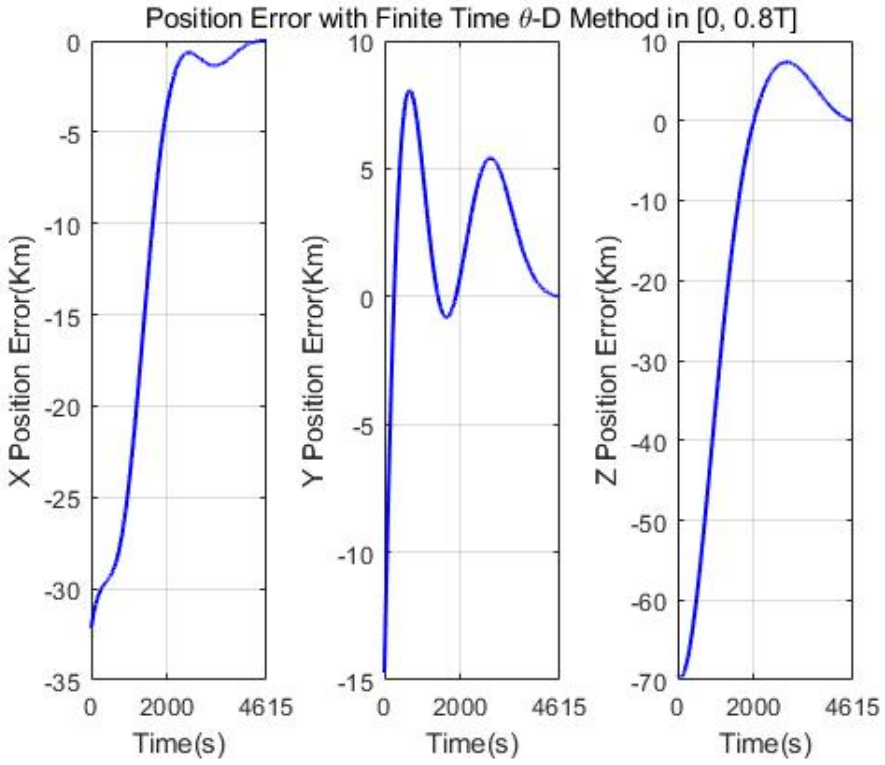

Figure 4.21. History of Position Error in [0,0.8T]

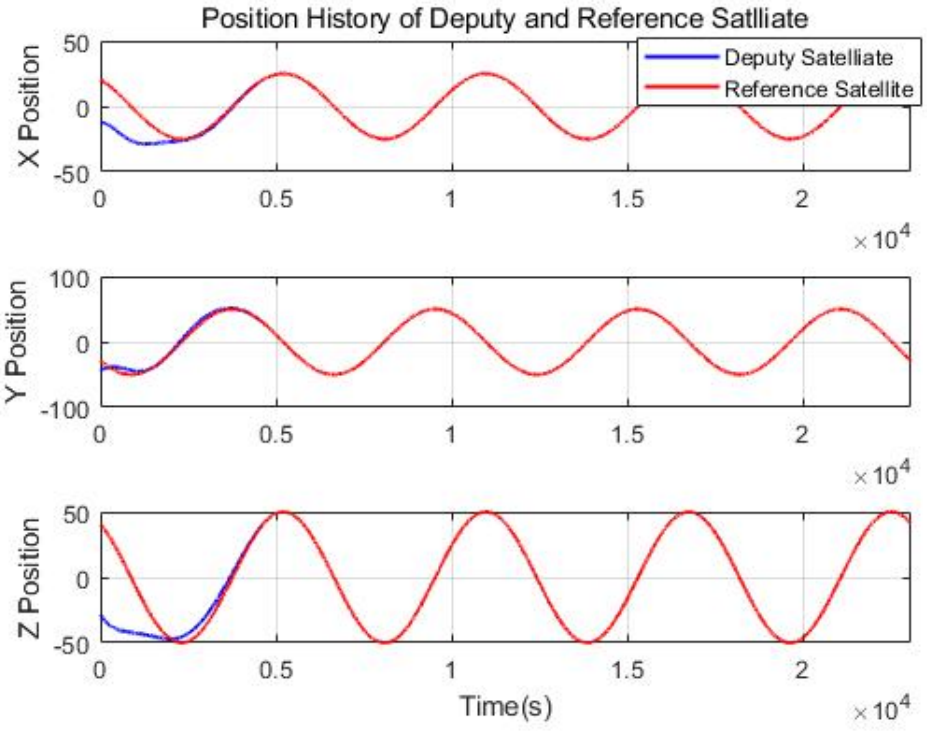

Figure 4.22. State History of Deputy and Reference Satellite

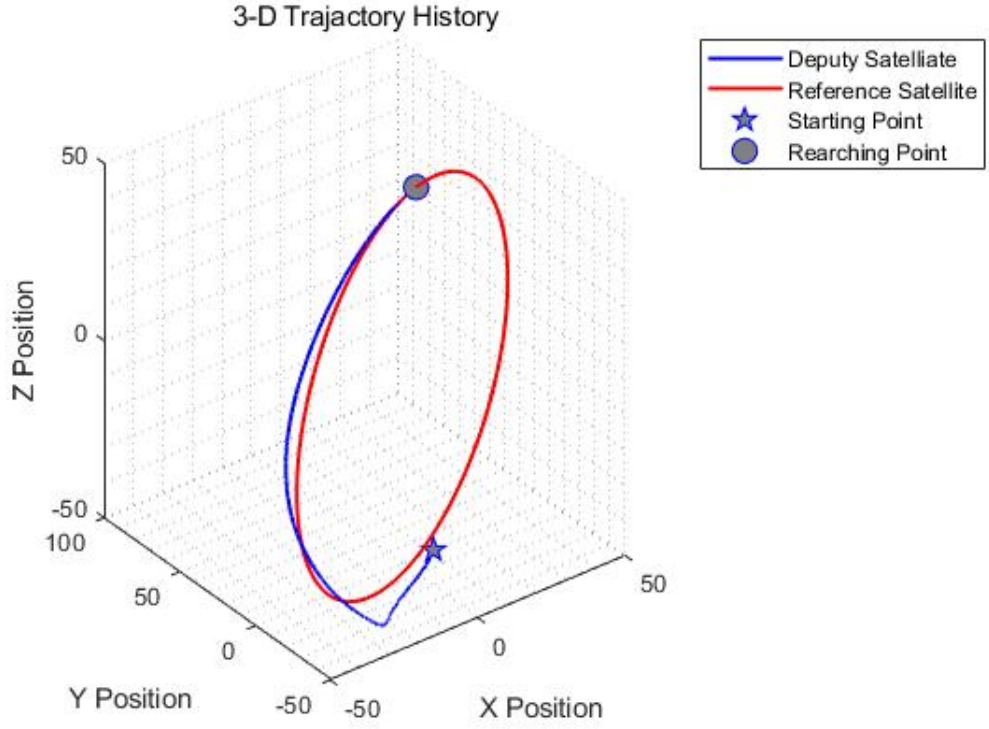

Figure 4.23. State History in 3 Dimensional Frame

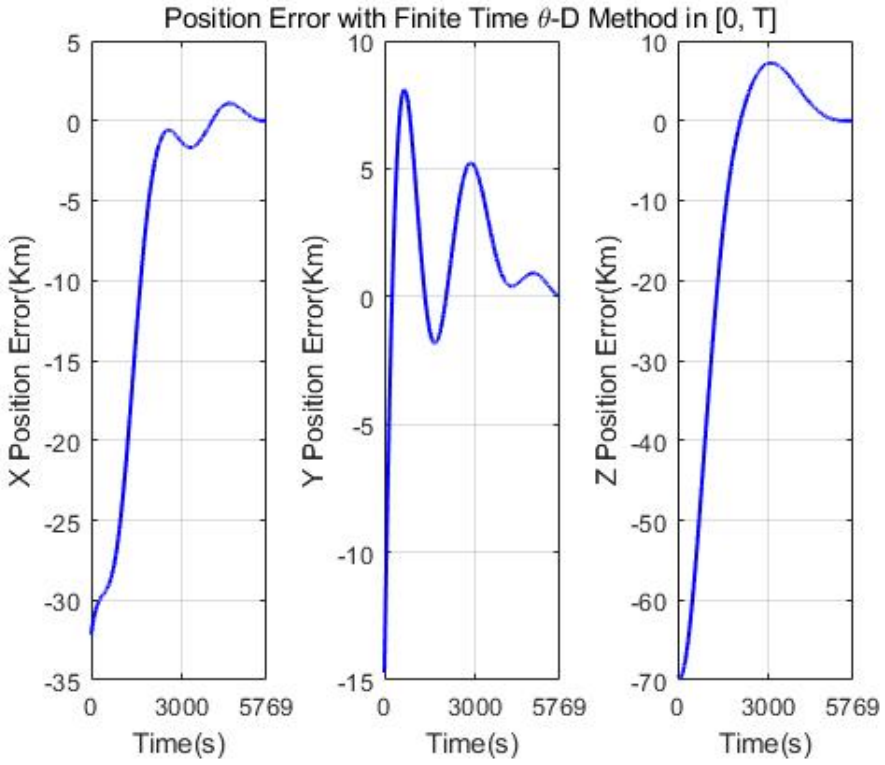

Figure 4.24. History of Position Error in [0,T]

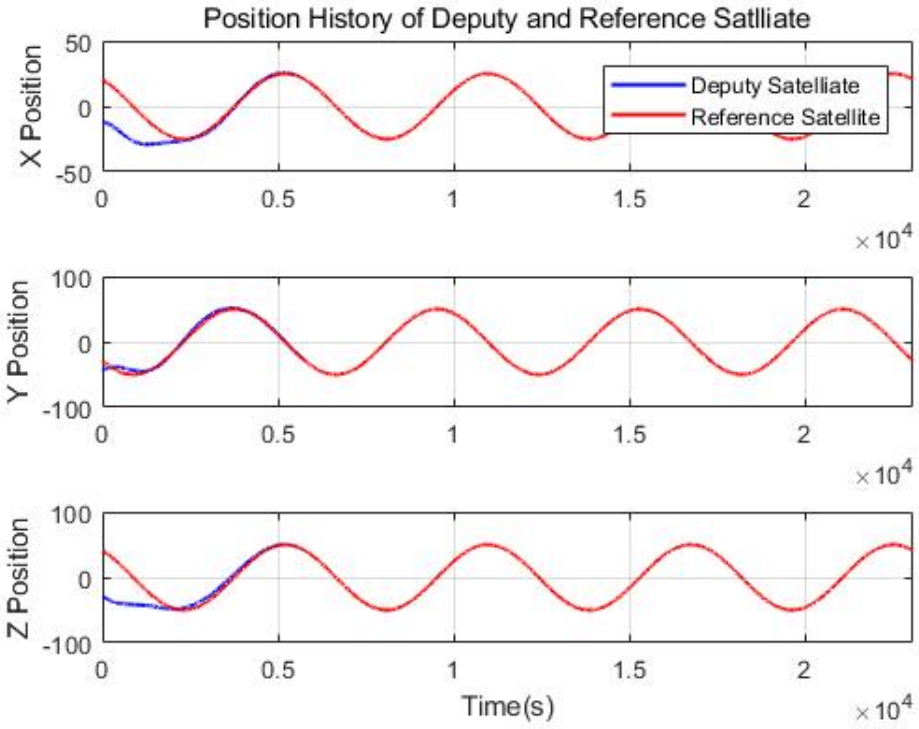

Figure 4.25. State History of Deputy and Reference Satellite

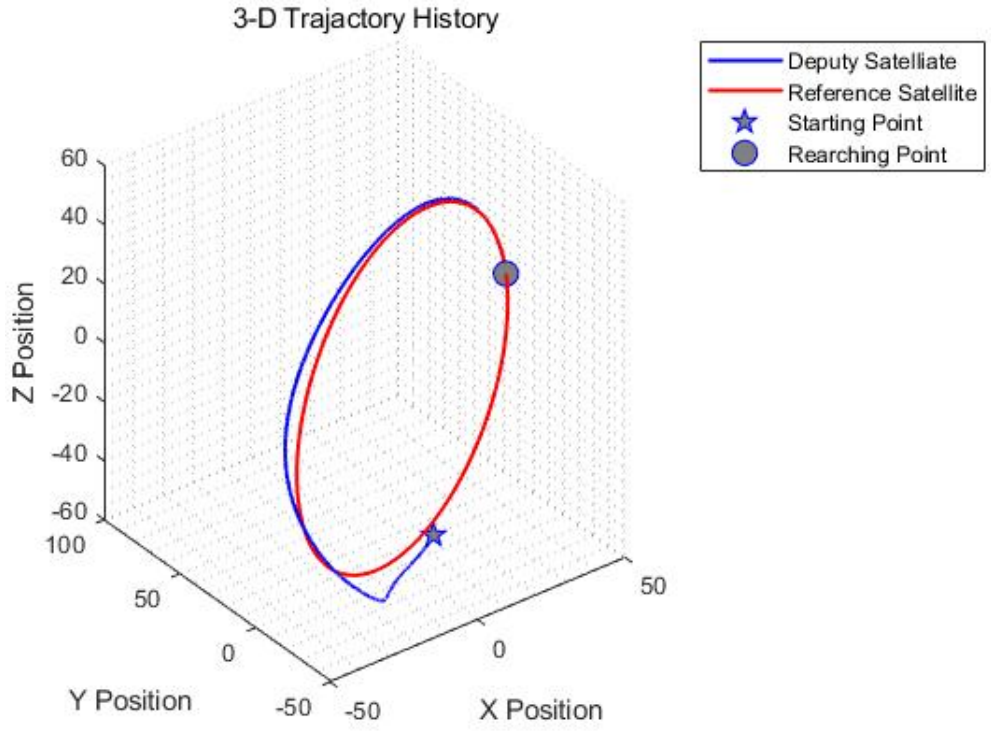

Figure 4.26. State History in 3 Dimensional Frame

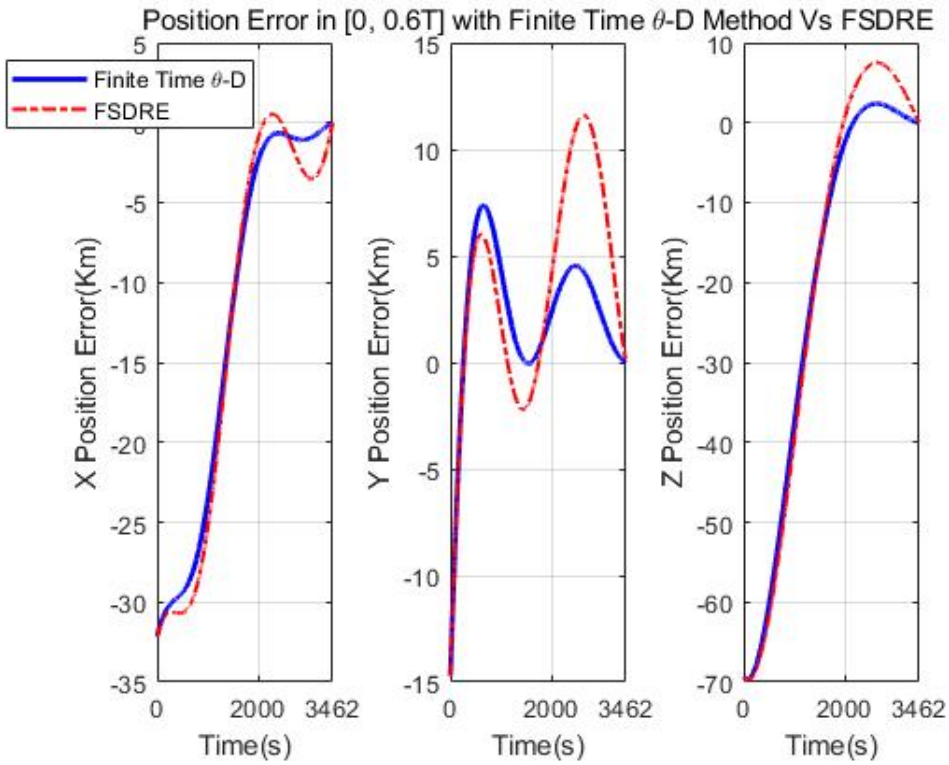

Figure 4.27. History of Position Error in [0, 0.6T] with Finite Time $\theta - D$ Vs FSDRE

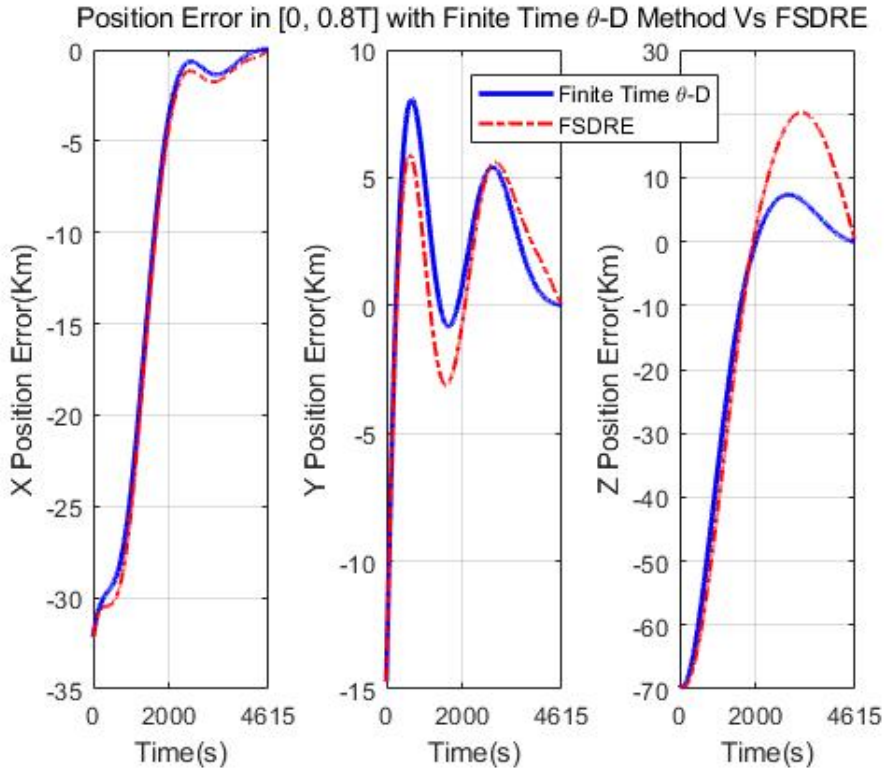

Figure 4.28. History of Position Error in [0, 0.8T] with Finite Time $\theta - D$ Vs FSDRE

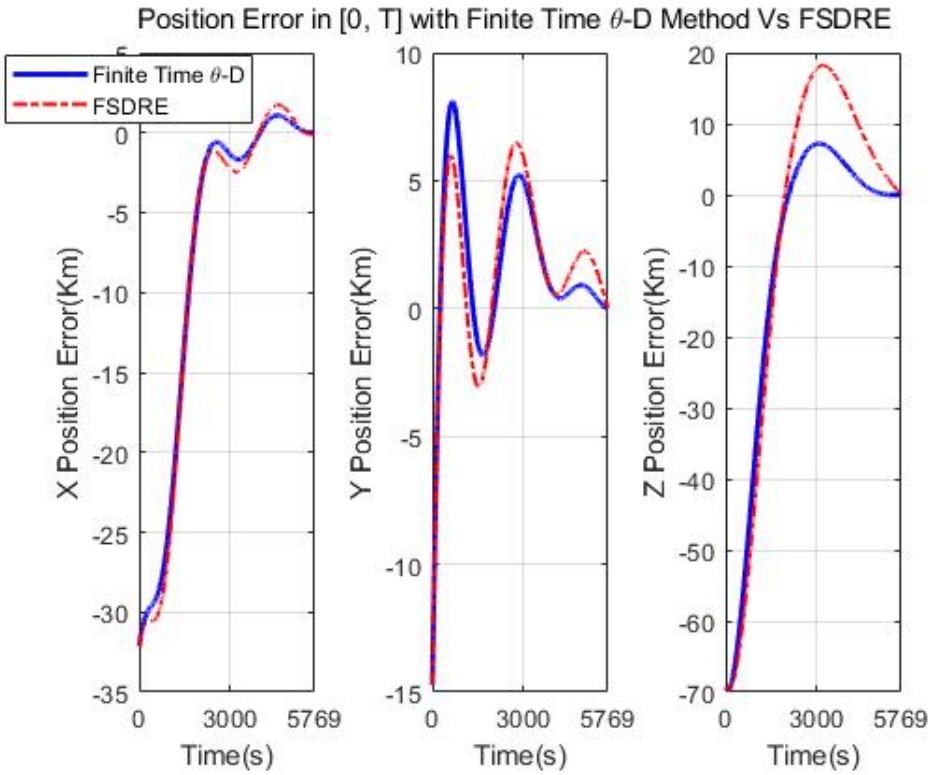

Figure 4.29. History of Position Error in [0, T] with Finite Time $\theta - D$ Vs FSDRE

5. CONCLUSIONS

5.1. CONCLUSION

In this dissertation, a novel finite time nonlinear optimal control synthesis technique, which is called finite time $\theta - D$ technique, was proposed. Originating from famous linear quadratic regulator (LQR) framework and State Dependent Riccati equation (SDRE) technique, the challenge of obtaining the closed form of finite time nonlinear optimal control problem was tackled successfully with the proposed finite time $\theta - D$ technique. Normally, LQR can get the optimal feedback control only for linear dynamics. SDRE can get optimal feedback control for nonlinear dynamics but with intensive computations. Different from other existing approximate expertise to get the sunoptimal finite time feedback controller, the finite time $\theta - D$ technique can guarantee the semi-global stability, and it was easy to implement online because the intensively computational load can be avoided. Practically, $T_0, T_1(x, \theta)$ and $T_2(x, \theta)$ are enough for engineering applications. Certainly, one can choose more $T_i(x, \theta)$ terms to get better performance with more computational time. The number of terms chosen was based on the design requirement. Dependent on the specific application and finite $T_i(x, \theta)$ terms, the semi-globally asymptotic stability and approximate closed form feedback controller was obtained. The phrase suboptimal property implies that the solution is not the analytical one, but an approximate one to the partial HJB equation because the exact analytical solution can not be obtained. By constructing the optimal cost expression, the power series of auxiliary parameter θ, and adding the perturbation term $D_i(k_i, l_i))$, the asymptotic stability based on Lyapunov theory and desired performance was guaranteed by tuning parameters k_i and l_i. This technique inherited the property of the LQR and that can be applied to the applications, which can be formulated as regulator or tracking problems. Most engineering applications can fall into this category.

Three aerospace applications were exemplified in this dissertation. Those three applications extended the originally proposed finite time $\theta - D$ technique. The RLV landing dynamics is a non-affine control nonlinear system. In order to apply the proposed technique into the RLV landing dynamics, a method was applied to transform the non-affine control to affine control by adding one more state variable. When one took the finite time $\theta - D$ technique to design control to nonlinear non-affine control application, this operation is routine practice. This application showed that other independent project-oriented variables (altitude, downrange,etc) can be viewed as "time" variable in the proposed finite time $\theta - D$ framework. That extends the application scope for this technique. As the LQR inherently held a certain robustness, this proposed technique also had robustness with different initial conditions. The most intriguing property was that this algorithm made online planning possible, which can guarantee the safe landing with a high probability. The second and third applications are satellite operations. The second one is the multiple satellites consensus control design from finite time optimal perspective. The proposed method can enrich the control design tool reservoir for the multiagent cooperative control. Also, the merit of time-saving computation can make it implementation on-board. The third application is to show how to implement the finite time $\theta - D$ technique with some model-known disturbance. In this application, a simple, but effective, way to handle the disturbance was shown. The final simulation result indicated that the disturbance rejection ability of this proposed technique was potential.

In conclusion, this dissertation provided an overall theoretical development procedure and applications of finite time $\theta - D$ technique characterised with nonlinear dynamics. Although the three applications are all from the aerospace engineering, it can also extend to other mechanical, electrical or even financial systems , whose dynamics are nonlinear and can be formulated to regulator or tracking tasks. This research is in its infants. The following are possible continuations for this work in the coming years.

5.2. FUTURE RESEARCH RECOMMENDATIONS

1. A systematic way to choose k_i and l_i needs to be developed.

2. In the third application, a simple way to address the model-known disturbance was presented. In the following research, the adaptive and robust way of tackling the disturbance or uncertainties should be developed. At the mean time, if the disturbances/uncertainties are unknown or partially known, one needs to determine how to address them.

3. Since the control algorithm should be processed by digital computer in those days, it is necessary to develop a discrete time version of $\theta - D$ control algorithm.

4. Since the filter/observer was the dual form of the controller, finite time $\theta - D$ filter can be presented to some applications.

5. In this dissertation, only a few applications were considered. It is necessary to find more interesting applications in different areas, whose mathematical models are characterized as nonlinear dynamics and the problems can be formulated as regulator or tracking form.

6. In this dissertation, the state constraints and input constraints problems were not addressed. It will involve many practical engineering problems; for example, control saturation, obstacle-avoidance in Unmanned Aerial Vehicle (UAV) or automatons cars, single-agent or multi-agent obstacle-avoidance, etc. Transforming the constraint conditions into the state penalty matrix $Q(x)$ and input penalty matrix $R(x)$ is needed. The question is how to transform, which deserves further investigation.

REFERENCES

Al'brekht, E., 'On the optimal stabilization of nonlinear systems,' Journal of Applied Mathematics and Mechanics, 1961, **25**(5), pp. 1254 – 1266, ISSN 0021-8928, doi: https://doi.org/10.1016/0021-8928(61)90005-3.

Ammar, A., Kheldoun, A., Metidji, B., Ameid, T., and Azzoug, Y., 'Feedback linearization based sensorless direct torque control using stator flux mras-sliding mode observer for induction motor drive,' ISA transactions, 2020, **98**, pp. 382–392.

Athans, M., 'The matrix minimum principle,' 1967.

Balakrishnan, S., Pernicka, H. J., and Xin, M., 'Multiple spacecraft formation control with θ-d method,' 2007.

Beard, R. W., Saridis, G. N., and Wen, J. T., 'Approximate solutions to the time-invariant hamilton–jacobi–bellman equation,' Journal of Optimization theory and Applications, 1998, **96**(3), pp. 589–626.

Bellman, R., 'Dynamic programming,' Science, 1966, **153**(3731), pp. 34–37.

Bertizzolo, L., D'oro, S., Ferranti, L., Bonati, L., Demirors, E., Guan, Z., Melodia, T., and Pudlewski, S., 'Swarmcontrol: An automated distributed control framework for self-optimizing drone networks,' arXiv preprint arXiv:2005.09781, 2020.

Bilal, M., Vijayan, R., and Schilling, K., 'Sdre control with nonlinear j2 perturbations for nanosatellite formation flying,' IFAC-PapersOnLine, 2019, **52**(12), pp. 448–453.

Blackmore, L., 'Autonomous precision landing of space rockets,' in 'in Frontiers of Engineering: Reports on Leading-Edge Engineering from the 2016 Symposium,' volume 46, 2016 pp. 15–20.

Brewer, J., 'Kronecker products and matrix calculus in system theory,' IEEE Transactions on circuits and systems, 1978, **25**(9), pp. 772–781.

Bryson, A. E., 'Optimal control-1950 to 1985,' IEEE Control Systems Magazine, 1996, **16**(3), pp. 26–33.

Byrnes, C. I., Isidori, A., Willems, J. C., *et al.*, 'Passivity, feedback equivalence, and the global stabilization of minimum phase nonlinear systems,' IEEE Transactions on automatic control, 1991, **36**(11), pp. 1228–1240.

Chen, C.-T., 'Linear system theory ans design,' International Edition, 1996.

Chen, X. and Chen, X., 'An iterative method for optimal feedback control and generalized hjb equation,' IEEE/CAA Journal of Automatica Sinica, 2017, **5**(5), pp. 999–1006.

Chen, X. and Zhao, L., 'Observer based finite-time attitude containment control of multiple spacecraft systems,' IEEE Transactions on Circuits and Systems II: Express Briefs, 2020.

Chen, Y., Edgar, T., and Manousiouthakis, V., 'On infinite-time nonlinear quadratic optimal control,' Systems & control letters, 2004, **51**(3-4), pp. 259–268.

Chiasson, J., 'A new approach to dynamic feedback linearization control of an induction motor,' IEEE Transactions on Automatic Control, 1998, **43**(3), pp. 391–397.

Çimen, T., 'State-dependent riccati equation (sdre) control: A survey,' IFAC Proceedings Volumes, 2008, **41**(2), pp. 3761–3775.

Çimen, T., 'Systematic and effective design of nonlinear feedback controllers via the state-dependent riccati equation (sdre) method,' Annual Reviews in control, 2010, **34**(1), pp. 32–51.

Cloutier, J. R., 'State-dependent riccati equation techniques: an overview,' in 'Proceedings of the 1997 American control conference (Cat. No. 97CH36041),' volume 2, IEEE, 1997 pp. 932–936.

Cloutier, J. R., D'Souza, C. N., and Mracek, C. P., 'Nonlinear regulation and nonlinear h control via the state-dependent riccati equation technique: Part 1, theory,' in 'Proceedings of the international conference on nonlinear problems in aviation and aerospace,' Embry Riddle University, 1996 pp. 117–131.

Curtis, H. D., *Orbital mechanics for engineering students*, Butterworth-Heinemann, 2013.

Dierks, T. and Jagannathan, S., 'Online optimal control of affine nonlinear discrete-time systems with unknown internal dynamics by using time-based policy update,' IEEE Transactions on Neural Networks and Learning Systems, 2012, **23**(7), pp. 1118–1129, ISSN 2162-2388, doi:10.1109/TNNLS.2012.2196708.

Ding, J. and Balakrishnan, S., 'Approximate dynamic programming solutions with a single network adaptive critic for a class of nonlinear systems,' Journal of Control Theory and Applications, 2011, **9**(3), pp. 370–380.

Drake, D., Xin, M., and Balakrishnan, S., 'Theta-d control technique for ascent phase of reusable launch vehicles,' in 'AIAA Guidance, Navigation, and Control Conference and Exhibit,' 2004 p. 5018.

Duan, D., Liu, C., and Sun, J., 'Adaptive periodic event-triggered control for missile-target interception system with finite-horizon convergence,' Transactions of the Institute of Measurement and Control, 2020, p. 0142331219897186.

Edwards, C. and Spurgeon, S., *Sliding mode control: theory and applications*, Crc Press, 1998.

Fakharian, A., Hamidi Beheshti, M., and Davari, A., 'Solving the hamilton–jacobi–bellman equation using adomian decomposition method,' International Journal of Computer Mathematics, 2010, **87**(12), pp. 2769–2785.

Franco, T. C. and dos Santos, W. G., 'Itasat-2: Formation flying maneuver and control considering 2 disturbances and differential drag,' 2020.

Franzini, G. and Innocenti, M., 'Relative motion dynamics with arbitrary perturbations in the local-vertical local-horizon reference frame,' The Journal of the Astronautical Sciences, 2020, **67**(1), pp. 98–112.

Gao, X. and Weng, Y., 'Chattering-free model free adaptive sliding mode control for gas collection process with data dropout,' Journal of Process Control, 2020, **93**, pp. 1–13.

Garg, K., Arabi, E., and Panagou, D., 'Prescribed-time convergence with input constraints: A control lyapunov function based approach,' in '2020 American Control Conference (ACC),' IEEE, 2020 pp. 962–967.

Garrard, W. L., McClamroch, N., and Clark, L., 'An approach to sub-optimal feedback control of non-linear systems,' International Journal of Control, 1967, **5**(5), pp. 425–435.

Gelfand, I. M., Silverman, R. A., *et al.*, *Calculus of variations*, Courier Corporation, 2000.

Geng, Y., Li, C., Guo, Y., and Biggs, J. D., 'Fixed-time near-optimal control for repointing maneuvers of a spacecraft with nonlinear terminal constraints,' ISA transactions, 2020, **97**, pp. 401–414.

Grandia, R., Taylor, A. J., Singletary, A., Hutter, M., and Ames, A. D., 'Nonlinear model predictive control of robotic systems with control lyapunov functions,' arXiv preprint arXiv:2006.01229, 2020.

Hao, Y., He, Y., Xie, Y., Sun, C., and Zhao, K., 'Neural-network based finite-time coordinated formation control for spacecraft without unwinding,' IEEE Access, 2020, **8**, pp. 127507–127518.

Harl, N. and Balakrishnan, S., 'Reentry terminal guidance through sliding mode control,' Journal of guidance, control, and dynamics, 2010, **33**(1), pp. 186–199.

Harl, N., Balakrishnan, S., and Phillips, C., 'Sliding mode integrated missile guidance and control,' in 'AIAA guidance, navigation, and control conference,' 2010 p. 7741.

Heydari, A. and Balakrishnan, S., 'Finite-horizon input-constrained nonlinear optimal control using single network adaptive critics,' in 'Proceedings of the 2011 American Control Conference,' IEEE, 2011a pp. 3047–3052.

Heydari, A. and Balakrishnan, S., 'Optimal online path planning for approach and landing guidance,' in 'AIAA Atmospheric Flight Mechanics Conference,' 2011b p. 6641.

Heydari, A. and Balakrishnan, S., 'Path planning using a novel finite horizon suboptimal controller,' Journal of guidance, control, and dynamics, 2013a, **36**(4), pp. 1210–1214.

Heydari, A. and Balakrishnan, S., 'Closed-form solution to finite-horizon suboptimal control of nonlinear systems,' International Journal of Robust and Nonlinear Control, 2015, **25**(15), pp. 2687–2704.

Heydari, A. and Balakrishnan, S. N., 'Finite-horizon control-constrained nonlinear optimal control using single network adaptive critics,' IEEE Transactions on Neural Networks and Learning Systems, 2012, **24**(1), pp. 145–157.

Heydari, A. and Balakrishnan, S. N., 'Fixed-final-time optimal control of nonlinear systems with terminal constraints,' Neural Networks, 2013b, **48**, pp. 61–71.

Heydari, A. and Balakrishnan, S. N., 'Fixed-final-time optimal tracking control of input-affine nonlinear systems,' Neurocomputing, 2014, **129**, pp. 528–539.

Hosseinabadi, P. A., Abadi, A. S. S., Mekhilef, S., and Pota, H. R., 'Chattering-free trajectory tracking robust predefined-time sliding mode control for a remotely operated vehicle,' Journal of Control, Automation and Electrical Systems, 2020, pp. 1–19.

Isidori, A., *Nonlinear control systems*, Springer Science & Business Media, 2013.

Jacobson, D., 'New conditions for boundedness of the solution of a matrix riccati differential equation,' Journal of Differential Equations, 1970, **8**(2), pp. 258–263.

James, J., 'Entry guidance training manual,' NASA Johnson Space Center, Flight Training Branch, Houston, TX, 1988.

Jin, X., 'Fault tolerant finite-time leader–follower formation control for autonomous surface vessels with los range and angle constraints,' Automatica, 2016, **68**, pp. 228–236.

Khalil, H. K. and Grizzle, J. W., *Nonlinear systems*, volume 3, Prentice hall Upper Saddle River, NJ, 2002.

Kim, J. W., Park, B. J., Yoo, H., Oh, T. H., Lee, J. H., and Lee, J. M., 'A model-based deep reinforcement learning method applied to finite-horizon optimal control of nonlinear control-affine system,' Journal of Process Control, 2020, **87**, pp. 166–178.

Krstic, M., Kokotovic, P. V., and Kanellakopoulos, I., *Nonlinear and adaptive control design*, John Wiley & Sons, Inc., 1995.

Kučera, V., 'A review of the matrix riccati equation,' Kybernetika, 1973, **9**(1), pp. 42–61.

Lewis, F. L. and Liu, D., *Reinforcement learning and approximate dynamic programming for feedback control*, volume 17, John Wiley & Sons, 2013.

Lewis, F. L., Vrabie, D., and Syrmos, V. L., *Optimal control*, John Wiley & Sons, 2012.

Lewis, F. L., Zhang, H., Hengster-Movric, K., and Das, A., *Cooperative control of multi-agent systems: optimal and adaptive design approaches*, Springer Science & Business Media, 2013.

Li, M. and Hu, J., 'An approach and landing guidance design for reusable launch vehicle based on adaptive predictor–corrector technique,' Aerospace Science and Technology, 2018, **75**, pp. 13–23.

Liao, X. and Chen, L., 'Integral sliding mode control based approach and landing guidance law with finite-time convergence,' Optik, 2016, **127**(20), pp. 8215–8230.

Liu, D. and Wei, Q., 'Finite-approximation-error-based optimal control approach for discrete-time nonlinear systems,' IEEE Transactions on Cybernetics, 2013, **43**(2), pp. 779–789, ISSN 2168-2275, doi:10.1109/TSMCB.2012.2216523.

Liu, D. and Wei, Q., 'Policy iteration adaptive dynamic programming algorithm for discrete-time nonlinear systems,' IEEE Transactions on Neural Networks and Learning Systems, 2014, **25**(3), pp. 621–634, ISSN 2162-2388, doi: 10.1109/TNNLS.2013.2281663.

Liu, D., Wei, Q., Wang, D., Yang, X., and Li, H., *Adaptive dynamic programming with applications in optimal control*, Springer, 2017.

Liu, H., Pan, Y., Cao, J., Wang, H., and Zhou, Y., 'Adaptive neural network backstepping control of fractional-order nonlinear systems with actuator faults,' IEEE Transactions on Neural Networks and Learning Systems, 2020a.

Liu, H., Tian, Y., and Lewis, F. L., 'Robust trajectory tracking in satellite time-varying formation flying,' IEEE Transactions on Cybernetics, 2020b.

Lukes, D. L., 'Optimal regulation of nonlinear dynamical systems,' SIAM Journal on Control, 1969, **7**(1), pp. 75–100, doi:10.1137/0307007.

Mashtakov, Y., Ovchinnikov, M., Petrova, T., and Tkachev, S., 'Two-satellite formation flying control by cell-structured solar sail,' Acta Astronautica, 2020, **170**, pp. 592–600.

Ming, X., Balakrishnanand, S., and Ohlmeyer, E. J., 'Integrated guidance and control of missiles with θ-d method,' Control Systems Technology IEEE Transactions, 2006, **14**(6), pp. 981–992.

Mori, T. and Deresei, I., 'A brief summary of the bounds on the solution of the algebraic matrix equations in control theory,' International Journal of Control, 1984, **39**(2), pp. 247–256.

Padhi, R., Unnikrishnan, N., Wang, X., and Balakrishnan, S., 'A single network adaptive critic (snac) architecture for optimal control synthesis for a class of nonlinear systems,' Neural Networks, 2006, **19**(10), pp. 1648–1660.

Qureshi, D. and Salim, M., 'A comprehensive survey of sliding mode-based control methodologies for robotic manipulator,' A Comprehensive Survey of Sliding Mode-Based Control Methodologies for Robotic Manipulator (June 11, 2020), 2020.

Rudin, W. *et al.*, *Principles of mathematical analysis*, volume 3, McGraw-hill New York, 1964.

Sachan, A., Al Ayubi, H., and Garg, M. K., 'Integral sliding mode for nonlinear system: A control-lyapunov function approach,' in 'Advances in Machine Learning and Computational Intelligence,' pp. 813–823, Springer, 2020.

Salkuyeh, D. K., 'Shifted skew-symmetric/skew-symmetric splitting method and its application to generalized saddle point problems,' Applied Mathematics Letters, 2020, **103**, p. 106184.

Sanfelice, R., 'Clf-based control for hybrid dynamical systems,' arXiv preprint arXiv:2009.03819, 2020.

Shamma, J. S. and Cloutier, J. R., 'Existence of sdre stabilizing feedback,' IEEE Transactions on Automatic Control, 2003, **48**(3), pp. 513–517.

Slotine, J.-J. E., Li, W., *et al.*, *Applied nonlinear control*, volume 199, Prentice hall Englewood Cliffs, NJ, 1991.

Stansbery, D. T. and Cloutier, J. R., 'Position and attitude control of a spacecraft using the state-dependent riccati equation technique,' in 'Proceedings of the 2000 American Control Conference. ACC (IEEE Cat. No. 00CH36334),' volume 3, IEEE, 2000 pp. 1867–1871.

Sussmann, H. J. and Willems, J. C., '300 years of optimal control: from the brachystochrone to the maximum principle,' IEEE Control Systems Magazine, 1997, **17**(3), pp. 32–44.

Tripathi, A. K., Patel, V. V., and Padhi, R., 'Autonomous landing design of uavs using feedback linearization controller with anti windup scheme,' IFAC-PapersOnLine, 2020, **53**(1), pp. 81–86.

Vadali, S., Schaub, H., and Alfriend, K., 'Initial conditions and fuel-optimal control for formation flying of satellites,' in 'Guidance, Navigation, and Control Conference and Exhibit,' 1999 p. 4265.

Wan, S., Li, X., Su, W., Yuan, J., and Hong, J., 'Active chatter suppression for milling process with sliding mode control and electromagnetic actuator,' Mechanical Systems and Signal Processing, 2020, **136**, p. 106528.

Wang, D., Liu, D., and Wei, Q., 'Finite-horizon neuro-optimal tracking control for a class of discrete-time nonlinear systems using adaptive dynamic programming approach,' Neurocomputing, 2012, **78**(1), pp. 14–22.

Wang, F., Zhang, H., and Liu, D., 'Adaptive dynamic programming: An introduction,' IEEE Computational Intelligence Magazine, 2009, **4**(2), pp. 39–47, ISSN 1556-6048, doi: 10.1109/MCI.2009.932261.

Wang, F.-Y., Jin, N., Liu, D., and Wei, Q., 'Adaptive dynamic programming for finite-horizon optimal control of discrete-time nonlinear systems with ε-error bound,' IEEE Transactions on Neural Networks, 2010, **22**(1), pp. 24–36.

Wang, J., Wang, C., Wei, Y., and Zhang, C., 'Filter-backstepping based neural adaptive formation control of leader-following multiple auvs in three dimensional space,' Ocean Engineering, 2020, **201**, p. 107150.

Wei, Q., Wang, F., Liu, D., and Yang, X., 'Finite-approximation-error-based discrete-time iterative adaptive dynamic programming,' IEEE Transactions on Cybernetics, 2014, **44**(12), pp. 2820–2833, ISSN 2168-2275, doi:10.1109/TCYB.2014.2354377.

Wernli, A. and Cook, G., 'Suboptimal control for the nonlinear quadratic regulator problem,' Automatica, 1975, **11**(1), pp. 75–84.

Westenbroek, T., Fridovich-Keil, D., Mazumdar, E., Arora, S., Prabhu, V., Sastry, S. S., and Tomlin, C. J., 'Feedback linearization for uncertain systems via reinforcement learning,' in '2020 IEEE International Conference on Robotics and Automation (ICRA),' IEEE, 2020 pp. 1364–1371.

Xiangdong, L., Zhang, F., Zhen, L., and Yao, Z., 'Approach and landing guidance design for reusable launch vehicle using multiple sliding surfaces technique,' Chinese Journal of Aeronautics, 2017, **30**(4), pp. 1582–1591.

Xin, M. and Balakrishnan, S., 'A new optimal nonlinear control method and its application to missile guidance law design,' in 'AIAA Guidance, Navigation, and Control Conference and Exhibit,' 2002 p. 5023.

Xin, M. and Balakrishnan, S., 'Missile longitudinal autopilot design using a new suboptimal nonlinear control method,' IEE Proceedings-Control Theory and Applications, 2003, **150**(6), pp. 577–584.

Xin, M. and Balakrishnan, S., 'Control of the wing rock motion using a new suboptimal control method,' Proceedings of the Institution of Mechanical Engineers, Part G: Journal of Aerospace Engineering, 2004, **218**(4), pp. 257–266.

Xin, M. and Balakrishnan, S., 'A new method for suboptimal control of a class of non-linear systems,' Optimal Control Applications and Methods, 2005, **26**(2), pp. 55–83.

Xin, M., Balakrishnan, S., and Pernicka, H., 'Deep-space spacecraft formation flying using theta-d control,' in 'AIAA guidance, navigation, and control conference and exhibit,' 2004a p. 4784.

Xin, M., Balakrishnan, S., and Pernicka, H., 'Multiple spacecraft formation control using θ–d method,' IFAC Proceedings Volumes, 2005, **38**(1), pp. 307–312.

Xin, M., Balakrishnan, S., and Pernicka, H. J., 'Position and attitude control of deep-space spacecraft formation flying via virtual structure and θ-d technique,' 2007.

Xin, M., Balakrishnan, S., and Pernicka, H. J., 'Libration point stationkeeping using the θ-d technique,' The Journal of the Astronautical Sciences, 2008, **56**(2), pp. 231–250.

Xin, M., Balakrishnan, S., and Stansbery, D., 'Spacecraft position and attitude control with theta-d technique,' in '42nd AIAA aerospace sciences meeting and exhibit,' 2004b p. 540.

Xin, M., Balakrishnan, S., Stansbery, D., and Ohlmeyer, E., 'Nonlinear bank-to-turn/skid-to-turn missile outer-loop/inner-loop autopilot design with theta-d technique,' in 'AIAA Guidance, Navigation, and Control Conference and Exhibit,' 2003 p. 5581.

Xin, M., Balakrishnan, S., Stansbery, D. T., and Ohlmeyer, E. J., 'Nonlinear missile autopilot design with theta-d technique,' Journal of guidance, control, and dynamics, 2004c, **27**(3), pp. 406–417.

Xin, M., Dancer, M., Balakrishnan, S., and Pernicka, H., 'Stationkeeping of an l/sub 2/libration point satellite with/spl theta/-d technique,' in 'Proceedings of the 2004 American Control Conference,' volume 2, IEEE, 2004d pp. 1037–1042.

Xin, M. and Pan, H., 'Nonlinear optimal control of spacecraft approaching a tumbling target,' Aerospace Science and Technology, 2011, **15**(2), pp. 79–89.

Xu, G. and Wang, D., 'Nonlinear dynamic equations of satellite relative motion around an oblate earth,' Journal of Guidance, Control, and Dynamics, 2008, **31**(5), pp. 1521–1524.

Xu, H. and Jagannathan, S., 'Neural network-based finite horizon stochastic optimal control design for nonlinear networked control systems,' IEEE transactions on neural networks and learning systems, 2014, **26**(3), pp. 472–485.

Xu, Z., Gao, S., Han, Y., and Yuan, J., 'Modeling and feedback linearization based sliding mode control of diesel engines for waterjet propulsion vessels,' Control Engineering Practice, 2020, **105**, p. 104647.

Yamasaki, T. and Balakrishnan, S., 'Sliding mode based pure pursuit guidance for uav rendezvous and chase with a cooperative aircraft,' in 'Proceedings of the 2010 American Control Conference,' IEEE, 2010 pp. 5544–5549.

Yedavalli, R. K., *Flight Dynamics and Control of Aero and Space Vehicles*, John Wiley & Sons, 2020.

Yu, C., Jiang, J., Zhen, Z., Bhatia, A. K., and Wang, S., 'Adaptive backstepping control for air-breathing hypersonic vehicle subject to mismatched uncertainties,' Aerospace Science and Technology, 2020, p. 106244.

Zambelli, M. and Ferrara, A., 'Constrained sliding-mode control: A survey,' in 'Variable-Structure Systems and Sliding-Mode Control,' pp. 149–175, Springer, 2020.

Zedek, M., 'Continuity and location of zeros of linear combinations of polynomials,' Proceedings of the American Mathematical Society, 1965, **16**(1), pp. 78–84.

Zhang, B. and Lu, S., 'Fault-tolerant control for four-wheel independent actuated electric vehicle using feedback linearization and cooperative game theory,' Control Engineering Practice, 2020, **101**, p. 104510.

Zhang, L., Wei, C., Wu, R., and Cui, N., 'Fixed-time extended state observer based non-singular fast terminal sliding mode control for a vtvl reusable launch vehicle,' Aerospace Science and Technology, 2018, **82**, pp. 70–79.

Zhang, S., Fei, L., CHENG, Y.-Q., and Kai-Feng, H., 'Aircraft trajectory control with feedback linearization for general nonlinear systems,' in '2020 Chinese Control And Decision Conference (CCDC),' IEEE, 2020 pp. 3937–3944.

Zhang, Y., Li, S., and Liao, L., 'Near-optimal control of nonlinear dynamical systems: A brief survey,' Annual Reviews in Control, 2019.

Zhao, Q., Xu, H., and Jagannathan, S., 'Neural network-based finite-horizon optimal control of uncertain affine nonlinear discrete-time systems,' IEEE transactions on neural networks and learning systems, 2014, **26**(3), pp. 486–499.

Zheng, X. and Yang, X., 'Improved adaptive nn backstepping control design for a perturbed pvtol aircraft,' Neurocomputing, 2020, **410**, pp. 51–60.

Zhou, J., Hu, Q., and Friswell, M. I., 'Decentralized finite time attitude synchronization control of satellite formation flying,' Journal of Guidance, Control, and Dynamics, 2013, **36**(1), pp. 185–195.

VITA

Jie Yao was born in SheXian County, Anhui Province, P.R.China. In September 1999, he enrolled at the Jingdezhen Ceramic Institute, where he studied Mechanical Design, Manufacturing, and Automation for his freshman year and sophomore years. In September 2001, he attended Nanjing University of Aeronautics and Astronautics, where he studied in the Department of Automatic Control and graduated as with a Bachelor of Science degree in July 2003. After graduation, he joined the Jingdezhen Ceramic Institute as a lecturer and research assistant. In August 2014, he enrolled at Missouri University of Science and Technology (formerly University of Missouri-Rolla) to pursue his doctoral degree in Mechanical Engineering. During this period, he held the position of Graduate Research Assistant and Graduate Teaching Assistant in the Department of Mechanical and Aerospace Engineering. He received his Ph.D.in Mechanical Engineering from the Missouri University of Science and Technology in December 2020. His research interests included nonlinear control, optimal control, adaptive dynamic programming, optimal estimation, adaptive control, neural network, reinforcement learning, computer vision, and machine learning, etc.